Philipps Universität Marburg

Community transcriptomics reveals drainage effects on paddy soil microbiome across the three domains of life

Dissertation

zur Erlangung des akademischen Grades

Doktor der Naturwissenschaften

(Dr. rer. nat)

dem Fachbereich Biologie

der Philipps-Universität Marburg/Lahn

vorgelegt von

Rehab Abdallah

aus Kairo, Ägypten

Marburg an der Lahn | 2018

The experimental work for this thesis was carried out from October 2014 to April 2018 at the Max Planck Institute for Terrestrial Microbiology under supervision of PD Dr. Werner Liesack in the Department of Biogeochemistry and the Department of Organismic Interactions.

The thesis was accepted by the Department of Biology of the Phillips University Marburg at the: 05/07/2018

First examiner: PD Dr. Werner Liesack

Second examiner: Prof. Dr. Ralf Conrad

Date of defense: 27/9/2018

Dedicated to my husband and my family

Publication

This thesis resulted in the following papers:

Abdallah R. Z., Wegner C.E., Liesack W., Community transcriptomics reveals drainage effects on paddy soil microbiome across the three domains of life, (Submitted to Soil Biology and Biogeochemistry)

Abdallah R. Z., Wegner C.E., Liesack W., The effect of incubation time on paddy soil microbial communities after drainage, (in preparation as short report)

“Science knows no country, because knowledge belongs to humanity, and is the torch which illuminates the world”

Louis Pasteur

Table of contents

Summary

Methane is a potent greenhouse gas that plays a major role in global climate change. Biogenic methane is produced solely by methanogens thriving in anoxic soil such as wetland rice fields. The wide use of rice straw as an organic fertiliser makes rice farming one of the major global sources of methane emission. It contributes approx. 10% to the total methane budget. The microbial communities in the rice field soil (paddy soil) are able to efficiently degrade rice straw under anoxic conditions. Bio-polymer breakdown is the rate-limiting step for methanogenesis. Drainage is a common practice in rice farming, and it serves as an important mitigation strategy to reduce methane emission from rice paddies. Moreover, it enhances soil health and productivity by increasing soil organic matter (SOM) decomposition and mineralization. The focus of my thesis research was to (i) elucidate how drainage shapes the structure and function of paddy soil microbial communities across all three domains of life and (ii) understand how the paddy soil microbial communities hydrolyse bio-polymers during drainage.

Initially, paddy soil microcosms amended with rice straw were pre-incubated for 7 or 28 days under flooded conditions, followed by 9 days of drainage. The analysis showed that except for saprophytic fungi and methanotrophic bacteria, the duration of the pre-incubation period had only a minor effect on the microbial community response to drainage. Therefore, I focused my research on microcosms pre-incubated for 28 days under flooded conditions.

During the flooding and drainage periods, the change in soil physical and chemical parameters was measured. The soil was sampled from flooded and drained microcosms, and the response of paddy soil bacterial, archaeal and eukaryotic communities was assessed using metatranscriptomics. With drainage, the oxygen concentration increased from suboxic (~1.6 µmol/l) to near-atmospheric (~240 µmol/l) levels. Concurrently, the moisture content decreased to ~ 11% and the water potential decreased to -0.87 MPa.

The changes in soil physical and chemical characteristics did not affect the absolute SSU rRNA transcript abundances of bacteria and archaea, while those of fungi increased with drainage. However, drainage induced significant changes in their taxonomic composition. *Firmicutes* (*Clostridiaceae*, *Ruminococcaceae*, and *Lachnospiraceae*) decreased in relative abundance, while *Actinobacteria* (*Nocardioidaceae*), *Proteobacteria* (*Comamonadaceae*) increased. These

taxon-specific dynamics were consistently observed on rRNA and mRNA levels. Significant increase of *Planctomycetes* abundance (*Planctomycetaceae*) was primarily observed on mRNA level. The abundance of methanogen mRNA significantly decreased with drainage, coinciding with complete inhibition of the methane production potential in dry soil. Among Eukarya, protists and *Amoebozoa* were prevalent under flooded conditions, while fungal rRNA and mRNA abundances were significantly increased upon drainage. In particular, *Pezizomycotina* (*Ascomycota*) and *Agaricomycotina* (*Basidiomycota*) were the most abundant fungal groups in dry soil.

Taking the level of mRNA expression as a proxy, the overall microbiota activity was not severely affected by the decrease in water potential. The proportion of microbial mRNA in total RNA was 1.7% under flooded conditions and 2% upon drainage. Moreover, transcripts affiliated with transcription and translation were enriched with drainage. The mRNA proportion in total RNA combined with stable or increased SSU rRNA abundances indicates that drainage did not have a detrimental effect but induced the development of a community well adapted to oxic and dry soil conditions. This microbial community was characterized by an increase in the relative abundance of transcripts involved in lignin degradation, peptidoglycan lysis and had the capacity to metabolize storage molecules such as glycogen. Under flooded conditions, the microbial community expressed a higher level of glycoside hydrolase transcripts involved in cellulose and chitin degradation.

Zusammenfassung

Methan ist ein potentes Treibhausgas, das erheblich zum Klimawandel beiträgt. Es wird biologisch ausschließlich durch methanogene Archaeen produziert, welche in anoxischen Böden weit verbreitet sind. Ein Beispiel ist der Nassreisanbau. Dieser trägt 10% zu dem global in die Atmosphäre emittierten Methan bei. Reisstroh wird im Reisanbau als organischer Dünger eingesetzt und von der mikrobiellen Gemeinschaft im gefluteten Reisfeldboden unter anoxischen Bedingungen abgebaut. Der ratenbegrenzende Schritt für die Methanproduktion im Reisfeldboden ist der Bio-polymer-Abbau. Entwässerung ist eine gängige Praxis im Reisanbau und repräsentiert eine wichtige Strategie zur Minderung der Methanemission aus Reisfeldern. Entwässerung fördert ferner die Bodengesundheit durch den beschleunigten Abbau und die Mineralisierung der organischen Substanz im Boden. Die vorliegende Arbeit sollte den Effekt von Entwässerung auf die Zusammensetzung und Funktion der mikrobiellen Gemeinschaft im Reisfeldboden mittels molekularökologischer Methoden untersuchen. Ein Schwerpunkt sollte die Analyse des Bio-polymer-Abbaus sein.

Reisfeldboden-Mikrokosmen wurden mit Reisstroh versetzt und anfänglich entweder für sieben oder 28 Tage unter gefluteten Bedingungen vorinkubiert und nachfolgend für neun Tage entwässert. Die Analyse zeigte, dass mit Ausnahme saprophytischer Pilze und methanoxidierender Bakterien die Dauer der Vorinkubation nur einen geringen Effekt auf die Antwort der mikrobiellen Gemeinschaft auf die Entwässerung des Bodens hat. Daher wurden die Mikrokosmen für die weiteren Untersuchungen ausschließlich für 28 Tage vorinkubiert. Bodenproben wurden jedem einzelnen Mikrokosmos entnommen und die Antwort der mikrobiellen Gemeinschaft auf Entwässerung wurde mittels Umwelttranskriptomik (= Metatranskriptomik) untersucht.

Physikalische Bodenparameter wurden während der Entwässerungsphase regelmäßig überprüft. Entwässerung führte zu einem Anstieg der Sauerstoffkonzentration von suboxischer (~1.6 µmol/l) zu nahezu atmosphärischer Konzentration (~240 µmol/l). Korrespondierend dazu fiel die Bodenfeuchte auf 11% und das Wasserpotenzial auf -0.87 MPa.

Der Effekt von Entwässerung auf die Bodenparameter hatte keinen Einfluss auf die mittels RT-qPCR quantifizierbaren rRNA-Transkriptmengen der bacteria und archaea. Hingegen stieg die

Transkriptmenge an pilzlicher rRNA signifikant an. Die taxonomische Zusammensetzung der mikrobiellen Gemeinschaft änderte sich während der Entwässerungsphase signifikant. Die relative Abundanz der Firmicutes (Clostridiaceae, Ruminococcaceae, Lachnospiraceae) nahm mit zunehmender Entwässerung ab, während die Abundanzen der Actinobacteria (Nocardioidaceae) und Proteobacteria (Comamonadaceae) anstiegen. Diese durch die Entwässerung induzierten Dynamiken wurden durch eine taxonomische Analyse der rRNA und mRNA bestätigt. Im Falle der Planctomycetes (Planctomycetaceae) wurde eine solche Dynamik nur auf Ebene der mRNA beobachtet. Im Gegensatz hierzu nahm die detektierbare Menge an mRNA methanogener Archaeen während der Entwässerungsphase signifikant ab; dies im Einklang mit der vollständigen Hemmung der Methanproduktion. Protisten und Amoebozoa waren die dominanten Vertreter innerhalb der Eukaryota. Entwässerung führte zu einer Verringerung der Protisten (Cercozoa) im Reisfeldboden, hatte aber keinen signifikanten Effekt auf die Abundanz der Amoebozoa. Die Entwässerung führte im Metatranskriptom zu einem signifikanten Anstieg pilzlicher rRNA und mRNA. Pezimycotina (Ascomycota) und Agarimycotina (Basidiomycota) waren die wichtigsten pilzlichen Gruppen im trockenen Reisfeldboden.

Der Anteil der mRNA an der Gesamt-RNA ist ein guter Indikator für mikrobielle Aktivität. Dieser Anteil lag für die bakterielle mRNA im gefluteten Reisfeldboden bei 1.7% und nach Entwässerung bei 2%. mRNA des Transkriptions- und Translationsapparates war unter den entwässerten Bedingungen signifikant angereichert. Dies weist darauf hin, dass die Entwässerung keinen negativen Effekt auf die metabolische Aktivität der mikrobiellen Gemeinschaft hatte. Vielmehr wurde durch die Entwässerung die Entwicklung einer an trockene und oxische Bedingungen angepasste mikrobielle Gemeinschaft induziert. Charakteristisch für diese Gemeinschaft war die Expression von mRNA, welche für an der Verstoffwechselung von Lignin, Peptidoglykan und Glykogen beteiligten Enzyme kodiert. Unter gefluteten Bedingungen wurde hingegen ein höheres Niveau an Transkripten detektiert, welche Glykosylhydrolasen kodieren. Diese sind am Abbau von Zellulose und Chitin beteiligt.

1 Introduction

Rice is a staple crop worldwide; rice cultivation, however, is one of the primary sources of atmospheric methane emissions. This chapter of my PhD thesis provides a thorough overview of paddy soil, the microbial communities thriving in it, how they contribute to the global methane cycle through the degradation of plant bio-polymer, and drainage as an effective mitigation strategy. Furthermore, I discuss how drainage affects the structure and function of certain paddy soil microbial guilds such as methanogens and methanotrophs. The scientific topics relevant to my thesis are organised by particular subheadings.

1.1 Methane budget, emissions, and global warming

Methane is one of the most abundant hydrocarbons on earth and an important greenhouse gas (GHG). It has been of interest to the public and the scientific community because of its substantial role in global warming. Over the last two centuries, estimated methane emissions have doubled from about 200 to 500–600 Tg/year (Le Mer and Roger, 2001; Conrad, 2009; Nisbet et al., 2014). This doubling corresponds to a 150% increase in atmospheric methane concentration, from 722 ppb in 1750 to 1,803 ppb in 2011 (IPCC, 2013). Methane is a potent GHG; it is 34 times more effective in trapping heat than CO_2. It is thus one of the drivers of the global temperature increase (with a 40% contribution), alongside CO_2 and NO_2 (Lelieveld et al., 1993; IPCC, 2013). Methane is produced from natural and anthropogenic sources. Nevertheless, the rise in its atmospheric concentration is correlated with the increase in anthropogenic methane emissions (IPCC, 2007). Anthropogenic methane emissions comprise 50–63% of the total methane emitted to the atmosphere (IPCC, 2013). Sources of anthropogenic methane are agriculture (27%), fossil fuels (18%), landfills and sewage treatment plants (11%), and biomass burning (7%) (Conrad, 2009).

Methane can be produced biogenically (biological methane) or abiogenically (inorganic methane). Biogenic methane represents 70% of the total methane emitted to the atmosphere (IPCC, 2007). Methanogens are the sole source of biogenic methane (Thauer et al., 2008). These microbes prevail in anoxic environmental systems such as rice paddies.

1.2 Paddy soil and rice farming

Rice is the second most cultivated crop after wheat (Leff et al., 2004). Worldwide, around 3.8 billion people consume rice as a staple food (Muthayya et al., 2014). Rice is farmed mostly under flooded conditions, also termed anthropogenic wetlands. Wetlands are soil bodies that are either permanently or seasonally flooded with water. They are considered to be the single leading source of methane (IPCC, 2007). In particular, wetland rice fields are estimated to produce between 25 and 150 Tg/year of methane (Le Mer & Roger 2001). Rice farming contributes to 10% of the total methane emitted to the atmosphere (Conrad, 2009). Moreover, in response to the growing human population, rice farming is expected to increase by at least 42% by 2050 (Ray et al., 2013). Therefore, the contribution of rice farming to the global methane budget is expected to increase over the coming decades.

During rice farming, rice paddies are flooded, which limits oxygen penetration and divides the ecosystem of paddy soil into three main soil compartments: surface soil, bulk soil, and rhizosphere soil (**Figure 1.1**). Each of these soil compartments has a unique biogeochemistry and, therefore, specific microbial communities.

1.3 Biogeochemistry of rice paddies

1.3.1 Microbial-biogeochemical cycles in surface and bulk soil

In flooded rice paddies, the carbon cycle is driven by the presence of organic carbon and electron acceptors such as oxygen, Fe(III), sulphate, and nitrate. In the presence of these electron acceptors, organic carbon is converted to CO_2, while in their absence, it is converted to methane and CO_2 (Conrad and Frenzel, 2002). In the light of these facts, the specific biogeochemical characteristics of each paddy soil compartment and the microbial communities thriving in it can be explained.

In surface soil, oxygen is the main electron acceptor. It diffuses through the floodwater, thereby providing oxic conditions in the upper 0.5 mm soil zone (Frenzel et al., 1992; Noll et al., 2005; Reim et al., 2012). Incubation conditions determine the concentration of oxygen in the surface layer and deeper soil layers. For instance, a prior study demonstrated that illuminating a paddy soil microcosm for 2.5 hours resulted in oxygen diffusion to a depth of 40 mm, compared to only 5 mm when the microcosm was incubated in the dark (Frenzel et al., 1992).

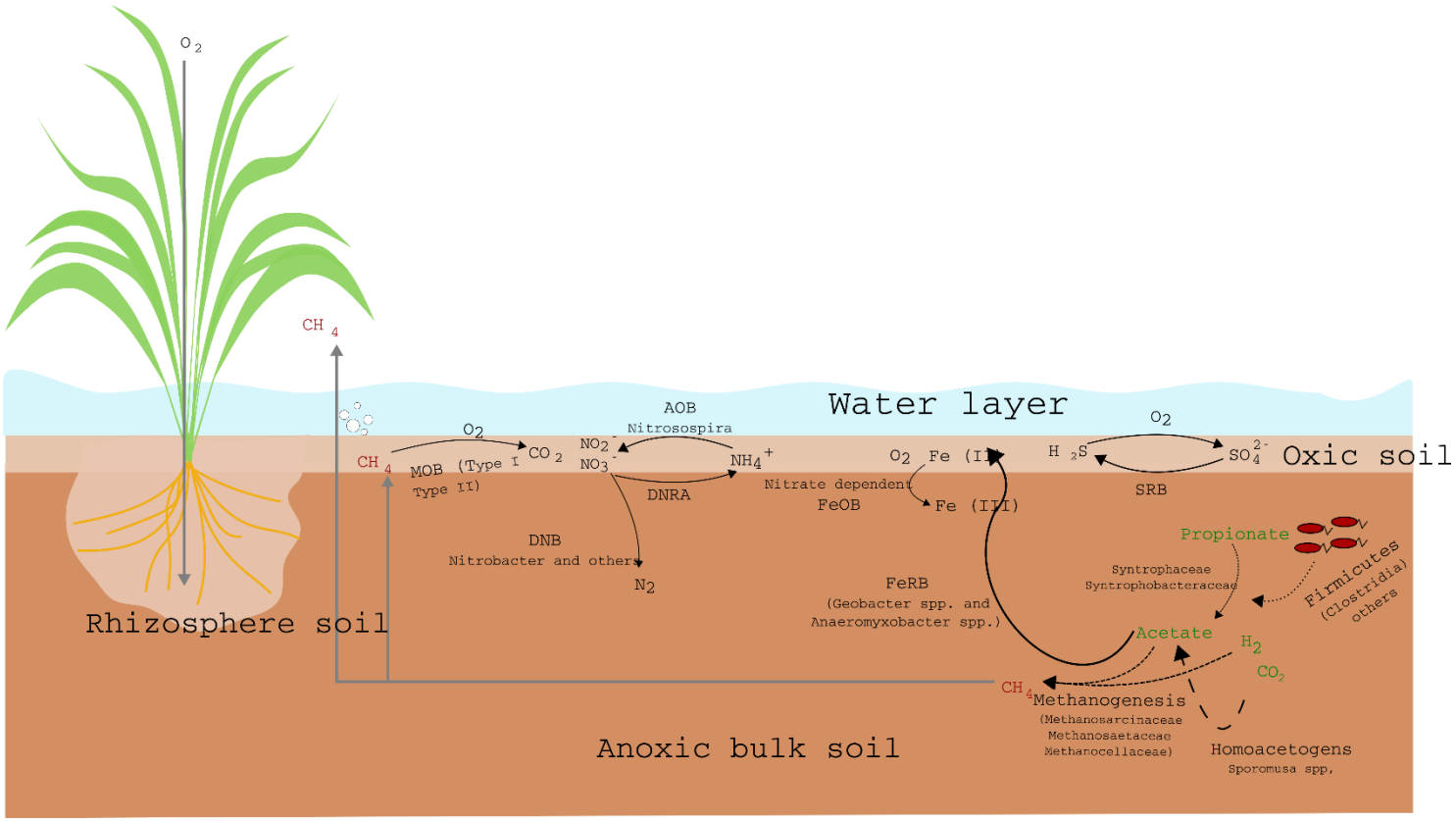

Figure 1.1: Paddy soil compartments, major biogeochemical cycles occurring in flooded paddy soil, and the microbial guilds involved in these processes.
MOB: Methane-oxidising bacteria; AOB: Ammonium-oxidising bacteria; DNB: Denitrifying bacteria; DNRA: Dissimilatory nitrate reduction to ammonia; FeOB: Iron-oxidising bacteria; FeRB: Iron-reducing bacteria; SRB: Sulphate-reducing bacteria.

In bulk soil, however, other electron acceptors contribute to the oxidation of organic matter (Conrad and Frenzel, 2002). These electron acceptors are depleted sequentially, and only after their reduction methanogenesis can be the dominant process. These reduced electron acceptors – nitrate, sulphate, and Fe(III) – are regenerated when exposed to O_2 (Conrad and Frenzel, 2002).

1.3.1.1 Bacterial nitrogen, iron, and sulphur cycles

Nitrogen cycle. The microbial nitrogen cycle starts with nitrogen fixation, or the conversion of N_2 to ammonia. Bacterial nitrogen fixation (BNF) occurs in all paddy soil compartments by free-living autotrophic and heterotrophic bacteria (Ladha and Reddy, 2003). The majority of BNF bacteria are cyanobacteria and photosynthetic bacteria inhabiting the surface layer; however, other heterotrophic BNF bacteria have been detected in bulk and rhizosphere soil (Ladha and Reddy, 2003). Nitrogen fixation is followed by (1) the aerobic oxidation (nitrification) of ammonia to nitrite and nitrate, and (2) the anaerobic reduction (denitrification) of the nitrification products to N_2 (Conrad and Frenzel, 2002). Nitrifiers, or bacterial ammonia oxidisers (AOB) and bacterial nitrite oxidisers (NOB), dwell in the surface soil. The main ammonia oxidisers in rice paddy soil are members of the genus *Nitrosospira* (Rotthauwe et al., 1997; Conrad and Frenzel, 2002; Ke et al., 2013). In addition to the aerobic oxidation of ammonia, anaerobic ammonia oxidation (anammox) has been detected in anoxic paddy soil fertilised with slurry manure (Zhu et al., 2011). The microbial community involved is closely related to the anammox bacteria Candidatus *Kuenenia* and Candidatus. *Anammoxoglobus*, and to the nitrite-dependent anaerobic ammonium and methane-oxidising bacteria Candidatus. *Brocadia fulgida*, Candidatus. *Brocadia anammoxidans*, and Candidatus. *Jettenia asiatica* (Zhu et al., 2011; Wang et al., 2012). Upon the formation of nitrite and nitrate in the surface and rhizosphere soil, these nitrogen species diffuse into the bulk soil where denitrifiers and dissimilatory nitrate reducers can use them as terminal electron acceptors. Nitrate is usually depleted a few millimetres below the surface (Conrad and Frenzel, 2002).

Iron cycle. Fe(III) is the most quantitatively important electron acceptor in paddy soil (Conrad and Frenzel, 2002). Oxygen is responsible for the abiotic iron oxidation of Fe(II) to Fe(III) in the upper 3 mm of rice paddy soil. Below this, at 3–6 mm, iron oxidation occurs through a bacterial nitrate-dependent mechanism (Ratering and Schnell, 2001). Fe(III) reduction is thermodynamically more favourable than sulphate reduction and methanogenesis (Hoh and

Cord-Ruwisch, 1996; Chidthaisong and Conrad, 2000b). Therefore, iron reduction suppresses methanogenesis by competing for the same substrates such as acetate and H_2 (Chidthaisong and Conrad, 2000b; Conrad and Frenzel, 2002). In paddy soil, the population of dissimilatory iron reducers was identified as belonging to the genera *Geobacter* and *Anaeromyxobacter*, and to novel *Betaproteobacteria* (Hori et al., 2010; Kim and Liesack, 2015).

Sulphur cycle. Sulphate reduction is known to primarily occur in the upper layer of soil (0–1 cm), mainly in the oxic-anoxic interface (Wind and Conrad, 1995; Wind and Conrad, 1997; Wind et al., 1999; Yao et al., 1999). Moreover, sulphate concentration was found to be highest in rhizosphere soil (Conrad and Frenzel, 2002). Sulphur-oxidising bacteria, present in the surface and rhizosphere soil, oxidise the reduced sulphur species (H_2S, FeS, and S^0) to sulphate (Conrad and Frenzel, 2002). Sulphate reducers in paddy soil were affiliated to the genera *Desulfovibrio*, *Desulfobulbus*, *Desulforhabdus*, *Desulfotomaculum*, and *Desulfobotulus* (Conrad and Frenzel, 2002). Recently, it has been demonstrated that under sulphidogenic conditions, sulphate reducers play a significant role in propionate degradation (Liu and Conrad, 2017).

1.3.1.2 Soil organic matter and bio-polymer degradation in paddy soil

Upon the sequential depletion of alternative electron acceptors, the microbial processes in paddy soil are dominated by plant bio-polymer breakdown and methanogenesis (Glissmann and Conrad, 2002; Wegner and Liesack, 2016). Organic carbon in paddy soil originates from rice root exudates, soil organic matter (SOM), and decaying rice straw. Rice straw is the major source of organic carbon in rice paddies because of its use as an organic fertiliser. Rice straw is composed mostly of cellulose (32–37%), hemicellulose (29–37%), and lignin (10–15%) (Watanabe et al., 1993; Saito et al., 1994; Conrad and Frenzel, 2002). Cellulose is made up of glucose units linked together by β-1, 4 glycoside bonds (Klemm et al., 2005). Hemicellulose comprises different sugars such as xylose, mannose, galactose, glucose, rhamnose, and fucose. Hemicellulose is also structurally more complex than cellulose (Sun et al., 2000). Lignin is a highly recalcitrant aromatic heteropolymer. It is produced enzymatically by radical polymerisation of three phenolic monomers (Brown and Chang, 2014).

In rice paddies, microbial communities mediate the degradation of these plant bio-polymers under anoxic conditions. The anaerobic degradation of organic carbon occurs in five steps. The first step is the hydrolysis of plant bio-polymers into monomers. Hydrolysis is followed by

fermentation of monomers to primary fermentation products such as alcohols and short-chain fatty acids. These products (e.g. propionate) are converted by syntrophic degradation into acetate, H_2, and CO_2. Homoacetogenesis also occurs in paddy soil, and homoacetogens compete with methanogens for H_2 and CO_2. The final step in organic matter decomposition is methanogenesis, with acetate being used as a substrate for acetoclastic methanogenesis and CO_2 /H_2 as substrates for hydrogenotrophic methanogenesis (Conrad and Frenzel, 2002). **Figure 1.2** summarises these steps.

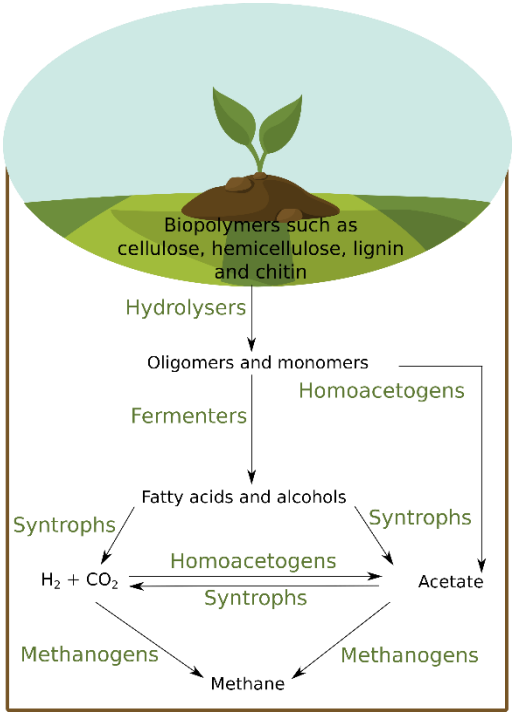

Figure 1.2: Anaerobic degradation of organic carbon in paddy soil.
In anoxic environments, fermentative bacteria hydrolyse and ferment bio-polymers into fatty acids and alcohols that are then syntrophically converted into acetate, H_2, and CO_2. Acetate and H_2/CO_2 serve as substrates for methanogenesis. Adapted from (Conrad and Frenzel, 2002)

A phylogenetically diverse range of bacteria play significant roles in polymer hydrolysis and fermentation in paddy soil. The important contribution of the *Clostridia* and *Bacteroidetes* to rice straw degradation is well-documented (Conrad and Frenzel, 2002; Rui et al., 2009; Wegner and Liesack, 2016). Recently, *Acidobacteria* and *Chloroflexi* were also identified to be actively involved in rice straw degradation (Rui et al., 2009; Wegner and Liesack, 2016). Bacterial families found to be involved in the decomposition of rice straw include *Lachnospiraceae*, *Ruminococcaceae*, and *Veillonellaceae*, in addition to *Myxococcaceae* (*Anaeromyxobacter*) and *Geobacteraceae* (Wegner and Liesack, 2016). Fermentation products arising from the

degradation of either SOM or rice straw are mainly acetate, followed by propionate and butyrate (Glissmann and Conrad, 2000; Conrad and Frenzel, 2002). The cellulose component of rice straw is preferentially degraded to acetate and CO_2, while propionate is assumed to be produced from other rice straw components such as xylan (Chin and Conrad, 1995; Chin et al., 1998). The decomposition of the lignin component of rice straw is not yet well-studied, presumably because classical lignin degradation is based on oxygen-dependent enzymes (Brown and Chang, 2014).

Propionate is a primary fermentation product that is syntrophically degraded in paddy soil (Conrad and Frenzel, 2002). Members of the *Syntrophaceae*, *Syntrophobacteraceae*, and *Syntrophomonadaceae* are thought to be responsible for the syntrophic degradation of propionate in paddy soil (Gan et al., 2012), resulting in acetate, H_2, and CO_2 (Krylova et al., 1997; Conrad and Frenzel, 2002). Moreover, the temporary accumulation of propionate is much more pronounced in soils amended with rice straw than in unamended soils (Krylova et al., 1997; Wegner and Liesack, 2016).

Aside from being a fermentation product, acetate can also be produced from H_2 and CO_2 by homoacetogens. In Vercelli paddy soil, these bacteria were identified to be members of the genus *Sporomusa* (Rosencrantz et al., 1999; Liesack et al., 2000; Conrad and Frenzel, 2002; Wegner and Liesack, 2016). Homoacetogens compete with hydrogenotrophic methanogens for H_2 and CO_2 (**Figure 1.2**). Thermodynamically, the reduction of CO_2 to acetate is not favourable unless H_2 is elevated (Conrad and Frenzel, 2002). This occurs mainly on rice roots. In flooded bulk soil, however, homoacetogenesis occurs when chloroform ($CHCl_3$) and 2-bromoethanesulphonate (BES) inhibit methanogenesis (Chidthaisong and Conrad, 2000a).

1.3.1.3 Carbohydrate Active Enzymes

Microbial communities in paddy soil require specific sets of enzymes to hydrolyse plant bio-polymers. These are termed the Carbohydrates Active Enzymes (CAZymes), which comprise six groups or classes: (1) glycosyl hydrolases (GH), (2) polysaccharide lyases (PL), (3) carbohydrate esterases (CE), (4) glycosyltransferases (GT), (5) carbohydrate-binding modules (CBM), and (6) auxiliary redox enzymes (AA). The first three classes are involved in the hydrolysis of carbohydrates, while glycosyltransferases are involved in the formation of glycosidic bonds (Cantarel et al., 2009; Lombard et al., 2014). Carbohydrate-binding modules are proteins that work in conjunction with other hydrolysing enzymes to offer substrate-specific

binding to carbohydrates (Cantarel et al., 2009). The majority of auxiliary redox enzymes are involved in lignin degradation. Glycosyl hydrolases are the most remarkable genes involved in bio-polymer breakdown. They constitute 47% of the classified CAZyme entries in the CAZyme database (Cantarel et al., 2009).

In flooded paddy soil, rice straw amendment leads to a significant increase in specific glycosyl hydrolases such as exoglucanase, glucosidase, and xylosidase (Glissmann and Conrad, 2002). As stated previously, various bacterial groups have been identified to be involved in rice straw degradation in paddy soil (Wegner and Liesack, 2016). These groups have been found to be involved in task-sharing, in which each bacterial group produces a particular set of glycoside hydrolases (Wegner and Liesack, 2016). *Firmicutes* produce cellulases, chitinases, and endo-xylanases, while *Proteobacteria* and *Bacteroidetes* are involved in the degradation of hemicelluloses via the production of arabinofuranosidase and fucosidase. Concurrently, *Acidobacteria* produce exo-xylanase (Wegner and Liesack, 2016). Even though the degradation of rice straw under flooded conditions has been investigated in some detail, little is known about its degradation under drained (oxic) paddy-soil conditions.

1.3.1.4 Methanogens and methanotrophs

Methane and CO_2 emission is the endpoint of SOM and bio-polymer degradation. Both hydrogenotrophic and acetoclastic methanogenesis occur in paddy soil. Hydrogenotrophic methanogenesis contributes to 20–30%, while acetoclastic methanogenesis contributes to 70–80% of methane emissions from paddy soil (Conrad and Klose, 1999). Shortly after flooding, the family *Methanosarcinaceae* dominates the anoxic zone in rice paddies worldwide, as demonstrated by DNA-based studies (Lueders and Friedrich, 2000; Ramakrishnan et al., 2001; Conrad and Frenzel, 2002; Conrad, 2007). *Methanobacteriaceae* and *Methanomicrobia* are also members of the methanogenic community in paddy soil, based on both DNA and RNA evidence, yet they are not as abundant as *Methanosaetaceae*, *Methanosarcinaceae*, and *Methanocellaceae* (Grosskopf et al., 1998; Lueders and Friedrich, 2000; Wegner and Liesack, 2016).

A recent metatranscriptome study has revealed that rice straw amendment affects the activity and composition of methanogens in paddy soil. The amendment of rice straw increased methane emissions and affected methanogen dynamics in flooded Vercelli paddy soil (Wegner and

Liesack, 2016). In rice-straw-amended soil, *Methanosarcinaceae* were the most abundant methanogens during an incubation period of 7 to 28 days (Wegner and Liesack, 2016). In unamended soil, during the early stages of methanogenesis (7 days), *Methanosarcinaceae*, *Methanosaetaceae*, and *Methanocellaceae* were similarly abundant (Wegner and Liesack, 2016). After 28 days of incubation of the unamended soil, *Methanosaetaceae* (acetoclastic pathway) became the most abundant methanogens, and *Methanocellaceae*, (formerly Rice Cluster I) (hydrogenotrophic pathway) exhibited a significant increase in relative abundance (Wegner and Liesack, 2016).

Recently, several papers have indicated that methanogenesis is not restricted to the phylum *Euryarchaeota*. Members of the new Candidatus phyla *Bathyarchaeota* and *Verstraetearchaeota* play a role in methane production as well (Evans et al., 2015; He et al., 2016; Vanwonterghem et al., 2016). *Bathyarchaeota* have recently been detected in paddy soils (Breidenbach and Conrad, 2015; Bai et al., 2017; Vaksmaa et al., 2017).

Before methane is emitted to the atmosphere, it becomes partially oxidised by aerobic methanotrophs in the oxic-anoxic soil layer, or the upper 2–3 mm zone (Conrad and Frenzel, 2002). Aerobic methanotrophs are classified as Type I methanotrophs (*Gammaproteobacteria*) and Type II methanotrophs (*Alphaproteobacteria*). Methanotrophic extremophiles belonging to the phylum *Verrucomicrobia* have only recently been identified (Dunfield et al., 2007). Anoxic bulk soil is considered to be the largest reservoir of methanotrophs (Conrad, 2007). Type II methanotrophs are the primary methane oxidisers in flooded paddy soil, as demonstrated by DNA-based research (Henckel et al., 2000; Mayumi et al., 2010; Fazli et al., 2013). While Type I methanotrophs are dominant in the oxic-anoxic interface, Type II methanotrophs are most abundant in bulk soil, below a depth of 2.2 mm (Reim et al., 2012). Even though Type II methanotrophs are the dominant methane oxidisers in paddy soil, Type I methanotrophs (such as *Methylobacter*) were found to be the most active methanotrophs involved in methane oxidation in the early incubation stage (3–19 days) on a polytetrafluoroethylene membrane, which divided the microcosm into an upper and a lower compartment. The upper compartment contained oxygen at atmospheric concentration, while the lower chamber was linked to an external reservoir that had nitrogen gas supplemented with 15% methane. The microcosms were incubated in the dark for 14 days at 25 °C (Krause et al., 2010; Reim et al., 2012). Furthermore, Type II methanotrophs start to become active in paddy

soil only after 25 days of incubation (Krause et al., 2010). This could be related to the fact that, unlike Type I methanotrophs, Type II methanotrophs are able to thrive in nutrient-poor conditions (Krause et al., 2010).

1.3.2 Rhizosphere soil

The microbial communities in rhizosphere soil are extremely heterogeneous and diverse (Lu et al., 2006). The release of oxygen from roots and the production of root exudates provide suitable niches for diverse microbial groups to dwell in rhizosphere soil (Conrad and Frenzel, 2002; Kogel-Knabner et al., 2010). The flow of carbon from rice roots provides suitable substrates for methane production. It is thought that in the early phase of the rice-growing season, methane is mostly produced from degradation of rice straw in bulk soil. Later, in the tillering and ripping stages, rice root exudates play a more important role in the production of methane and its emission to the atmosphere (Kogel-Knabner et al., 2010). It has even been demonstrated that methane production is more significant in rhizosphere soil than in bulk soil (Lu et al., 2000). The key methanogen in the rhizosphere soil is *Methanocellaceae* (rice cluster I) (Lu et al., 2005). Due to the presence of oxygen in the rhizosphere soil, methane oxidation occurs. Interestingly however, only 10% to 50% of the methane produced is oxidised in the rhizosphere soil, compared to 80% in the oxic-anoxic interface layer (Conrad and Frenzel, 2002; Kogel-Knabner et al., 2010). Furthermore, Type II methanotrophs are the dominant methanotrophs in the rhizosphere soil (Shrestha et al., 2010).

The presence of oxygen also allows for nitrification to occur in rhizosphere soil, coupled with denitrification. This leads to the production of N_2 (Conrad and Frenzel, 2002), which can be fixed by nitrogen-fixing bacteria such as *Azospirillum* (Lu et al., 2006). Additionally, oxygen released from roots leads to coupled iron-oxidation and iron-reduction processes. Iron reducers such as *Anaeromyxobacter* spp. and *Geobacter* spp. were found to be slightly more abundant in rhizosphere soil than in bulk soil (Conrad and Frenzel, 2002; Lu et al., 2006). Sulphur-oxidising bacteria regenerate sulphate in the presence of oxygen, which is why sulphate concentration has been found to be highest in rhizosphere soil (Conrad and Frenzel, 2002). This process is linked to sulphate reduction by sulphate reducers such as *Desulfovibrioaceae* (Lu et al., 2006). In rhizosphere soil, organic matter is thought to be degraded by both aerobic and anaerobic microorganisms such as *Clostridia*, *Burkholderiaceae*, and *Comamonadaceae* (Lu et al., 2006). The different developmental stages of the rice plant have a major effect on the

successional change of dominant bacterial groups in rhizosphere soil (Ikenaga et al., 2003; Lu et al., 2006).

1.4 Drainage and its importance to paddy soil

Drainage is a common practice in rice farming (Conrad and Frenzel, 2002). It results in drying of soil and proliferation of oxygen into the anoxic bulk soil, leading to the reoxidation of reduced electron acceptors. Drainage is used as a mitigation strategy to decrease GHG emissions from paddy soil. The different drainage types in rice farming are described below.

- **Mid-season drainage**

  It consists of a distinct and extended period (between 5 and 20 days) of drainage during rice growth (in the tillering stage). Mid-season drainage has been found to decrease methane emissions by 27% to 52% when compared to permanently flooded soil in two different studies (Sass et al., 1992; Towprayoon et al., 2005). Moreover, it is considered by many researchers to be the best option to mitigate GHG emissions from rice paddies (Hussain et al., 2015).

- **Intermittent irrigation**

  In intermittent irrigation, water is not provided continuously to the rice field, allowing the field to dry, thereby decreasing GHG emissions. Intermittent irrigation is followed during the non-sensitive stage of rice growth. Farmers in Japan implement this practice during the rice-growing season, following mid-season drainage (Wichelns, 2016; Leon et al., 2017).

- **Alternate wetting and drying periods**

  Through multiple aeration periods, the soil undergoes numerous drying and re-flooding cycles. The drying period, in this case, is shorter – for example, three days (Towprayoon et al., 2005; Hussain et al., 2015). Hussain et al. (2015) found that alternate wetting and drying periods resulted in a 72% decrease in methane emissions compared to permanently flooded soil; however, this practice led to increased N_2O emissions. Moreover, it lowered crop production by 12% (Towprayoon et al., 2005).

Drainage is also implemented for prolonged periods after the rice-growing season. During the dry season, the moisture content of soil can be as low as 6% (Soontranon et al., 2014). During drainage periods, SOM decomposition is accelerated; waterlogged or flooded soil is known to have slower SOM decomposition rates compared to aerated soil (Zhou et al., 2014).

1.5 Oxygen and desiccation as environmental variables of drainage

During drainage, changes in the activity and dynamics of the microbial community are influenced mainly by the intrusion of oxygen and soil drying. Oxygen and its effect on the zonation of the microbial community in paddy soil have been studied previously in two studies by Lüdemann et al. (2000) and Noll et al. (2005). Both studies used unplanted microcosms incubated in the dark.

Lüdemann et al. (2000) demonstrated a depth-specific distribution of abundant bacterial groups along the oxic-anoxic interface. In the oxic zone, *Alphaproteobacteria* (genus: *Sphingomonas*) and *Gammaproteobacteria* were most abundant. In the anoxic zone, members of *Clostridial* 'Cluster I' were dominant (Lüdemann et al., 2000). This study was conducted on DNA and RNA levels using Terminal restriction fragment length polymorphism (T-RFLP) fingerprinting. The DNA and RNA signatures were similar.

Noll *et al.* (2005) studied the effect of both oxygen and incubation time on the composition of the microbial community in flooded paddy soil. This study also involved both DNA and RNA analyses. It was revealed that the RNA-based analyses were more responsive to community dynamics than the DNA-based analysis (Noll et al., 2005). In early succession, the oxic zone was colonised by members of the *Betaproteobacteria*, while – as in the study by Lüdemann *et al.* – *Clostridial* 'Cluster I' was most abundant in the anoxic zone (Noll et al., 2005). In late succession, *Nitrospira*, *Verrucomicrobia*, and *Myxococcales* (*Anaeromyxobacter*) were the most abundant groups in the oxic zone (Noll et al., 2005).

The effects of desiccation on methanogenesis and methanotrophy in paddy soil have been studied by Jackel et al. (2001). In their study, soil-drying inhibited the oxidation of methane by methanotrophs and lowered methanogenesis rates. Soil with 20% (v/v) moisture content accumulated only about 10 µmol of methane after 30 days of incubation under anoxic conditions, while soil with 50% (v/v) or higher moisture content accumulated more than 100 µmol (Jackel et al., 2001).

1.6 Current knowledge on the response of microbial communities in paddy soil to drainage

The intrusion of oxygen during drainage changes the physico-chemical characteristics of soil. This change affects the microbial communities in paddy soil. Previous research on paddy soil has focused on how drainage affects particular microbial guilds such as methanogens and methanotrophs (Henckel et al., 2000; Ma and Lu, 2011; Ma et al., 2012, 2013).

In the anoxic bulk soil, drainage decreased methane emissions (Henckel et al., 2000; Ma and Lu, 2011; Ma et al., 2012, 2013). However, despite the lower methane emissions, the methanogenic community appeared to be stable during both flooded and drained conditions (Ma and Lu, 2011; Ma et al., 2012; Breidenbach and Conrad, 2015). Under drained conditions, members of the family *Methanocellaceae* were found to be abundant in desiccated or drained lake sediments and in Chinese paddy soil, based on the analysis of small Subunit Ribosomal RNA (SSU rRNA) genes (Ma and Lu, 2011; Conrad et al., 2014) and *mcrA* transcripts (Watanabe et al., 2009; Ma et al., 2012). In Philippine paddy soil, *Methanosarcina* were the main methanogens detected under dry conditions (Breidenbach and Conrad, 2014).

In surface soil, methane oxidation potential was found to increase, and methanotrophs proliferated in deeper soil sections (up to a depth of 8 mm instead of 2 mm) after eight days of drainage (Henckel et al., 2001). More interestingly, during drainage, Type I methanotrophs outcompeted Type II methanotrophs based on the analysis of SSU rRNA and particulate methane monooxygenase subunit alpha (*pmoA*) genes (Henckel et al., 2001). The community change from Type II to Type I methanotrophs could be due to the increase in oxygen concentration, which may have favoured Type I methanotrophs (Roslev and King, 1994). Similar results were reported by (Ma et al., 2013). Moreover, this last study revealed that extended drainage periods had different effects on methanotrophs. A moisture content of about 65% favoured the activity of Type I methanotrophs, while the methane oxidation activity decreased in both rhizosphere and surface soil at a moisture content of about 45% (Ma et al., 2013).

Recently, the response of bacterial and archaeal communities in soil to drainage, crop rotation, and desiccation has been assessed by three consecutive studies (Breidenbach et al., 2015; Breidenbach and Conrad, 2015; Reim et al., 2017). Based on the analysis of the SSU rRNA gene and transcripts, a slight shift in the composition of the bacterial community in the soil of

a Philippine rice field was observed after drainage and crop rotation (Breidenbach et al., 2015; Breidenbach and Conrad, 2015). *Spartobacteria*, *Sphingobacteria*, *Acidobacteria*, *Anaeromyxobacter*, and *Myxococcales* increased in relative abundance after drainage (Breidenbach and Conrad, 2015). The increase in abundance of these bacterial lineages was linked to a high oxygen concentration in the case of *Spartobacteria* and *Sphingobacteria*, and to the decrease in substrate availability for *Acidobacteria* (Breidenbach and Conrad, 2015). In a SSU rRNA survey by Reim *et al.* (2017) desiccation of paddy soil in Thailand followed by re-flooding resulted in a significant increase in the relative abundance of *Firmicutes* (*Clostridia*), *Cyanobacteria*, and *Bacteroidetes*. Moreover, *Firmicutes* outcompeted *Proteobacteria*, which were dominant in the original wet soil sample (Reim et al., 2017).

1.7 Desiccation and oxygen as environmental stressors in pure culture studies

The effect of oxygen and desiccation has been studied on particular members of the paddy-soil microbial community, with a focus on methanogens. *Methanosarcina* spp. in general and *Methanosarcina barkeri* specifically are well-known for tolerating oxygen stress. In a study by (Fetzer et al., 1993), oxygen stress (up to 200 h) did not affect the viability of *Methanosarcina barkeri*; however, it significantly reduced methane production. The reason for *M. barkeri's* oxygen tolerance is that it possesses sets of genes known to encode stress-responsive enzymes – in particular, those for oxidative stress, such as superoxide dismutase and catalase (Maeder et al., 2006). The genome of a member of the hydrogenotrophic *Methanocellaceae* (Rice Cluster I) is also known to contain these genes (Erkel et al., 2006; Lü and Lu, 2012). A study of methanogenic consortia, in which either *Methanosaeta* or *Methanosarcina* had been enriched, demonstrated that the effect of long-term aeration (72 h) inhibited acetoclastic methanogenesis but not the fermentation processes upstream of methanogenesis (Wu and Conrad, 2001). Moreover, in a recent study, (Jasso-Chavez et al., 2015) demonstrated that after adaptation to air, *Methanosarcina acetivorans* can grow and produce methane under 0.4–1% O_2, similarly to control cells (under anoxic conditions). Furthermore, increased levels of catalase, superoxide dismutase, and peroxidase transcripts were observed in the air-adapted cells relative to control cells (Jasso-Chavez et al., 2015). In contrast, methanogens have been revealed to be sensitive to desiccation. Desiccation decreased the viability of *M. barkeri* by 10% under anoxic conditions and by less than 5% under oxic conditions (Fetzer et al., 1993).

It is also worth noting that methanogens were found to be active and to produce methane (in lower rates) through the hydrogenotrophic pathway under oxic conditions in arid biological soil crusts (Angel et al., 2011). Once the conditions switched to anoxic, methane was produced through the acetoclastic pathway. The responsible archaea for methane production in arid biological soil crusts were identified to be *Methanosarcina* and *Methanocella* (Angel et al., 2011).

1.8 Desiccation and its effect on microbial communities in other soil systems

Desiccation is one of the main factors that shape the composition and dynamics of microbial communities in soil. The effect of desiccation and extreme drying events on these communities has captured the interest of soil microbial ecologists. Some researchers have focused on how desiccation affects microbial processes and microbial biomass. A fourfold decrease in colony-forming units (CFU) was observed upon desiccation of grassland rhizosphere soil (Griffiths et al., 2003). However, no difference in microbial community composition was observed between drained and control soil (Griffiths et al., 2003). This could be due to the techniques used in the study. The study used Denaturing gradient gel electrophoresis (DGGE) of the SSU rRNA gene and transcript from environmental nucleic acid. In the DGGE technique, DNA fragments are separated using a denaturing buffer during gel electrophoresis. This technique is known to produce false negative results as DNA sequences from different bacterial species can display the same separation on the gel because of the same bacterial GC (guanine-cytosine) content. Additionally, repeated drying and re-wetting cycles were found to result in reduced bacterial growth but stable fungal growth (Bapiri et al., 2010). With regard to microbial biomass, the literature reveals conflicting results. Generally, bacterial biomass decreased with desiccation (Hueso et al., 2012; Alster et al., 2013; Naylor and Coleman-Derr, 2018). However, some reports indicate that bacterial and fungal biomass slightly decreased or remained stable under drought conditions (Bapiri et al., 2010; Hartmann et al., 2017).

Soil microbial alpha-diversity is often used as a metric for greater metabolic potential and, hence, higher nutrient mineralisation and decomposition (Naylor and Coleman-Derr, 2018). Desiccation is thought to have little effect on the microbial alpha-diversity of soil (Acosta-Martinez et al., 2014; Armstrong et al., 2016; Toth et al., 2017; Naylor and Coleman-Derr, 2018). However, in some studies, desiccation resulted in significant shifts in the composition of microbial communities in soil (Barnard et al., 2013; Bouskill et al., 2013; Acosta-Martinez

et al., 2014; Evans et al., 2015; Naylor and Coleman-Derr, 2018). In general, upon the drying of soil, a decrease or increase in relative abundance of certain microbial groups is detected, rather than the disappearance of certain microbial groups and the rise of desiccation-tolerant taxa (Naylor and Coleman-Derr, 2018). A general phenomenon is an increase in Gram-positive bacteria (*Firmicutes* and *Actinobacteria*) and a decrease in Gram-negative bacteria (Acosta-Martinez et al., 2014; Chodak et al., 2015).

Upon desiccation, members of the phylum *Actinobacteria* usually exhibit a rapid increase in the relative abundance of SSU rRNA. This is in contrast to the *Bacteroidetes* and *Verrucomicrobia*, which display an opposite trend; see **Figure 1.3** (Evans et al., 2011; Barnard et al., 2013; Bouskill et al., 2013; Acosta-Martinez et al., 2014). Mostly, the changes observed in abundance relate to a single member or a few particular members of the respective phylum (Barnard et al., 2013; Bouskill et al., 2013). For example, the increase in *Actinobacteria* in a rainfall exclusion study was mainly attributed to the order *Actinomycetales* (Bouskill et al., 2013). Unlike *Actinobacteria*, several bacterial phyla – such as *Proteobacteria*, *Firmicutes*, *Planctomycetes*, and *Acidobacteria* – exhibit varying responses to drying of soil; see **Figure 1.3** (Naylor and Coleman-Derr, 2018). *Proteobacteria* (Evans et al., 2011; Hartmann et al., 2017) and *Firmicutes* (Evans et al., 2011) have been found to favour wet soils. In contrast, in other studies, the members of these phyla preferred a dry environment (Bouskill et al., 2013; Acosta-Martinez et al., 2014; Chodak et al., 2015; Hartmann et al., 2017). These discrepancies in phylum-level responses to drying of soil can be explained by the presence of resident sub-phyla specific to each study and soil. These sub-phyla may occupy distinct ecological niches or have specific morphological features that increase their tolerance level to desiccation (Naylor and Coleman-Derr, 2018).

The response of the eukaryotic soil community to soil desiccation is not well-studied (Naylor and Coleman-Derr, 2018). Little is known about desiccation effects on the fungal community in soil (Gordon et al., 2008; Barnard et al., 2013; Fuchslueger et al., 2016). Nevertheless, the few studies that have been conducted reveal that the soil fungal community is not affected by desiccation. The research involved Phospholipid-derived fatty acids (PFLA) of fungal cells (Gordon et al., 2008; Fuchslueger et al., 2016), SSU rRNA gene and transcript (Barnard et al., 2013) analyses.

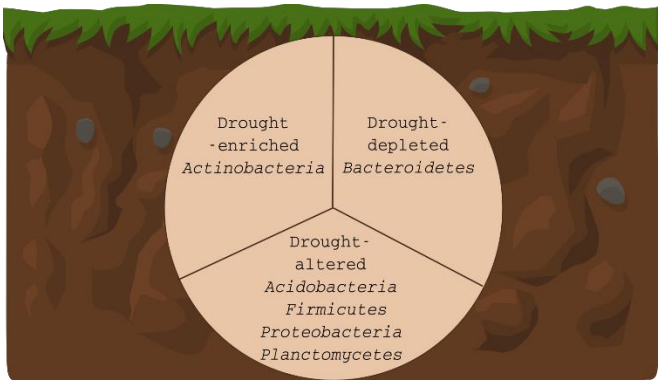

Figure 1.3: The effect of drought on bacterial communities in soil.
Drought leads to major abundance shifts in the composition of bacterial communities in soil. *Actinobacteria* (Gram-positive bacteria) are favoured by drought, while *Bacteroidetes* (Gram-negative ones) are sensitive to it. Other phyla – such as *Proteobacteria*, *Firmicutes*, *Acidobacteria*, and *Planctomycetes* – exhibit varying responses to drying of soil.

1.9 Molecular-ecology techniques used to assess the responses of microbial communities to environmental cues

As mentioned in the previous sections, soil represents a fascinating but challenging environment because of the complex and dynamic interaction of physical, biogeochemical, and biological factors. Molecular ecology provides the means to explore soil microbiology in a cultivation-independent manner, with various approaches being available depending on the research questions and objectives. The 'Omics' era provides us with the ability to directly analyse the microbial communities in soil, including dominant and rare members, and presents us with deep insights into the identity of not only the uncultured but also the hidden players in an environmental system. While metagenomics is an excellent approach to understand the structure and metabolic potential of microbial communities, it becomes limiting when the effect of a specific environmental factor is sought to be discovered. This is mainly because metagenomics and fingerprinting approaches are based on environmental DNA extracted from both viable and non-viable cells (Moran, 2010; Van Elsas and Boersma, 2011).

Alternatively, studies based on RNA provide a more precise picture of active microbial communities and their response to environmental changes including stress. Moreover, metatranscriptomics (RNA-Seq) is less prone to bias towards individual members of the microbial community because the technique uses random priming to generate cDNA libraries (Croucher and Thomson, 2010). The use of random hexamer primers allows us to simultaneously analyse the microbiome across all three domains of life and thus provides us

with insights into microbial communities (Croucher and Thomson, 2010). Metatranscriptomics ideally includes the analysis of both ribo-tags (SSU rRNA) and mRNA. Ribo-tags are used for identifying the taxonomic affiliations of the community-wide rRNA pool, while mRNA sequence datasets are used to understand functional gene expression, including a taxonomic source analysis of the transcripts.

1.10 Engineered systems (microcosms) to study environmental stress under controlled conditions

Soil is a heterogeneous environment with highly complex biological, physical, and biogeochemical processes. Obtaining conceptual data directly from field-sampling of a soil ecosystem is challenging, especially if one aims to study the effect of particular environmental factors on microbial communities in soil (Verhoef, 1996). Field-sampling may be suitable for understanding *in situ* microbial community structure; however, engineered soil microcosms are preferably used to understand the response of microbial communities to a defined factor or to study a specific biogeochemical process (Verhoef, 1996). It is also a well-known practice in microbial ecology to use highly reproducible systems, such as soil microcosms, in order to reduce the experiment to known variables. The general results obtained in such engineered microcosms may later be challenged and tested by analysing native, heterogeneous field samples that are defined by much higher complexity than engineered microcosms.

Paddy-soil microcosms planted with rice are more indicative of the actual processes occurring in the field than unplanted microcosms. The latter, however, have been successfully used as model systems to study the microbial communities in bulk and surface soil (Henckel et al., 2000; Lüdemann et al., 2000; Noll et al., 2005; Shrestha et al., 2007). Two types of unplanted microcosms are described in the literature. One type is incubated in the dark (Noll et al., 2005), while the other type is incubated under alternating dark and light cycles (Henckel et al., 2000). This second microcosm type is characterised by cyanobacterial growth on the surface layer, resulting in an oxygen profile different to that in unplanted microcosms incubated under dark conditions (Frenzel et al., 1992; Henckel et al., 2000).

1.11 Aim of the study and working hypothesis

Oxygen and moisture content are important regulators of diversity, structure, and functioning of microbial communities in soil (Lüdemann et al., 2000; Noll et al., 2005; Shrestha et al., 2009; Barnard et al., 2013; Bouskill et al., 2013; Evans et al., 2014; Kim and Liesack, 2015). The

effect of drought on grassland soil has been previously studied (Fierer and Schimel, 2002; Griffiths et al., 2003; Bapiri et al., 2010; Evans et al., 2011; Barnard et al., 2013; Bouskill et al., 2013). In paddy soil, studies until now have focused mainly on how drainage affects particular microbial guilds such as methanogens and methanotrophs (Henckel et al., 2000; Watanabe et al., 2009; Ma and Lu, 2011; Ma et al., 2012). Besides, most studies have used PCR-based amplification of the rRNA gene and transcripts, a methods approach that is prone to bias (Henckel et al., 2000; Watanabe et al., 2009; Ma and Lu, 2011; Ma et al., 2012; Breidenbach et al., 2015; Breidenbach and Conrad, 2015; Reim et al., 2017). Furthermore, the effect of drainage on the eukaryotic community in paddy soil has barely been addressed in previous papers. Moreover, a significant gap in knowledge exists regarding the impact of drainage on paddy-soil microbial communities involved in the degradation of plant bio-polymer and in their gene expression patterns. This calls for a large-scale study that targets the effects of drainage on the three domains of life and their functional profiles. Hence, this project is intended to assess how drainage and, consequently, oxygen and a low moisture content affect the activity, structure, and function of microbial communities in paddy soil, with a particular focus on plant bio-polymer breakdown.

To address the aims of my PhD study, the physical parameters of soil before and after drainage were measured; total RNA and DNA from flooded and drained samples were extracted; cDNA libraries for Illumina RNA-Seq, qPCR, and RT-qPCR assays were constructed; and a bioinformatics analysis pipeline for handling next-generation sequencing (NGS) data was set up. To mimic field conditions and simultaneously conduct a controlled experiment, the study was set up in soil microcosms and incubated under day and night cycles. The experiment was carried out for two pre-incubation periods of 7 days (short term) and 28 days (long term), followed by 9 days of drainage.

We expect that penetration of oxygen into the anoxic paddy soil will induce a drastic change in the active microbial community, leading to the revival of dormant groups. As a result, changes in functional gene expression will occur, particularly with regard to specific pathways such as methanogenesis and breakdown of plant bio-polymers. It is also anticipated that desiccation effects will modulate the development of a paddy-soil microbial community adapted to oxic and dry conditions.

2 Material and Methods

2.1 Materials

2.1.1 Soil sample

Paddy soil was provided by the Italian Rice Research Institute from a drained rice field in Vercelli (GPS coordinates 45°19′12.72″N, 8°25′6.959″E). The soil was collected in 2013. The characteristics of the Vercelli soil have previously been described (Christensen, 1986; Pump and Conrad, 2014).

2.1.2 Instruments used

Instruments	Manufacturer	City
Microx4 portable fiber-optic oxygen meter	Presences	Regensburg, Germany
Redox platinum electrode with an Ag/AgCl reference electrode	Ecotech	Bonn, Germany
WP4C - a Chilled Mirror dew point hygrometer	Decagon Devices	Pullman, USA
T5x tensiometer	Decagon Devices	Pullman, USA
GC-8A gas chromatograph	Shimadzu	Duisburg, Germany
FastPrep®-24 bead beater	MP Biomedicals	California, USA
NanoDrop® ND-1000 UV-Vis spectrophotometry	NanoDrop Tech. Inc.	USA
Qubit® 2.0 Fluorometer	Invitrogen	California, USA
Experion automated electrophoresis system	Bio-Rad	Hercules, USA
C1000 Touch™ Thermal Cycler	Bio-Rad	Hercules, USA
Magnetic stand	Invitrogen	California, USA
CFX Connect Real-Time PCR detection system	Bio-Rad, USA	Hercules, USA

2.1.3 Chemicals and reagents

Items	Manufacturer	City
Absolve™	PerkinElmer	Boston, USA
DEPC-treated water	Ambion	Austin, USA
Tris-HCl	Sigma	Steinheim, Germany
Polyvinylpyrrolidone K25	Fluka	Buchs, Switzerland
Water-saturated phenol (pH 8.0)	Carl Roth	Karlsruhe, Germany
Phenol-chloroform-isoamyl alcohol (pH 8.0)	Carl Roth	Karlsruhe, Germany
Chloroform-isoamyl alcohol [24:1 (v/v)]	Carl Roth	Karlsruhe, Germany
Magnesium chloride ($MgCl_2$)	Carl Roth	Karlsruhe, Germany
Sodium acetate ($C_2H_3NaO_2$)	Sigma	Steinheim, Germany
Isopropanol	Carl Roth	Karlsruhe, Germany
Ethanol (Nuclease-free)	Applichem	Darmstadt, Germany
RNase-free TE buffer	Applichem	Darmstadt, Germany
Sodium Chloride (NaCl)	Carl Roth	Karlsruhe, Germany
Glass beads (0.17-0.18 mm)	Sartorius	Goettingen, Germany
Sodium hydroxide (NaOH) solution (10M)	Sigma	Buchs, Switzerland
SeaKem Agrose	Lonza	Basel, Switzerland

2.1.4 Kits

Items	Manufacturer	City
FastDNA® SPIN kit for soil	MP Biomedicals	California, USA
Turbo™ DNase	Ambion	Austin, USA
RNasin® Ribonuclease Inhibitor	Promega	Madison, USA
RNA Clean & Concentrator™-5	Zymo Research	California, USA
Qubit® RNA assay kit	Invitrogen	California, USA
Qubit® DNA assay kit	Invitrogen	California, USA
Experion™ RNA HighSens Analysis Kit	Bio-Rad	Hercules, USA
Experion™ DNA 12K HighSens Analysis Kit	Bio-Rad	Hercules, USA
DNA Smart Ladder	Eurogentec	Seraing, Belgium
GoScript Reverse Transcription System and random primers	Promega	Madison, USA
Oligonucleotides (primers)	Eurofins	Constance, Germany
Sybr Green kit	Sigma-Aldrich	Missouri, USA
NEBNext® Ultra™ Directional RNA Library Prep Kit for Illumina	New England Biolabs	Ipswich, USA
AMPure XP Beads	New England Biolabs	Ipswich, USA

2.2 Methods

2.2.1 Microcosm preparation, incubation, and drainage

Air-dried paddy soil (stored at room temperature) was crushed and sieved using a 2-mm mesh size. The dry, crushed and sieved soil was thoroughly mixed with grinded rice straw (500 g soil + 6.25 g rice straw). The soil/rice-straw mix was then used to fill a polyethylene plant pot (8 × 8.5 × 10.5 cm). Soil slurries were prepared by adding 500 ml deionized water. **Figure 2.1** shows an overview of the experimental design. Microcosms were submerged in a water-filled container to maintain floodwater at a constant level (Henckel et al., 2000) (**Figure 2.2**).

Incubation was done under greenhouse conditions with day/night cycles in summer 2015. 6 soil microcosms were incubated for 7 days (short-term) and another set of 8 soil microcosms were incubated for 28 days (long-term). Upon incubation, 9 day drainage was applied for half of the microcosms. Drainage microcosms were drained through 8 holes in the bottom of the polyethylene plant pots (3 mm in diameter). During the drainage period, we lost 1 of the polyethylene pots from the 28-day pre-incubated pots. Long-term incubation was set to 28 days because it is known that the most easily degradable polymer substances are utilized after 4 weeks of incubation, thereby leading to a stable community driven by polymer hydrolysis as the rate-limiting step for activity. Short-term incubation was set to 7 days because it marks the onset of methanogenesis (Wegner and Liesack, 2016). Except for section 3.8, I only present results of the long-term incubation experiment in my thesis because the focus of the thesis is to show the effect of drainage after 28-day pre-incubation as an approximation to field conditions. In addition the 7-day pre-incubation experiment was done to show the deferential effect of pre-incubation time with drainage.

2.2.2 Sampling

Upon incubation and drainage, microcosms were destructively sampled using inverted syringes for soil-core sampling. One core (3.8 cm in diameter) was used for nucleic acid extraction and another core (3.8 cm in diameter) was stored at -80°C. Upon sampling, cores were immediately cut into1-cm depth sections. The 1-2 cm depth sections were later used for extraction of nucleic acids. The 1-2 cm section was aliquoted into 2-ml tubes (0.5 g per tube). Tubes were then shock-frozen in liquid nitrogen. Cores used for storage were immediately shock-frozen (**Figure 2.2 C**). A 2-cm core depth for molecular analysis was selected to ensure anoxic condition for the control treatment under flooded conditions (Noll et al., 2005).

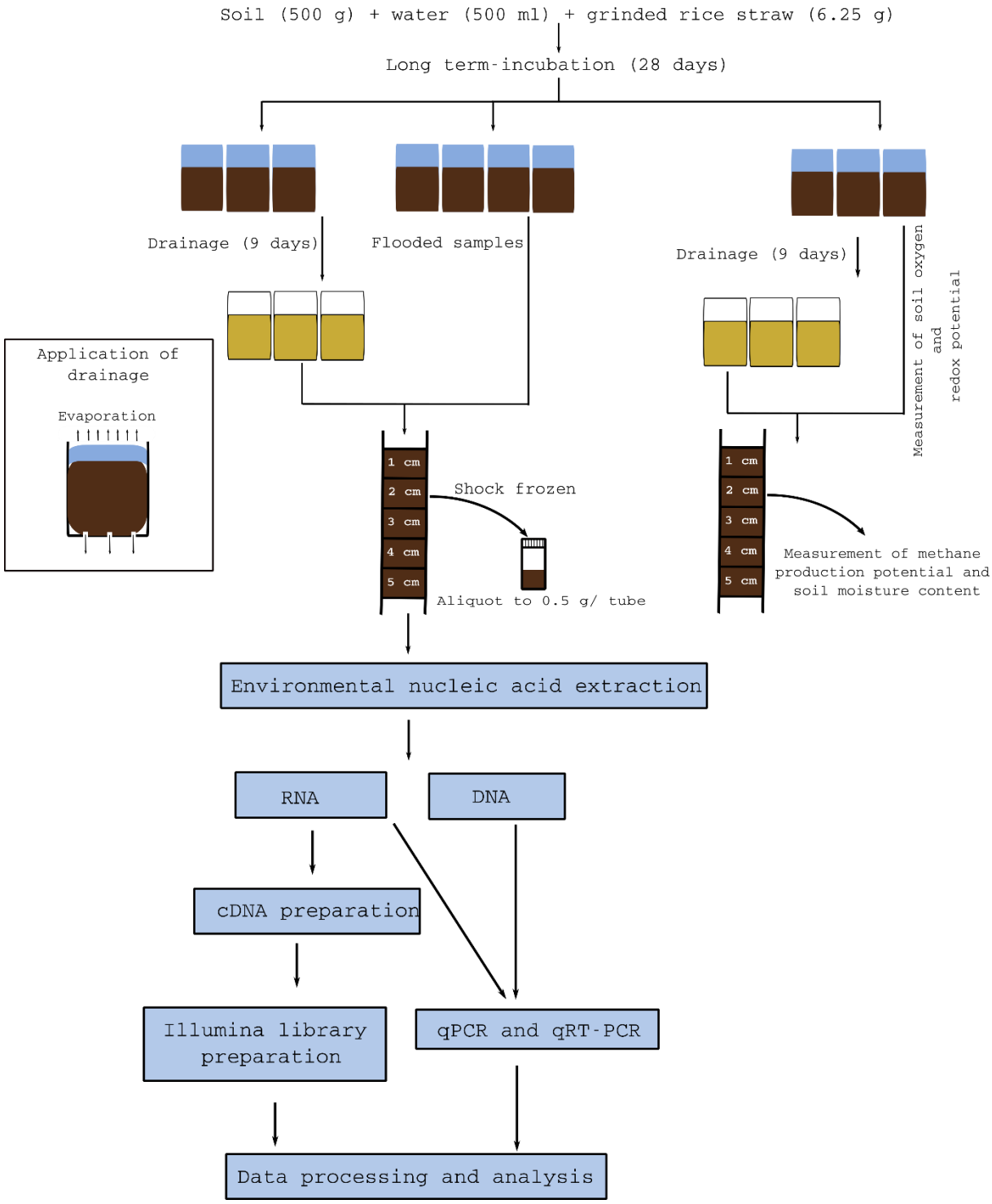

Figure 2.1: Overview of the experimental design for 28 day flooding followed by drainage. The same experimental setup was used for 7-day flooding followed by drainage, with the exception that three flooded microcosms were used for molecular analysis.

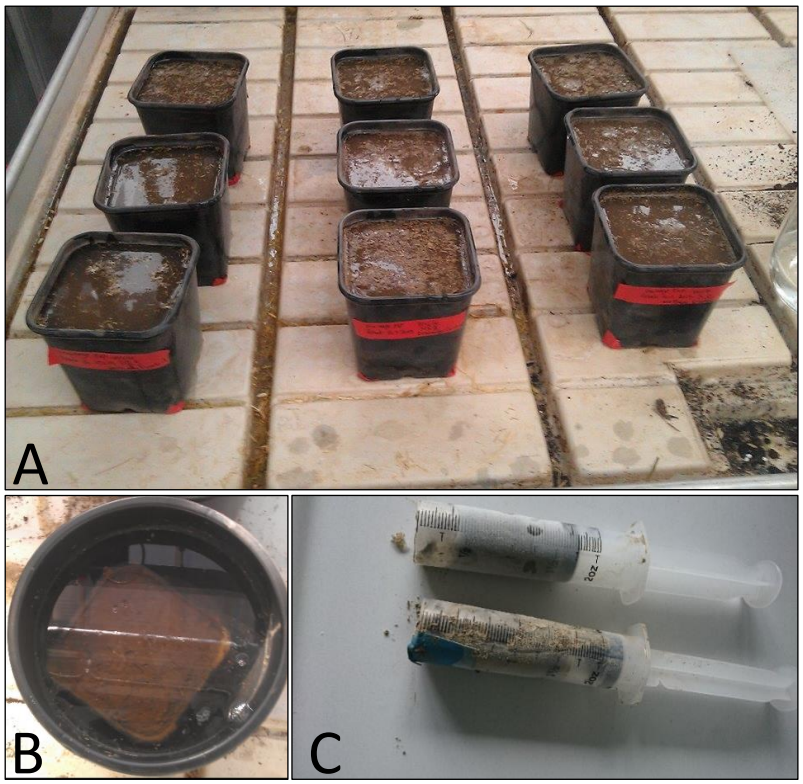

Figure 2.2: Microcosm preparation and soil-core sampling using 5-ml inverted syringes.
A) Soil slurry microcosms in polyethylene plant pots. B) Submerged microcosm in a water-filled container. C) Two soil cores shock-frozen in liquid nitrogen.

2.2.3 Measurement of soil physical and chemical parameters

Two separate sets of three soil microcosms (one each for short-term and long-term incubation) were used for the measurement of soil physical and chemical parameters. During drainage period, the oxygen concentration was determined using the Microx4 device, which is a portable fiber-optic oxygen meter connected to an optical oxygen probe (Presences). In addition, the soil redox potential was measured using a platinum rod with an Ag/AgCl reference electrode (Ecotech). One core (2.9 cm in diameter) was used to determine the gravimetric soil moisture content. Soil moisture content was calculated based on the gravimetric method (120°C overnight) (Christensen, 1986). One gram of soil was used to determine the gravimetric moisture content of each sample. After 9 day drainage, the soil water potential was determined using the WP4C device - a Chilled Mirror dew point hygrometer - and a T5x tensiometer (Decagon Devices). One core (2.9 cm diameter) was used to analyse methane production potential. Methane production potential was determined using the 1-2 cm depth sections. The soil section was transferred into 120 ml serum bottles and incubated under N_2 for 2 days. Over the two days, a total of five methane measurements were done: after 14, 20, 28, 40, and 48

hours of incubation. Methane production potential (µmol h^{-1}) was calculated by linear regression analysis of the methane concentrations over time. Rates were then divided by the dry weight of the soil section (µmol h^{-1} gdw^{-1}). Methane concentrations were measured using a GC-8A gas chromatograph (Shimadzu) containing a Hayeseq Q column. Data were analysed with PeakSimple software (SRI Instruments).

2.2.4 DNA and total RNA extraction and quality assessment

Environmental DNA was extracted from 0.5 g soil (wet weight) of each replicate sample, from both flooded and drained soil. The extraction of DNA was done with the FastDNA® SPIN kit for soil (MP Biomedicals) according to the manufacturer`s instructions. DNA concentrations were measured using the Qubit® DNA assay kit (Invitrogen).

RNA was extracted from 1.5 g flooded soil (wet weight) and 3 g drained soil (wet weight) of each replicate sample. Prior to RNA extraction, all plastic and glassware were made RNase free. Pipettes and working bench were treated with 2 % Absolve. Total RNA extraction was done according to Mettel et al. (2010), with the modification that high pH buffers (7.5) were used. In order to remove DNA and RNases, the RNA extracts were incubated with 5 U Turbo™ DNase (Ambion), 1x DNase buffer and 10 U RNasin® RNase inhibitor (Promega) for 30 min at 37 °C. Finally, another round of incubation (30 min) with Turbo™ DNase was performed (Mettel et al., 2010).

RNA quality was checked using UV absorbance at 400 nm (A_{400}) with NanoDrop ND-1000. A sample having an A_{400} value of less than 0.03 was considered good-quality, humic-acid-free RNA. RNA integrity was assessed on a 1 % agarose gel. The RNA concentration was quantified by the Qubit® RNA assay kit (Invitrogen).

2.2.5 cDNA synthesis and Illumina sequencing

Total RNA was converted into cDNA immediately upon extraction. Total RNA (~100 ng) was fragmented and reverse transcribed into cDNA by random priming using the NEBNext® Ultra™ Directional RNA Library Prep Kit for Illumina (New England Biolabs) according to the manufacturer`s protocol with few modifications. Modifications were as follow: (i) fragmentation was done for 8 min instead of 10 min; and (ii) conditions for cDNA size selection were adjusted to 42.5 µl bead volume in the first bead selection and 20 µl for the second bead selection. Appropriate cDNA size distribution was checked by the Experion™ DNA 12K

HighSens Analysis Kit (Bio-Rad) according to the manufacturer´s protocol. The final library size ranged from 300 to 550 bp (~ 200 to 490 bp insert size). cDNA concentration of each library was determined using Qubit® DNA assay kit (Invitrogen). In total, seven cDNA libraries were constructed from the 28-day pre-incubation experiment, with 4 independent replicate samples of the flooded soil and 3 independent replicate samples of the drained soil. Six cDNA libraries were constructed from the 7-day pre-incubation experiment, with 3 independent replicate samples of each flooded and drained soils. The cDNA libraries were mixed in equal molar ratio and sequenced on an Illumina HiSeq 2500 platform in paired-end mode (2 × 250 bp) at the Max Planck Genome Centre Cologne (Germany).

cDNA for RT-qPCR was prepared by random priming using the GoScript Reverse Transcription kit (Promega) according to the manufacturer`s protocol. Aliquots of total RNA (~100 ng per reaction) were used as the starting material in RT-qPCR. Single-stranded cDNA concentrations were measured with NanoDrop ND-1000.

2.2.6 qPCR and RT-qPCR

Gene (qPCR) and transcript (RT-qPCR) numbers of the bacterial and archaeal small subunit (SSU) rRNA were quantified using previously described SybrGreen-based assays (Stubner, 2004; Kemnitz et al., 2005; Wegner and Liesack, 2016). In addition, gene and transcript numbers of the methyl-coenzyme M reductase subunit alpha (*mcrA*) were determined (Steinberg and Regan, 2009). Fungal SSU rRNA genes and transcripts were quantified using the primer pair FR1/FF390 (Vainio and Hantula, 2000). Calibration curves for bacterial, archaeal and fungal SSU rRNA were constructed using DNA of the following reference organisms: *Escherichia coli* (genomic DNA, 10 to 10^9 copies); *Methanosarcina barkeri* (PCR amplicon, 7 to 7×10^8 copies); and *Ustilago maydis* (genomic DNA, 10^4 to 10^8 copies). The calibration curve (30 to 3×10^5 copies) for *mcrA* quantification was based on a *mcrA* fragment cloned into the pGEM®-T Easy plasmid (Promega, WI, USA). The *mcrA* fragment used for PCR-cloning was amplified from genomic DNA with the primer set mlas and mcrA-rev (Steinberg and Regan, 2009). qPCR and RT-qPCR were carried out using a CFX Connect Real-Time PCR detection system (Bio-Rad). The PCR efficiency was at least 80% ($R^2 > 0.98$). Melt curve analysis was used to check for the possible presence of unspecific products.

2.2.7 Computational analysis

2.2.7.1 Demultiplexing and quality control

All programs applied for demuliplexing and quality control are open source software and used in a stand-alone version installed on our Linux servers. Barcode and primer sequences were trimmed from raw sequences using fastq-mcf (Aronesty, 2011). Next, forward and reverse reads were merged using PEAR- Paired-End reAd mergeR software package (version v0.9.8) (Zhang et al., 2014). The quality of Illumina paired-end reads was checked using fastq filter (Usearch version 7) with one as the expected number of errors (Edgar, 2010). Paired-end reads passed the quality control if the following criteria were met: (i) ambiguous bases (N) ≤ 1% and read length ≥ 180 bp.

2.2.7.2 Extraction of SSU rRNA and mRNA datasets

The software SortMeRNA version 2.0 was used to specifically extract SSU rRNA and mRNA reads from the total sequence datasets (Kopylova et al., 2012). SortMeRNA was applied twice. In the first round, SSU rRNA reads were specifically filtered. In the second round, large subunit (LSU) rRNA reads were filtered. The remaining dataset was considered putative mRNA. SSU rRNA and mRNA reads were further processed. Paired-end reads were used for downstream analysis if the read lengths were ≥ 250 bp (SSU rRNA) and ≥ 180 bp (mRNA).

2.2.7.3 Diversity analyses

SSU rRNA reads used for downstream analysis were grouped into Operational Taxonomic Units (OTUs) to determine the diversity indices of the samples. OTU clustering was performed using Uclust, 0.95 identity threshold, and was guided by a tree based on the SSU rRNA Silva 123 database (Quast et al., 2013). Alpha and beta diversity were calculated using samples normalized to a sequencing depth of 150,000. The calculation was done by applying scripts in the "Quantitative Insights Into Microbial Ecology" package (Caporaso et al., 2010). Differences in the beta-diversity patterns between the 7-day and 28-day pre-incubation periods under flooded conditions were visualized by principle coordinate analysis (PCoA) using Bray-Curtis dissimilarity matrices deduced from SUU rRNA-based taxonomic assignment of OTUs.

2.2.7.4 Analysis of SSU rRNA reads

SSU rRNA was used as a marker to understand the compositional changes in the active microbial community between flooded and drained conditions. Quality-filtered SSU rRNA

reads were processed using a workflow of scripts employed in QIIME (version 1.9.1) (Caporaso et al., 2010). SSU rRNA reads were clustered into OTUs using Uclust and 0.95 identity threshold (Caporaso et al., 2010; Edgar, 2010). Taxonomic assignment of OTUs was done using SILVA 123 database and the RDP classifier at a confidence threshold of 95% (Wang et al., 2007; Quast et al., 2013). In addition, downstream processing involved the following criteria: (i) removal of OTUs containing only a single read (singletons) and (ii) OTUs had to be detected in at least three independent replicate samples. OTUs analysis was done on different taxonomic ranks: phylum, class, family and genus level for bacteria and archaea; and on super-group and phylum level for eukarya.

2.2.7.5 Analysis of mRNA transcripts

2.2.7.5.1 Taxonomic classification of mRNA

Putative mRNA sequences were queried against the non-redundant protein database (nr; year 2017) using Ublast software (Usearch version 7) (Edgar, 2010). Local Ublast involved the following criteria: E-value of e-2 and 50 hits maximum accept. The resulting tabular outputs were then processed using MEGAN v6 (Ultimate Edition) software (Huson et al., 2016). Taxonomic assignment was based on the lowest common ancestor (LCA) approach with a minimum bit score of 50 and the top 10% hits. Taxonomic analysis was done using the normalized reads option in MEGAN.

2.2.7.5.2 Functional annotation of mRNA

Functional annotation was done by mapping the BLAST output to the "Kyoto Encyclopedia of Genes and Genomes" (KEGG) database (November 2016). KEGG levels 2, 3 (KEGG pathway) and KEGG 4 (KEGG genes) were used in this analysis. Functional annotation was done using the normalized reads option in MEGAN.

Taxonomic classification of mRNA affiliated with a functional category was performed by extracting the mRNA sequences involved in this category into a new MEGAN6 file. Then this mRNA sequence dataset was analysed as in section 2.2.7.5.1.

2.2.7.5.3 Carbohydrate-active enzymes

The DataBase for automated Carbohydrate-active enzyme ANnotation (dbCAN) (June 2016) (Yin et al. 2012) was used to categorize mRNA transcripts encoding carbohydrate-active enzymes (CAZymes). The quality-filtered mRNA datasets were queried against the dbCAN

database using a local Ublast sequence similarity search and a minimum E-value of e-5. The best hit for each mRNA sequence was considered as the CAZymes` functional annotation. Taxonomic classification of mRNA transcripts annotated as CAZymes was done using MEGAN v6 following the same approach as used for taxonomic assignment of total mRNA sequences (section 2.2.7.5.1).

2.2.8 Analysis of differential drainage effects

Differential drainage effects between the short-term (7 days) and long-term (28 days) pre-incubation periods were analysed using the package DESeq2 (Love et al., 2014). On rRNA level, the comparison was done between a merged flooded soils dataset (7 and 28-day pre-incubation) and a merged drained soils dataset (7 and 28-day pre-incubation followed by drainage). Additionally, drained soils after either 7-day or 28-day pre-incubation period were comparatively analysed. Comparison of the taxonomic composition was performed using a DESeq2 script employed in QIIME on the rRNA OTUs matrix generated from section 2.2.7.4. Taxa that had less than ten mean normalized count and P value ≤ 0.05 were discarded from the analysis. The functional profiles of the flooded and drained datasets were compared using the DESeq2 employed in the MicrobiomeAnalyst (http://www.microbiomeanalyst.ca/) web server on the mRNA transcripts KEGG level 4 functional annotation profiles (Dhariwal et al., 2017). MicrobiomeAnalyst was also used to generate PCoA plot (beta-diversity) using the Bray-Curtis dissimilarity matrices and the heatmap based on the mRNA transcripts KEGG level 4 functional annotation.

2.2.9 Statistical analysis and figures generation

Welch's t-test was applied to assess whether diversity indices, qPCR and RT-qPCR data significantly ($P \leq 0.05$) differed between flooded and drained soils (Welch, 1947). Datasets generated in the course of this study were checked for significant differences between flooded and drained conditions using STAMP software with White's non-parametric t-test and Storey false discovery rate (FDR) multiple test correction (White et al., 2009). A taxon or a functional category with a corrected P value ≤ 0.1 was considered significantly different between the two experimental treatments unless stated otherwise in the figure legend. Dot-plots, box-polts and bar-graphs were generated using the software sigma-plot 12.5, while PCoA plots were generated using the MicrobiomeAnalyst webserver, and QIIME. The colours and fonts of the graphical visualizations were modified using Inkscape.

3 Results

3.1 Soil physical and chemical parameters

Soil physical and chemical parameters were measured across the drainage period for oxygen, redox potential, soil gravimetric moisture content, and temperature. Soil water potential was measured only at the end of the drainage period. The flooded soil was characterized by suboxic conditions (~1.68 µmol/l), a redox potential of -184±9, and a temperature of 29 °C (**Table 3.1**). After nine-day drainage, the oxygen concentration was increased to 240 µmol/l. Concurrently, the redox potential was increased to 421±8 mV (**Table 3.1, Figure S1**). The gravimetric moisture content decreased during drainage to ~ 11%. Correspondingly, the water potential decreased to -0.875±0.150 MPa (**Table 3.1**). The methane production potential of the flooded soil was 0.53 µmol h^{-1} gdw^{-1}.

Table 3.1: *Physical and chemical parameters of the soil before and after nine-day drainage* [1]

Parameters	***Flooded***	***Drainage***
Oxygen (µmol/l)	1.68±0.3	240.5±5.3
Temperature (◦C)	29.2±0.85	28.175±0.9
Redox (mV)	-184±9	421±8.3
Water potential (Kpa)	0.3±0.2	-875±150
Moisture content % (w/w)	121.3±8.5	11.5±1
Methane production potential (µmol h^{-1} gdw^{-1})	0.53±0.08	0

[1] Pre-incubation under flooded conditions for 28 days prior to 9-day drainage

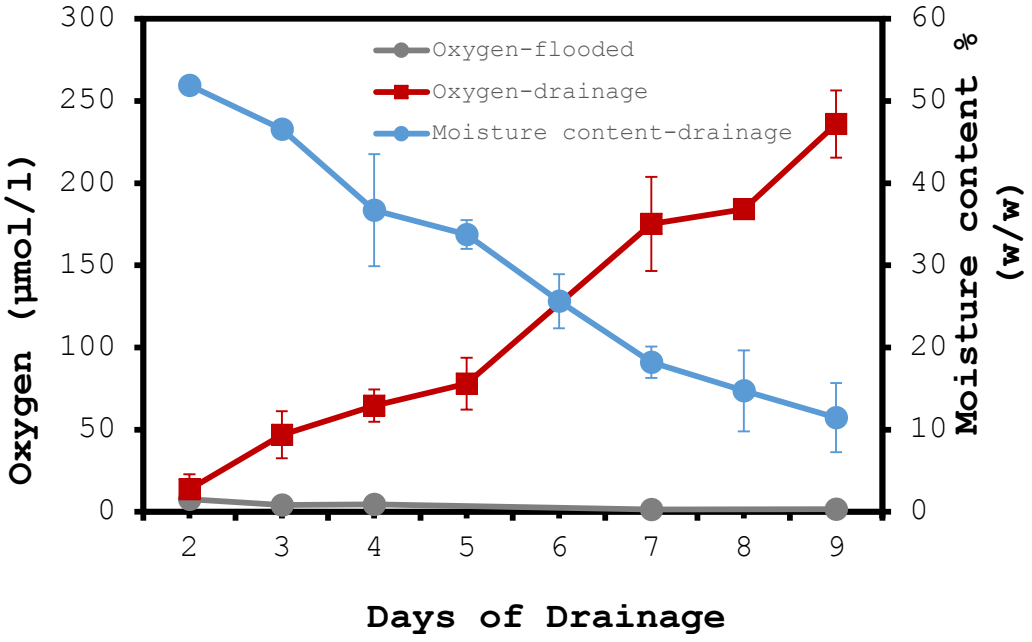

Figure 3.1 : Oxygen and gravimetric moisture content profiles.
The graph shows the profiles of oxygen and gravimetric moisture content across 9 days of drainage and, in addition, the oxygen profile of the flooded soil. Oxygen profile is shown on y_1 axis and gravimetric moisture content on the y_2 axis. Standard deviation is based on three biological replicates.

3.2 Sampling, extraction and purification of total RNA

Samples from both flooded and drained soils were collected for extraction of total RNA. **Figure 2.2 (C)** shows sampled and shock-frozen soil cores. Neutral pH (pH 7) extraction resulted in pure RNA characterized by low humic acids content. Ultraviolet (UV) absorbance values are indicated in **Table 3.2**. The values showed that no further Q-Sepharose column purification was required. RNA integrity was checked by 1% agarose gel electrophoresis. The concentration of total RNA per g dry weight of soil is shown in **Table 3.2**.

Table 3.2: *RNA concentration per g dry weight of soil* [1]

Treatment	*Sample*	*RNA (µg/g dry weight)*	*UV absorbance at 400 nm*	*RNA Integrity*
Flooded	**28F1**	2.816	0.014	Intact
	28F2	5.854	0.010	Intact
	28F3	1.404	0.012	Intact
	28F4	2.438	0.011	Intact
Drained	**28F9D1**	1.169	0.007	Intact
	28F9D2	1.021	0.010	Intact
	28F9D 3	2.963	0.009	Intact

[1] Pre-incubation under flooded conditions for 28 days prior to 9-day drainage

3.3 Absolute abundance of *Bacteria*, *Archaea*, and *Fungi*

The absolute abundance of bacteria, archaea, and fungi was determined by qPCR (total DNA) and RT-qPCR (total RNA). The qPCR assay was used to calculate SSU gene copy numbers as a proxy for cell biomass, while RT-qPCR was used to calculate copy numbers of SSU rRNA as a proxy for metabolic activity. Drainage significantly decreased the number of bacterial SSU rRNA gene copies, but no significant difference in bacterial SSU rRNA transcript numbers was observed between flooded and drained soils (**Figure 3.2, Table S1**). The numbers of archaeal SSU rRNA transcripts did not significantly change with drainage (**Figure 3.2**). Fungal SSU rRNA genes significantly increased, while fungal SSU rRNA had near significant increase ($P \leq 0.06$) (**Figure 3.2, Table S1**).

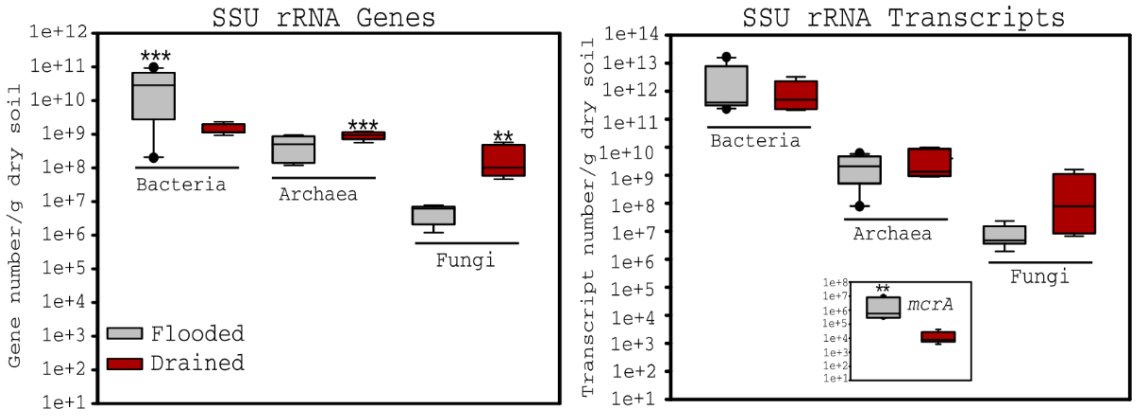

Figure 3.2: SSU rRNA gene and transcript numbers of bacteria, archaea, and fungi.
Box plots show the number of bacterial, archaeal, and fungal SSU genes (top) and transcripts (bottom) per g dry weight of soil. The transcript numbers of the *mcrA* gene are shown in the inset. Asterisks ** ($P \leq 0.05$) and *** ($P \leq 0.01$) indicate significant difference between flooded and drained soils.

3.4 cDNA synthesis for Illumina RNA-Seq

Total RNA from flooded and drained soils was used to prepare double-stranded cDNA libraries for Illumina RNA-Seq. Removal of cDNA fragments smaller than 300 bp was done using AMpure beads (New England Biolabs). Size-separated cDNA fragments ranged in size from 300 to 600 bp (**Figure 3.3**). The Illumina HighSeq 2500 (2 x 250 bp) platform was used for metatranscriptomic sequencing.

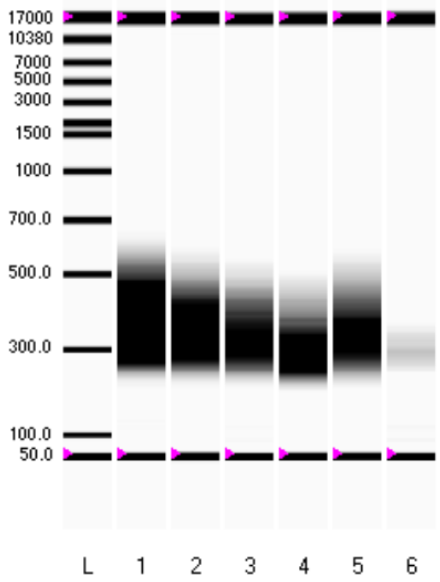

Figure 3.3*:* Size distribution of cDNA libraries analysed by the Experion automated electrophoresis system.
Lane L: Experion DNA ladder. Lanes 1 to 3: Replicate samples from drained soils; lane 1, 28F9D1; lane 2, 28F9D2; lane 3, 28F9D3. Lanes 4 to 6: Replicate samples from flooded soils; lane 4, 28F1, lane 5, 28F2, lane 6 28F3.

3.5 Sequencing statistics of Illumina RNA-Seq

The number of raw reads ranged from 6,267,294 to 19,299,651 reads per library (**Table 3.3**). The reads were grouped into sample-specific datasets based on multiplex identifiers. On average, 99 % of forward and reverse reads were assembled. 74% and 73% of the assembled reads passed the quality control with an average read length of 250 bp from the flooded and drained soils, respectively (**Table 3.3**). The SSU rRNA reads represented around 44% of the total RNA. The SSU rRNA datasets used for downstream analysis had an average read length of 300 bp. The number of SSU rRNA reads used for downstream analysis ranged from 985,030 (sample 28F9D3) to 7,009,347 (sample 28F1) (**Table 3.3**). LSU rRNA reads made ~54% of total RNA (data not shown). Putative mRNA ratio to total RNA was 1.7% and 2% for the flooded and the drained soils, respectively (**Table 3.3**). On average, 47% of the flooded soil and 67% of the drained soil putative mRNA transcripts had a hit to the NCBI (GenBank) nr database, 97% of these reads had taxonomic assignment (**Table 3.4**). The proportion of mRNA transcripts with nr hits that could be functionally annotated was as low as 38.5% and 36.3% for flooded and drained soils, respectively.

Table 3.3: *General statistics of the metatranscriptome libraries from flooded (28F) and drained (28F9D) samples*

Conditions	***Replicates***	***Raw reads***	***Assembled reads***	***Passed QC reads***		***SSU rRNA*** [1]		***SSU rRNA*** [2]	***Putative mRNA transcripts*** [1]	
Average read length				260 bp		260 bp		300 bp	260 bp	
Flooded	**28F1**	19,299,651	99.5 %	16,118,003	83 %	7,009,347	43.4 %	3,970,349	340,390	2.1%
	28F2	17,374,064	99.5 %	11,287,872	65 %	5,265,992	46.6 %	1,923,643	199,713	1.8%
	28F3	13,079,226	99.2 %	10,243,215	78.3 %	4,436,637	43.4 %	2,144,992	123,011	1.2%
	28F4	13,079,226	99.2 %	10,020,886	71.9%	4,201,560	41.9 %	1,541,602	150,869	1.5%
Average		15,708,042	99.2 ± 0.3%	11,917,494	74.6±8 %	5,228,384	43.8±2%	2,395,147	203,496	1.7 ± 0.4%
Drainage	**28F9D1**	9,656,112	99.4 %	6,368,767	65.9 %	2,889,797	45.3 %	1,420,367	149,101	2.3 %
	28F9D2	6,436,509	99.5 %	4,759,434	73.9 %	2,138,327	44.9 %	1,125,184	86,864	1.8 %
	28F9D3	6,267,294	98.8 %	4,970,126	79.3 %	2,331,977	46.9 %	985,030	98,926	2.0 %
Average		7,453,305	99.2± 0.4%	5,366,109	73±6 %	2,453,367	45.7±1%	1,176,860	111,630	2 ± 0.3%

[1] Relative abundance of SSU rRNA and mRNA calculated based on the number of reads that passed quality control.
[2] The dataset of SSU rRNA reads used for downstream analysis (diversity indices and taxonomic composition).

Table 3.4: *Sequencing statistics of putative mRNA from flooded (28F) and drained (28F9D) samples*

Conditions	*Replicates*	*Reads assigned to mRNA*	*% processed reads* [1]	*Reads with NCBI nr hit*	*% assigned* [2]	*Phylum*	*% assigned* [3]	*KEGG (functional annotation)*	*% assigned* [4]
Flooded	**28F1**	340,390	2.1	136,639	40.1	133,045	97.3	50,684	37
	28F2	199,713	1.8	97,634	48.8	94,727	97	40,681	41
	28F3	123,011	1.2	72,353	58.8	70,383	97.2	28,229	39
	28F4	150,869	1.5	60,699	40.2	58,712	96.7	22, 005	37
Average		203,496	1.7 ± 0.4	91,831	47± 8.8	89,217	97± 0.2	39,865	38.5± 1.9
Drainage	**28F9D1**	149,101	2.3	97,267	65.2	94,266	96.9	35,605	36.6
	28F9D2	86,864	2	57,659	66.3	55,906	96.9	21,139	36.6
	28F9D3	98,926	1.5	68,669	69.4	66,706	97.1	24,646	35.8
Average		111,630	2 ± 0.3	74,532	67± 2.1	72,292.7	97± 0.1	27,130.0	36.3± 0.4

[1] Percentage of putative mRNA reads in processed reads (mRNA to total RNA ratio) calculated by eliminating rRNA and non-coding small RNA using SortMeRNA
[2] Total numbers of mRNA reads that had a homolog in NCBI (GenBank) nr database using BLASTx (e-value cut-off of 1e-5).mRNA reads with NCBI (GenBank) nr hits were subjected to taxonomic assignment using MEGAN 6
[3] Percentage of mRNA reads that could be assigned on phylum level
[4] Among mRNA reads with NCBI (GenBank) nr hits, the percentage of reads that could be functionally annotated to KEGG

3.6 Effect of drainage on the microbial community composition

3.6.1 Microbial diversity and richness

SSU rRNA reads were grouped into OTUs to determine the diversity indices of flooded and drained samples. Rarefaction curves showed that flooded soils contained between 46,436 to 61,231 OTUs, while drained soils had between 50,455 and 54,096 OTUs. The OTU numbers are based on random selection of 150,000 SSU rRNA reads per replicate sample (**Figure 3.4**). Communities' evenness and diversity were measured by Simpson and Shannon indices. They indicated that the microbial community in drained soil is slightly less diverse than in flooded soil (**Table 3.5).**

Table 3.5: *Alpha-diversity indices*

Indices [1]	28F1	28F2	28F3	28F4	28F9D1	28F9D2	28F9D3	Flooded (Average)	Drainage (Average)
Simpson	0.9998	0.9998	0.9999	0.9999	0.9997	0.9997	0.9998	0.9998	0.9997
Shannon	14.3	14.1	14.8	14.9	14.2	14.3	14.5	14.54	14.31
Chao1	132451	108989	137812	152307	118667	124680	127226	132890	123524
Observed OTUs	52483	46435	58452	61231	50455	51782	54096	54651	52111

[1] Diversity indices are calculated based on random subsampling of 150,000 SSU rRNA reads

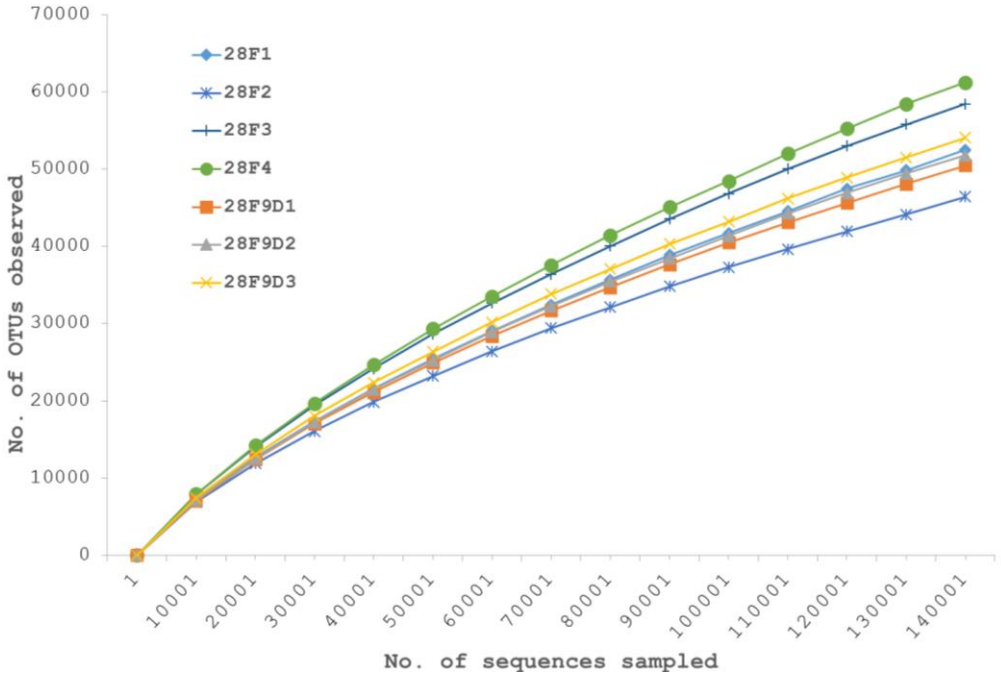

Figure 3.4: Microbial diversity in flooded and drained soils.
The graph shows the rarefaction curve of each replicate sample. The rarefaction curves are based on the number of OTUs observed by random sampling of 150,000 SSU rRNA reads at 95 % sequence similarity.

3.6.2 Drainage effects on domain level (*Bacteria, Archaea,* and *Eukarya*)

Taxonomic assignment of SSU rRNA and mRNA was performed to elucidate the effect of drainage on the three domains of life. Drainage did not affect the relative abundance of bacterial and archaeal SSU rRNA (**Figure 3.5**). Eukarya SSU rRNA abundance increased with drainage, but this was not supported by statistical significance (**Figure 3.5**). On mRNA level, bacterial abundance increased from 85.4% to 93.8% but archaeal abundance decreased significantly from 8.3% to 1.9 % (P [FDR] < 0.01) with drainage (**Figure 3.5**).

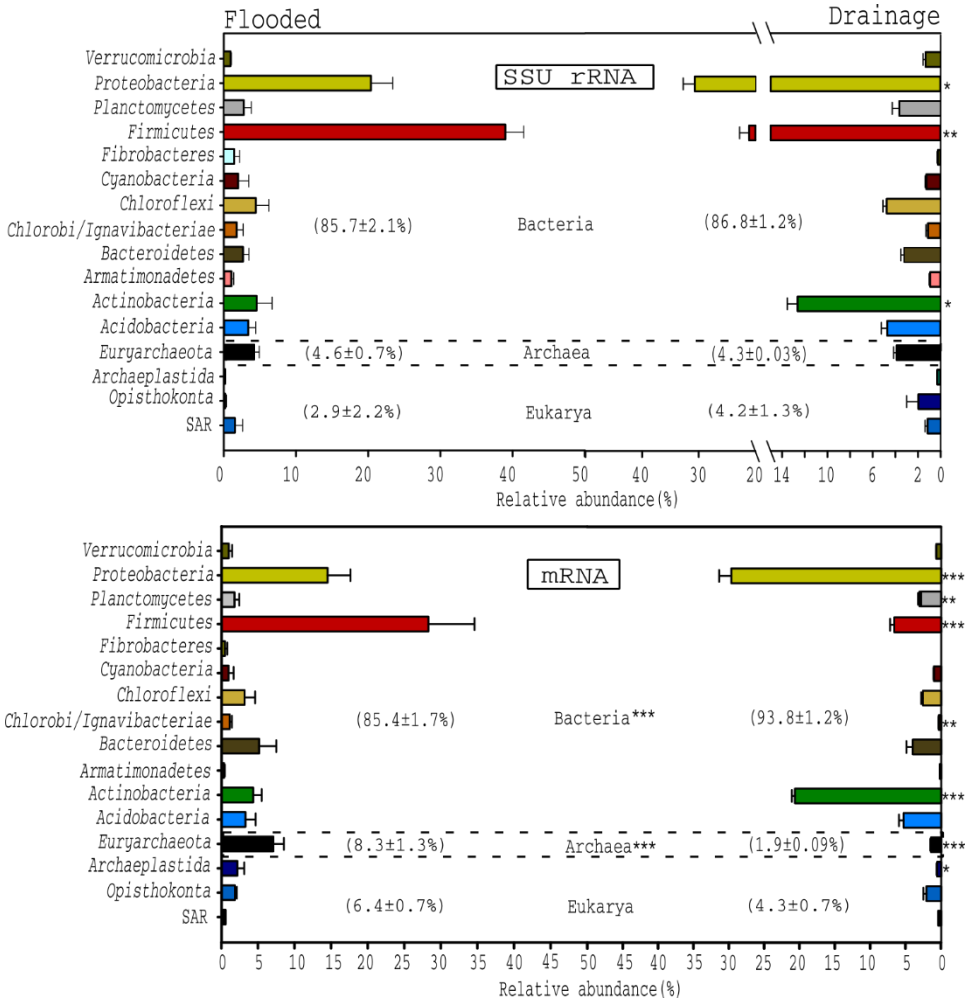

Figure 3.5: Community-wide response to drainage on phylum level (bacteria, archaea) and super-group level (eukarya)**.**
Taxon-specific abundances relate to the community-wide SSU rRNA and mRNA datasets. Taxa > 1 % relative SSU rRNA and/or mRNA abundance(s) are shown. Asterisks * ($P \leq 0.1$), ** ($P \leq 0.05$) and *** ($P \leq 0.01$) indicate significant difference between flooded and drained soils. P values are FDR corrected.

3.6.3 Effect of drainage on bacterial community composition

Among bacteria, *Firmicutes* was the most abundant phylum in flooded soil. The *Firmicutes* phylum was negatively affected by drainage with a decrease in relative SSU rRNA abundance from 39% to 21%. The decrease in *Firmicutes* mRNA abundance was even more pronounced; from 28% to 6.5% (**Figure 3.5, Figure S2**). The relative abundance of the *Firmicutes* families – *Ruminococcaceae* and *Lachnospiraceae*-were signifcantly higher in flooded soil than in drained soil; on both SSU rRNA (P [FDR] ≤ 0.1) and mRNA levels (P [FDR] ≤ 0.05) (**Figure 3.6, Figure S3**). The families *Clostridiaceae*, and *Bacillaceae* were signifcantly higher in flooded soil than in drained soil only on mRNA level (P [FDR] ≤ 0.05) (**Figure 3.6, Figure S3**).

Drainage induced proliferation of *Proteobacteria*, *Actinobacteria*, and *Planctomycetes* (**Figure 3.5, Figure S2**). After drainage, the *Comamonadaceae* were the most abundant family-level group among the *Proteobacteria*, on both SSU rRNA (5.5 %) and mRNA (2.9%) levels (**Figure 3.6, Figure S3**). The abundance of methanotrophic bacteria (MOB) increased from 2.5% in flooded soil to 3.2% in drained soil (relative to the total bacterial SSU rRNA) (**Figure 3.7, Table S2**). Their relative mRNA abundance did not significantly change with drainage (**Table S2**). In flooded soil, Type II MOB were more abundant than Type I MOB. Drainage specifically favored proliferation of Type I MOB **(Figure 3.7**). Actinobacterial SSU rRNA and mRNA abundances significantly (SSU rRNA P [FDR] ≤ 0.1 and mRNA P [FDR] ≤ 0.01) increased with drainage (**Figure 3.5, Figure S2**). Upon drainage, the two major actinobacterial families were *Nocardioidaceae* (5.5% SSU rRNA and 3.5% mRNA) and *Streptomycetaceae* (0.9% SSU rRNA and 4.8% mRNA) (**Figure 3.6, Figure S3**). Particular species within the *Nocardioidaceae*, such as *Marmoricola* sp., increased in relative abundance from almost 0% to greater than 1% (**Table S3**).

Unlike *Proteobacteria* and *Actinobacteria, Planctomycetes* showed no significant drainage-induced increase in SSU rRNA abundance (P [FDR] ≥ 0.1), but their mRNA abundance significantly (P [FDR] ≤ 0.01) increased from 1.3% to 2.8% (**Figure 3.6, Figure S3**).

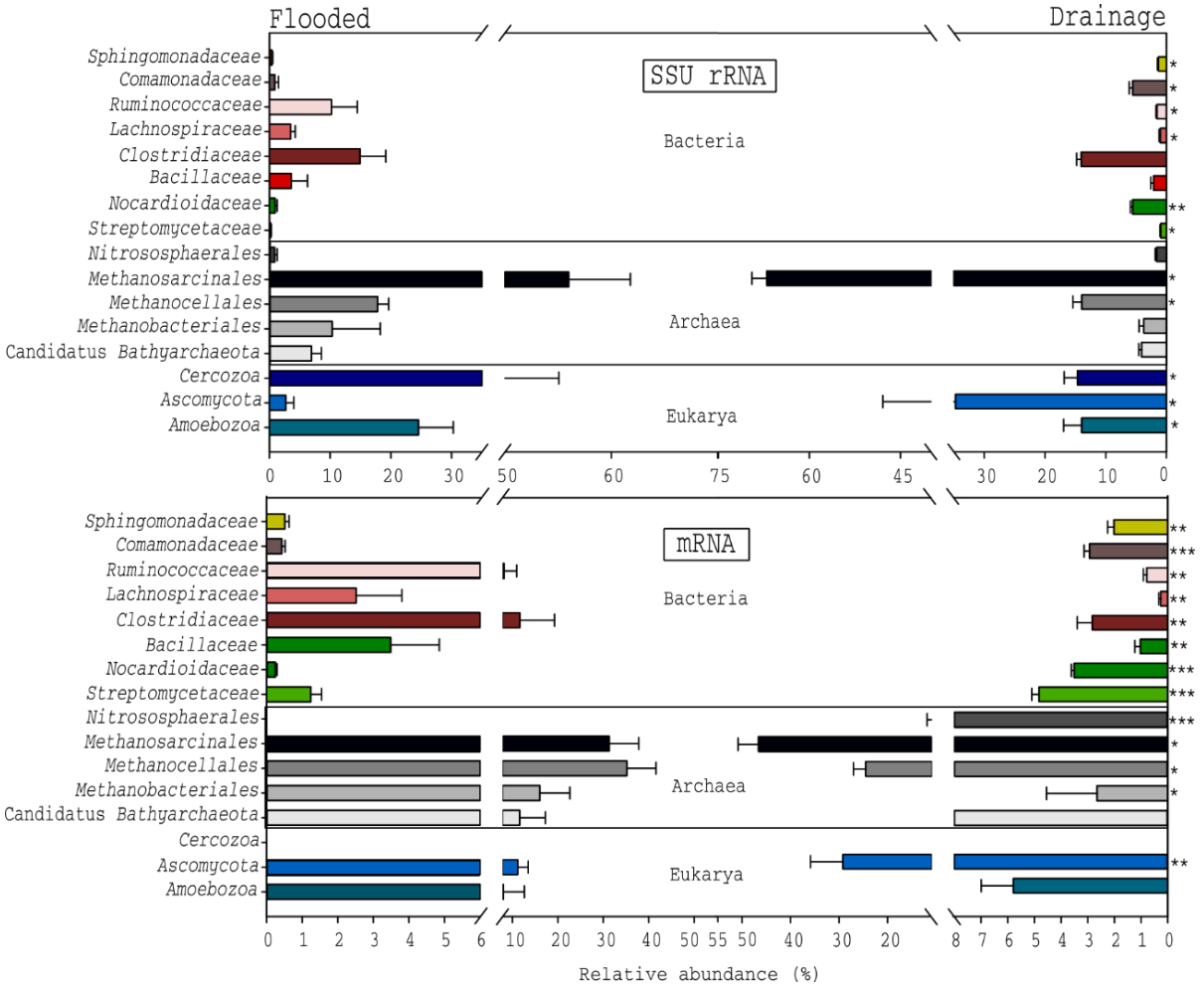

Figure 3.6: Community-wide response to drainage on family (bacteria), order (archaea) and phylum (eukarya) levels.
Taxon-specific abundances relate to the community-wide SSU rRNA and mRNA datasets. Selected taxa > 1 % relative SSU rRNA and/or mRNA abundance(s) are shown. Asterisks * ($P \leq 0.1$), ** ($P \leq 0.05$) and *** ($P \leq 0.01$) indicate significant difference between flooded and drained soils. *P* values are FDR corrected.

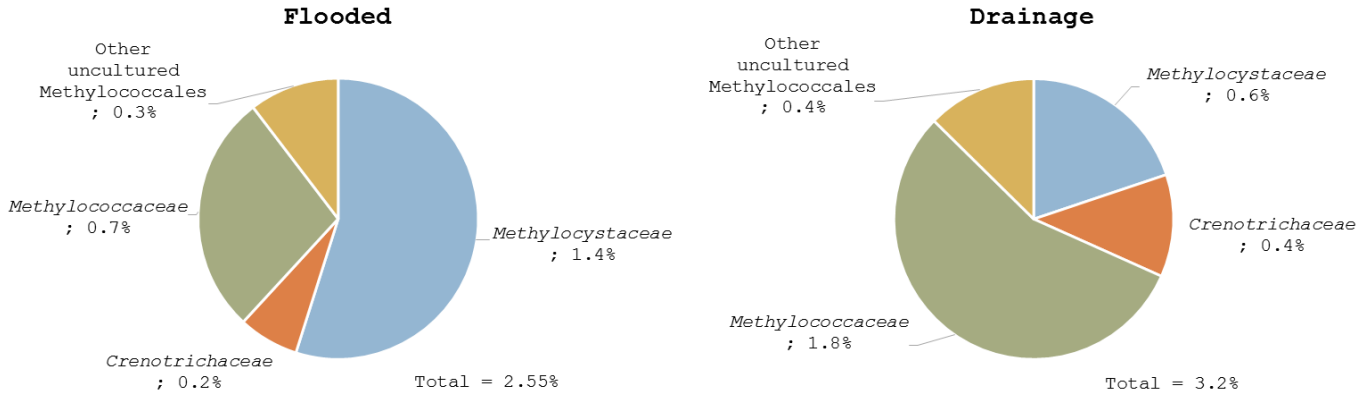

Figure 3.7: Family-level composition of the methanotrophic community (MOB) in flooded and drained soils.
Taxon-specific abundances relate to the bacterial community-wide SSU rRNA datasets.

3.6.4 Effect of drainage on archaeal community composition

Euryarchaeota was the most abundant archaeal phylum. Within *Euryarchaeota*, methanogens dominated the flooded soil with *Methanosarcinales* being the most abundant order (**Figure 3.6, Figure S3**). In fact, 36.3% of the total archaeal SSU rRNA was assigned to the genus *Methanosarcina* (**Table S4**). Members of the newly recognized potential methanogen group Candidatus *Bathyarchaeota* were also identified in the flooded soil on both SSU rRNA (5.7 %) and mRNA (11.6%) levels (**Figure 3.6, Figure S3**).

Drainage had no significant effect on the relative SSU rRNA abundance of the *Euryarchaeota*. Their mRNA abundance, however, significantly (P [FDR] ≤ 0.01) decreased with drainage, from 7% to 1.4% (**Figure 3.5, Figure S2**). Relative to total archaeal community, SSU rRNA and mRNA abundances of the *Methanosarcinales* increased with drainage, while those of the *Methanocellales* and *Methanobacteriales* decreased (**Figure 3.6, Figure S3**).

Overall, the archaeal diversity increased with drainage. In particular, drainage induced a significant abundance increase of non-methanogenic taxa, such as *Halobacteriaceae* and *Nitrososphaerales*, but this increase was primarily observed on mRNA level (**Figure 3.6, Figure S3**).

3.6.5 Effect of drainage on eukaryotic community composition

The SAR super-group (*Stramenopiles*, *Alveolates*, and *Rhizaria*) was abundant in the flooded soil, with *Cercozoa* (based on SSU rRNA) being the most prominent taxon (**Figure 3.6, Figure**

S3). Concurrently, the phylum *Amoebozoa* was an abundant member of the eukaryotic community in flooded soil (**Figure 3.6, Figure S3**), with *Acanthamoeba* being their most prominent member (~ 5 % of the eukaryotic SSU rRNA) (**Table S5**).

Drainage had a major impact on the eukaryotic community composition. It primarily induced a significant abundance increase of *Fungi*. Among the *Fungi*, members of the phyla *Ascomycota* and *Basidiomycota* significantly increased in the drained soils, on both rRNA (P [FDR] ≤ 0.1) and mRNA levels (P [FDR] ≤ 0.05) (**Figure 3.6, Figure S3**). The sub-division *Pezizomycotina* (35 % of eukaryotic SSU rRNA in drained soils) was the most abundant member of the *Ascomycota*, while *Agaricomycotina* (4 % of eukaryotic SSU rRNA in drained soils) was most abundant among the *Basidiomycota* (**Table S5**). Drainage also induced a significant abundance decrease of *Cercozoa* and *Amoebozoa* on SSU rRNA (P [FDR] ≤ 0.1) (**Figure 3.6, Figure S3**).

Taxonomic classification of eukaryotic mRNA corresponded well to the SSU rRNA-based classification only for fungi *(Ascomycota* and *Basidiomycota*) and *Amoebozoa*, but not for any other eukaryotic group. This is well exemplified by the *Archaeplastida*. This taxon made ~ 8 % of eukaryotic rRNA but ~ 51 % of eukaryotic mRNA in the flooded soil.

3.7 Effect of drainage on community functioning

The proportion of mRNA in total RNA was proposed to be an excellent proxy for short-term effects on community-wide gene expression (Peng et al., 2017). Nine-day drainage had no significant effect on the relative mRNA expression level between flooded (mRNA proportion in total RNA = 1.7±04%) and drained soils (mRNA proportion in total RNA = 2±0.3%) (**Table 3.4**).

3.7.1 Effect of drainage on the gene expression of particular functional categories

3.7.1.1 General cellular processes and stress response genes

Functional categories linked to maintenance metabolism (e.g., "oxidative phosphorylation" and "energy metabolism") showed a stable gene expression level in both flooded and drained soils (**Figure 3.8**, **Figure S4**). Functional gene expression involved in "cell motility" was significantly overrepresented in flooded soil, with 1% of total transcripts encoding flagellin-related proteins (**Figure 3.8**). The majority of these transcripts were encoded by *Firmicutes* and, to a lesser extent, *Proteobacteria* (**Figure S5**).

The abundance of transcripts involved in genetic information processing (e.g. "transcription machinery," "DNA repair and recombination", and "translation factors") significantly increased (*P* [FDR] ≤ 0.05) in drained soil (**Figure 3.8**). Correspondingly, the expression level of transcripts encoding RNA polymerase subunit β (*rpoB*) significantly increased (*P* [FDR] ≤ 1.5) from 0.61 % to 1.26 % during drainage (**Figure 3.8**, and **Table S6**). These transcripts were mainly expressed by *Proteobacteria* and *Actinobacteria* (**Figure S5**). Likewise, there was a significant increase (*P* [FDR] ≤ 0.05) in transcripts involved in "fatty acid metabolism", "glycerophospholipid metabolism," and KEGG level 2 "metabolism of terpenoids and polyketides" (**Figure 3.8**, **Figure S4**).

No significant difference in the expression level between flooded and drained soils was observed for transcripts involved in stress response (e.g., *DnaK*) (**Figure 3.8**) and reactive oxygen species. The only exception were transcripts encoding catalase-peroxidase (KO3782) (**Figure 3.8**).

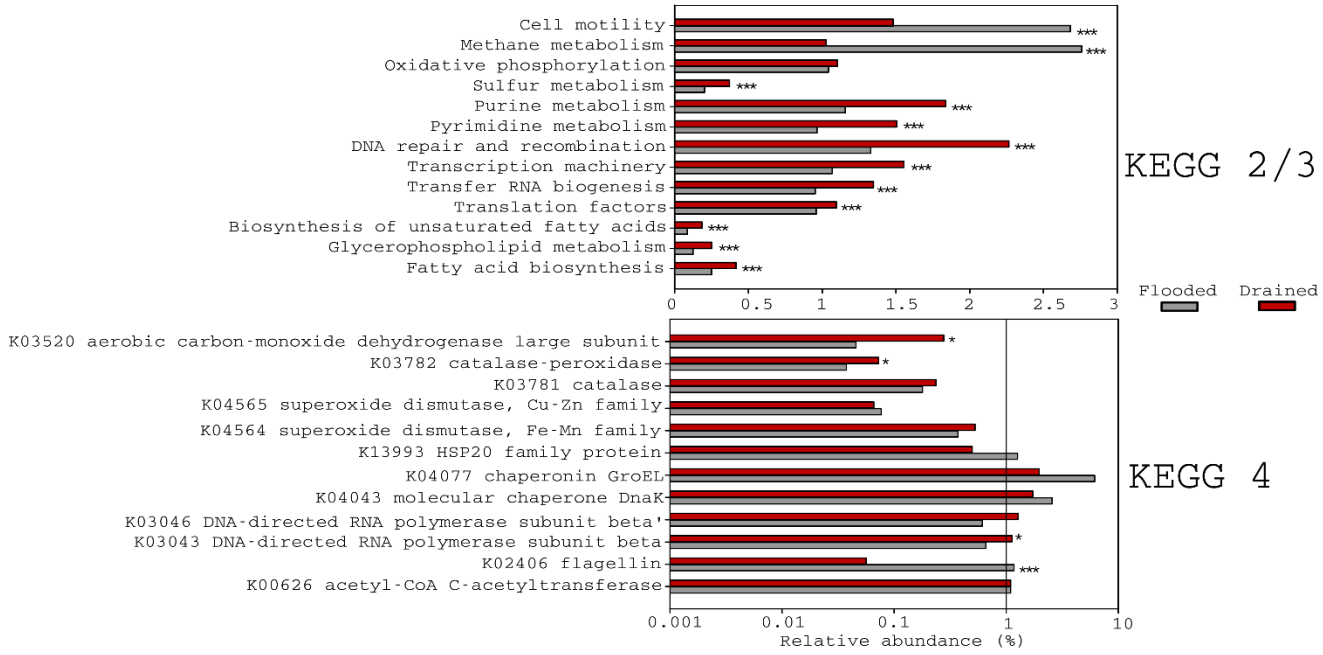

Figure 3.8: Community-wide mRNA response to drainage (KEGG levels 2/3)
The bar graphs show drainage-induced changes in mRNA expression on KEGG levels 2 (cell motility), 3 and 4. Asterisks * ($P \leq 0.15$), ** ($P \leq 0.1$) and *** ($P \leq 0.05$) indicate significant difference between flooded and drained soils. *P* values are FDR corrected.

3.7.1.2 Transcripts involved in methane cycling

Methanogenesis is one of the primary processes occurring in flooded paddy soil, with *mcrA* commonly used as the marker gene for methanogenesis. Drainage induced a nearly 300-fold decrease in *mcrA* transcripts; from 5.79×10^6 to 1.52×10^4 copies per gram of dry soil (**Figure 3.3**). In the mRNA dataset, transcripts assigned to subunits of the methyl-co enzyme M (*mcr*) gene significantly decreased (P [FDR] ≤ 0.15) with drainage (**Figure 3.9**). Likewise, transcripts assigned to the 5,10-methylenetetrahydromethanopterin reductase (*mer*) gene and subunits of the coenzyme F420 hydrogenase (*frh*) gene significantly decreased with drainage (P [FDR] $\leq$ 0.15) (**Figure 3.9**).The key gene in acetoclastic methanogenesis-the anaerobic carbon monoxide carboxylase (*cdh*) catalytic subunit- decreased with drainage but this was not backed up with statistical significance (**Figure 3.9**). On the contrary, the aerobic homologue of CODH was significantly (P [FDR] ≤ 0.15) enriched in drained soil (**Figure 3.8**, **Table S6**).

In contrast to the drainage-induced increase in SSU rRNA abundance of Type I MOBs (**Figure 3.7**), the transcript level of their key enzyme - particulate methane monooxygenase (pMMO) - decreased with drainage (**Table S7**).

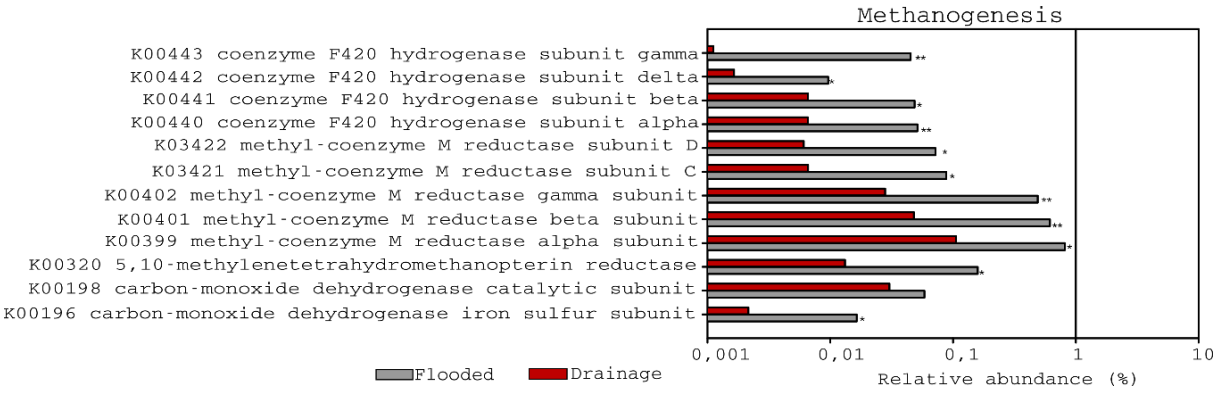

Figure 3.9 Methanogenesis mRNA response to drainage (KEGG 4).
The bar graphs show drainage-induced changes in mRNA expression on KEGG level 4 (genes involved in methanogenesis). Asterisks * ($P \leq 0.15$), ** ($P \leq 0.1$) and *** ($P \leq 0.05$) indicate significant difference between flooded and drained conditions. *P* values are FDR corrected.

3.7.1.3 Plant bio-polymer degradation

The CAZyme database was used to compare the CAZyme transcript pattern expressed by the paddy soil microbial communities in flooded and drained soils. Drainage did not change the relative abundance of CAZyme transcripts within the total mRNA (2.89 %) (**Table 3.6**), but it altered the relative abundance of particular CAZyme categories and the taxa involved in their expression (**Figure 3.10, Table S8**).

Rice straw is commonly used as a fertilizer in rice farming and thus one of the most important components of soil organic matter (SOM) in rice field soil. Cellulose and hemicellulose CAZymes represented 18% and 12% of the total CAZymes transcripts in flooded and drained soils, respectively (**Figure 3.10)**. The relative abundance of transcripts involved in hemicellulose degradation and encoding glycosyl hydrolases (GHs) and carbohydrate esterases (CEs) was not significantly affected by drainage (CE4, GH2, and GH36) (**Figure 3.10**); however, drainage altered the taxa involved in their expression (**Figure 3.10**). The situation was different for CAZymes involved in cellulose degradation. Their abundance significantly (*P* [FDR] ≤ 0.1) decreased with drainage (GH9, GH8, CBM 3 and 6) (**Figure 3.10**). The phyla associated with cellulose and hemicellulose degradation under flooded conditions were *Firmicutes* (*Clostridia* and *Bacilli*) and, to a lesser extent, *Proteobacteria*, *Actinobacteria* and *Bacteroidia* (**Figure 10**, **Figure S7**). Under drained conditions, CAZyme transcripts involved in the decomposition of cellulose and hemicellulose were expressed by *Actinobacteria* and *Proteobacteria* (**Figure 3.10, Figure S7**).

Among eukaryota, *Ascomycota* transcripts involved in the expression of GHs, CEs and carbohydrate-binding modules (CBMs) increased twofold in their expression level during drainage (**Table S8**). Specifically, members of the classes *Sordariomycetes* and *Saccharomycetes* contributed to the production of CAZymes involved in cellulose and hemicellulose degradation (**Figure S7**).

Transcripts encoding enzymes degrading the lignin component of rice straw (AA family) significantly (*P* [FDR] ≤ 0.05) increased with drainage (**Figure 3.10**, **Table 3.6**, **and Figure S6**). Most of the AA transcripts were expressed by *Actinobacteria* and *Proteobacteria* (**Table S8**).

Alpha-glucans (glycogen and starch) degradation represented 7% of the CAZyme transcripts in both flooded and drained soils. CAZymes of the GH13 subfamily was enriched in drained soil but with no statistical significance, and its accompanying CBM48 was significantly enriched (*P* [FDR] ≤ 0.05) (**Figure 3.10**). GH13 (α-amylase) and CBM48 are involved in glycogen breakdown (Lombard et al., 2014). Most of the transcripts involved in Alpha-glucans were expressed by *Firmicutes* in flooded soil (*P* [FDR] ≤ 0.05) and by *Actinobacteria* (*P* [FDR] ≤ 0.1) and *Proteobacteria* (*P* [FDR] ≤ 0.01) (**Figure 3.10**).

The relative abundance of transcripts involved in chitin degradation significantly decreased (*P* FDR ≤ 0.1) with drainage (CBM 54, CBM 50) (**Figure 3.10**). *Firmicutes*, specifically *Clostridia* were the primary source of chitinase transcripts (**Figure 3.10, Figure S7**).

Drainage induced the enrichment of transcripts affiliated with GHs involved in the degradation of substrates other than rice straw (**Figure 3.10**). One example is GH23 (*P* [FDR] ≤ 0.1) subfamily that contains enzymes catalysing the lysis of the bacterial peptidoglycan (Lombard et al., 2014). Drainage enriched CAZyme transcripts affiliated with *Cyanobacteria* and *Planctomycetes* (**Figure S8**). These taxon-specific transcripts belonged to the GH, CBM and GT families (**Table S8**).

Table 3.6: *Transcripts assigned to carbohydrate-active enzymes (CAZyme) families*

CAZyme families	**Transcript numbers** [1]		**Relative abundance (%)** [2]	
	Flooded	Drainage	Flooded	Drainage
Auxiliary Activities (AA) *	117	112	2±0.3	3±0.4
Carbohydrate-Binding Module (CBM) *	2244	901	40±2.3	24±1.6
Carbohydrate Esterase (CE)	336	229	6±1.2	6±0.5
Glycoside Hydrolase (GH)	1754	1228	31±1.4	33±1.0
Glycosyltransferase (GT) *	1158	1204	20±1.8	32±0.1
Polysaccharide Lyase (PL)	66	43	1±0.4	1±0.1
	Transcript numbers		**Relative abundance (%) in total mRNA**	
Total CAZymes	5667	3265	2.89±0.8	2.89±0.6

* *P* [FDR] ≤ 0.05.
[1] Mean read number of 4 independent flooded samples and 3 indepented drained samples.
[2] Percentage of specified CAZyme family in relation to the total number of CAZyme-annotated reads.

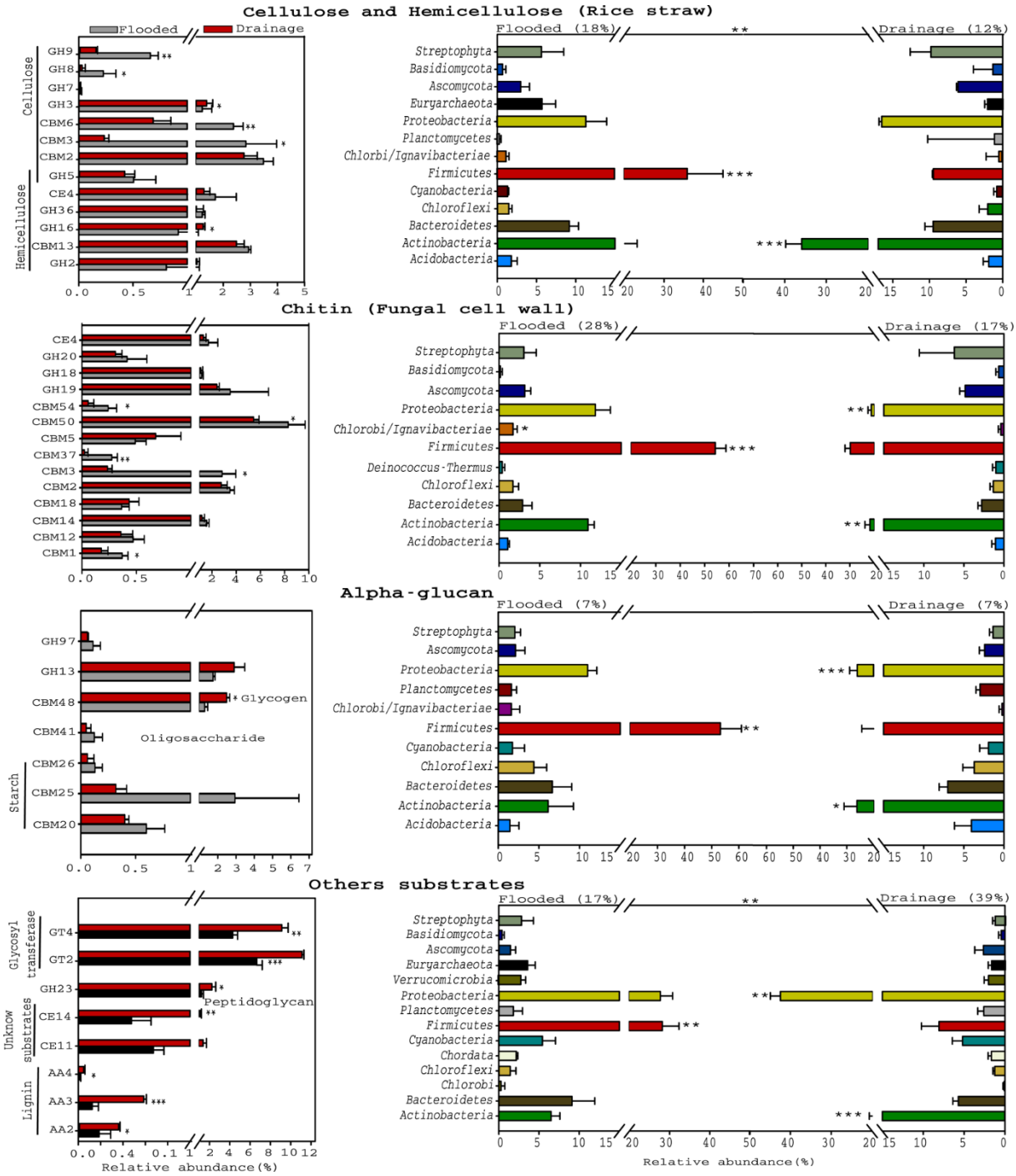

Figure 3.10: Drainage-induced changes in the expression of CAZyme transcripts.
The bar graphs show drainage-induced changes in the taxon-specific (right) and functional (left) abundances of CAZyme transcripts involved in cellulose, hemicellulose, chitin, and alpha-glucan degradation. Relative abundance values relate to the total number of CAZyme-affiliated mRNA transcripts. Asterisks * ($P \leq 0.1$), ** ($P \leq 0.05$) and *** ($P \leq 0.01$) indicate significant difference between flooded and drained soils. *P* values are FDR corrected.

3.8 The impact of the pre-incubation period on the community response to drainage

The differential impact of short-term (7-day) and long-term (28-day) pre-incubation under flooded conditions on the response of the microbial community to 9-day drainage was assessed in this section. This assessment was made on structural (rRNA) and functional (mRNA) level. The statistical data obtained from metatranscriptomic libraries of the flooded and drained soil samples after 7–day pre-incubation period are shown in **Table 3.7**.

3.8.1 The effect of pre-incubation period on SSU rRNA level

The OTUs datasets from flooded soils of both pre-incubation periods were merged to a single dataset. Likewise, the two OTUs datasets from the drained soils were merged to a single dataset. Calculation of alpha-diversity (Simpson index) showed that drainage slightly decreased soil microbial diversity (**Figure 3.11 A**). Bray-Curtis dissimilarity distance matrix was used to calculate the relatedness of the microbial communities in the flooded and drained soils after short-term and long-term pre-incubation (beta-diversity). The microbial communities of the drained soils clustered together, while those in flooded soils clustered distinctly from each other (**Figure 3.11 B**).

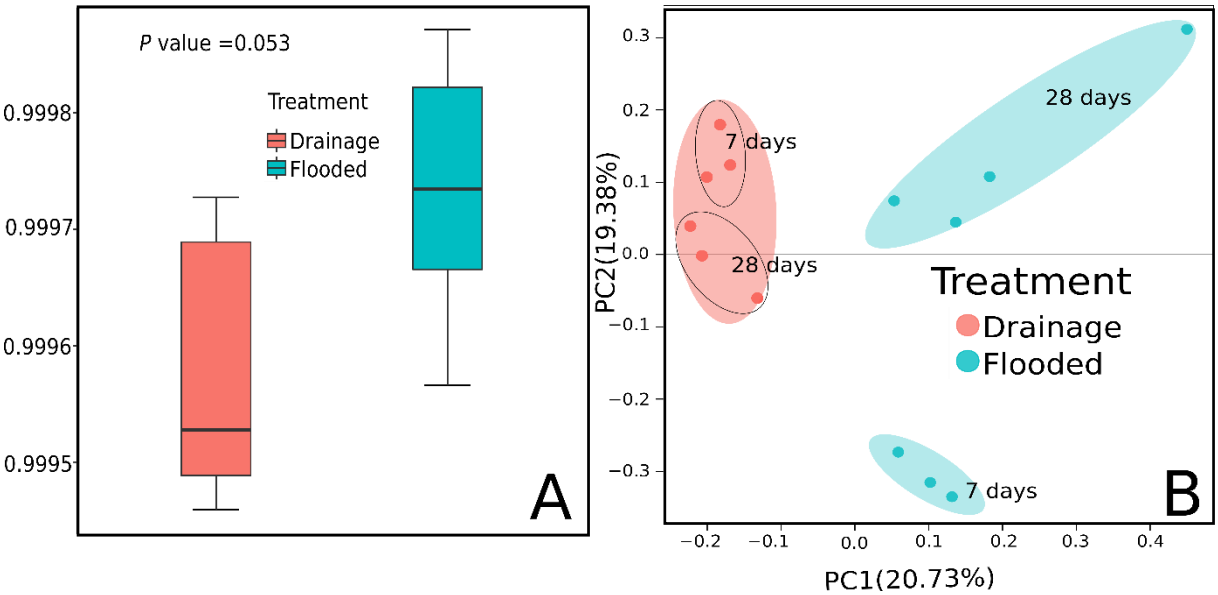

Figure 3.11: Alpha-diversity and beta-diversity of microbial communities in flooded and drained soils.
(A)Alpha-diversity based on Simpson diversity index. Welch's t-test applied to test for statistically significant difference. (B) Beta-diversity indicated by the principal coordinate analysis (PCoA) derived from the Bray–Curtis dissimilarity matrix based on 95% OTUs similarity across flooded and drained soils.

Table 3.7: *General statistics of the metatranscriptome libraries from short-term* (7-day) *flooded (7F) and drained (7F9D) sample*

Conditions	***Replicates***	***Raw reads***	***Assembled reads***	***Passed QC reads***		***SSU rRNA*** [1]		***SSU rRNA*** [2]	***Putative mRNA transcripts*** [1]	
Average read length				260 bp		260 bp		300 bp	260 bp	
Flooded	**7F1**	8,403,802	98.8%	5,724,960	68.1%	2,782,680	43.36%	1,525,863	69,595	1.91%
	7F2	5,954,192	98.85%	3,352,782	56.3%	1,658,932	40.37%	5,93,793	46,881	1.91%
	7F3	6,077,803	99.3%	3,750,075	61.7%	1,754,529	40.11%	819,159	65,234	2.49%
Average		6,811,932	99±0.03%	4,275,939	60±5%	2,065,380	41.3±1.8%	1,172,511	60,570	2.1±0.3%
Drainage	**7F9D1**	9,221,992	99.7%	4,526,605	49 %	3153269	49.38%	3,153,269	135,590	4.19%
	7F9D2	6,985,587	99.6%	2,965,493	42 %	2145213	45.23%	716,979	72,558	2.79%
	7F9D3	7,266,365	99.5%	4,006,163	56 %	1571209	43.34%	709,018	63,724	3.10%
Average		7,824,648	99.±0.01%	3,832,754	49±7%	2,289,897	46±3.1%	1,526,422	90,624	3.4±0.7%

[1] Relative abundance of SSU rRNA and mRNA calculated based on the number of reads that passed quality control.
[2] The dataset of SSU rRNA reads used for downstream analysis (diversity indices and taxonomic composition).

The DESeq2 R package was used to identify the taxa that, regardless of pre-incubation period, were differently abundant between flooded and drained soils. The DESeq2 table (**Table 3.8**) showed that the phylum *Firmicutes* had the greatest number of differentially abundant OTUs. In particular, uncultured *Ruminococcaceae, Mobilitalea* and "*Clostridium* sensu stricto 1" had a 2.9 to 2.1 $\log_2$ fold greater abundance in flooded soil than in drained soil (**Table 3.8**). The only archaeal taxon that had a significant $\log_2$ fold increase in flooded soil was an uncultured member of *Methanobacterium* (**Table 3.8**). A total of 43 OTUs of *Proteobacteria*, 2 OTUs of *Acidobacteria*, 4 OTUs of *Bacteroidetes*, 2 OTUs of *Cyanobacteria*, and 24 OTUs of *Fibrobacteres* showed significantly (P [FDR] ≤ 0.05) increased abundance under flooded conditions (**Table 3.8**). Regardless of the pre-incubation period, a total of 420 OTUs of *Proteobacteria*, 73 OTUs of *Actinobacteria*, and 116 OTUs of fungi had at least a two-fold abundance increase in drained soils (**Table 3.8**). Representative taxa of *Actinobacteria* were uncultured members of the *Marmoricola* and *Streptomycetaceae*. Members of the genus *Ramlibacter* (*Proteobacteria*) showed a 3.1 fold abundance increase in drained soils (**Table 3.8**). Type I MOB were also differentially abundant between flooded and drained soils (**Table 3.8**).

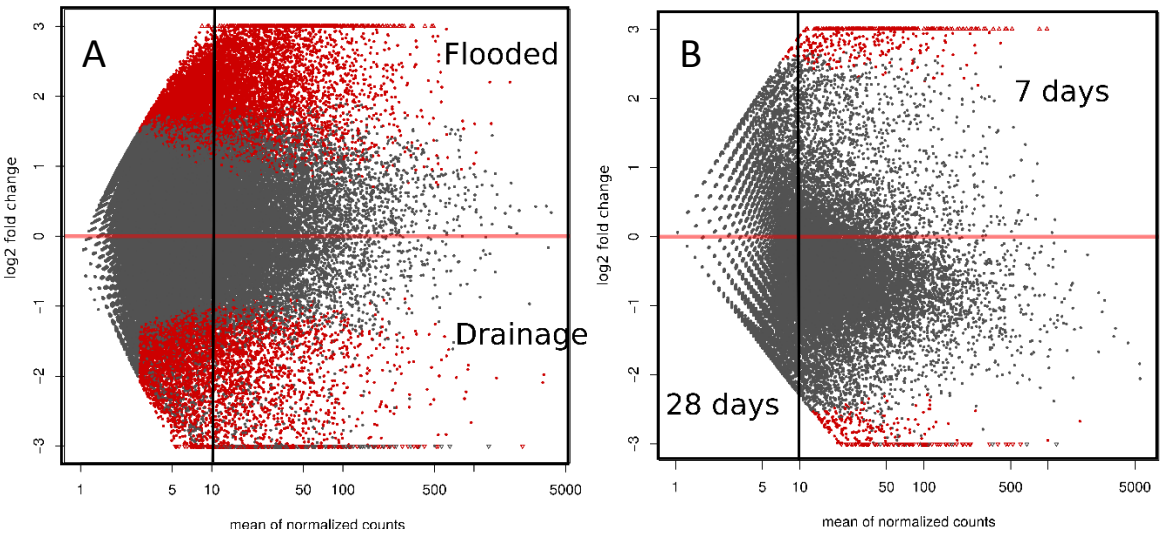

Figure 3.12: DESeq2 diagnostic plots.
The graphs show the diagnostic plots of the DESeq2 analysis; red dots indicate OTUs that show a significant difference in their abundance between the treatments, while grey dots indicate OTUs that are not affected by the treatment. (A) Differential OTU abundance between flooded and drained soils (combined samples from either 7-day or 28-day pre-incubation period). (B) Differential OTU abundance between soils exposed to drainage after either 7-day or 28-day pre-incubation period.

Table 3.8: *List of taxa with differential OTU abundance between flooded and drained soils*

Phyla	***Number of significant OTUs*** [1]	***log_2 fold change flooded/drainage*** [2]	***P value*** [3]	***Representative OTU*** [4]
Acidobacteria	2	2.9	0.007	*Acidobacteriaceae* (subgroup 1)
Bacteroidetes	4	2.7	0.001	*Bacteroidetes VC2.1 Bac22*
Chloroflexi	1	2.0	0.001	Uncultured *Roseiflexus*
Cyanobacteria	2	2.7	0.008	Uncultured *Aphanizomenon*
Euryarchaeota	2	2.2	0.010	Uncultured *Methanobacterium*
Fibrobacteres	24	2.6	0.010	Possible family 01
Firmicutes	1853	2.9	0.000	Uncultured *Ruminococcaceae*
Firmicutes	1853	2.3	0.000	Uncultured *Mobilitalea*
Firmicutes	1853	2.1	0,006	*Clostridium* sensu stricto 1
Firmicutes	1853	2.4	0.007	Uncultured *Bacillaceae*
Proteobacteria	43	3.8	0.0001	Uncultured *Beijerinckiaceae*
Unassigned	115	3.4	0.0000	Unassigned
Verrucomicrobia	1	2.8	0.008	Uncultured *Opitutus*
Acidobacteria	10	-2.4	0.0003	Uncultured *Holophagae* subgroup 7
Actinobacteria	73	-2.0	0.0040	Uncultured *Marmoricola*
Actinobacteria	73	-2.8	0.0000	Uncultured *Streptomycetaceae*
Armatimonadetes	4	-3.4	0.0000	Uncultured *Armatimonadetes* bacterium
Bacteroidetes	21	-2.6	0.0046	Uncultured *Sufflavibacter*
Firmicutes	6	-2.9	0.0026	Uncultured *Cohnella*
Fungi	116	-3.4	0.0003	Uncultured *Sordariales*
Planctomycetes	5	-2.2	0.0011	Uncultured *Gemmata*
Proteobacteria	420	-3.1	0.0000	Uncultured *Ramlibacter*
Proteobacteria	420	-2.2	0.0104	Uncultured *Methylococcales*
Unassigned	54	-3.2	0.0000	Unassigned

[1] Number of significant OTUs within each phyla (archaea and bacteria) or super group (eukarya)
[2]log2 foldchange between flooded and drained soil, blue color (positive value) indicates an OTU that is enriched in flooded soils, while dark pink colour (negative value) indicates an OTU that is enriched in drained soils.
[3] FDR corrected *P* values
[4] Representative OTU/taxa from each phylum or super group are shown. Taxonomic assignment is based on SILVA 123 database

We also aimed to assess whether the pre-incubation period had a differential drainage effect on particular community members. Using DESeq2, the SSU rRNA datasets obtained from drained soils after either 7-day or 28-day pre-incubation period were comparatively analysed. The diagnostic plot showed that, regardless of pre-incubation period, the majority of OTUs were shared between the two SSU rRNA datasets; however, a few OTUs could be detected only after 7-day or 28–day pre-incubation (red dots) (**Figure 3.12 B**).

Signature OTUs for 7-day pre-incubation were affiliated with the *Actinobacteria* (2 OTUs), *Cyanobacteria* (2 OTUs), and *Opisthokonta*/fungi (52 OTUs) (**Table 3.9**). Signature OTUs for 28-day pre-incubation were affiliated with *Chlorobi* (1 OTU), *Planctomycetes* (2 OTUs), and *Bacteroidetes* (58 OTUs). The phylum *Firmicutes* was detected in drained soil regardless of pre-incubation period; however, the number of significant OTUs was higher after 7-day than 28-day pre-incubation period (**Table 3.9**). Likewise, *Proteobacteria* were present in the drained soils after 7-day and 28-day pre-incubation period (**Table 3.9**). Nevertheless, 28 days incubated soil followed by drainage was characterized by three log2fold increase in type I methanotrophs (**Table 3.9**).

Table 3.9: *List of taxa with differential OTU abundance between drained soils after either 7-day or 28-day pre-incubation period.*

Phyla	***Number of significant OTUs*** [1]	***log_2 fold change 7 days /28 days*** [2]	***P value*** [3]	***Representative taxa/OTU*** [4]	***Pre-incubation period [days]***
Actinobacteria	2	3.1	0.003	*Corynebacteriales* uncultured	7
Cyanobacteria	2	3.3	0.001	ML635J-21	7
Firmicutes	97	5.2	0.000	*Bacillus* sp.	7
Fungi	52	4.4	0.000	*Mucorales* sp.	7
Proteobacteria	23	3.4	0.002	*Magnetospirillum* sp.	7
Unassigned-1	41	3.8	0.000	Unassigned	7
Bacteroidetes	58	-4.2	0.000	*Bacteroidetes* vadinHA17	28
Firmicutes	4	-2.7	0.007	*Oxobacter* sp.	28
Chlorobi	1	-2.8	0.010	OPB56	28
Planctomycetes	2	-3.1	0.005	AKAU3564 sediment group	28
Proteobacteria	21	-3.6	0.001	*Methylomonas* sp.	28
Unassigned-2	4	-3.0	0.004	Unassigned	28

[1] Number of significant OTUs within each phyla (archaea and bacteria) or super group (eukarya)
[2]log2 foldchange between drained soils after 7 days and drained soil after 28 days pre-incubation, light pink colour (positive value) indicates an OTU that is enriched in drained soils after 7-day pre-incubation, while dark pink colour (negative value) indicates an OTU that is enriched in drained soils after 28-day pre-incubation.
[3] FDR corrected *P* values
[4] Representative OTU/taxa from each phylum or super group are shown. For other OTU/taxa, please see **Table S9**. Taxonomic assignment is based on SILVA 123 database

3.8.2 The effect of pre-incubation period on mRNA level

The mRNA datasets from flooded and drained soils were queried against the NCBI (GenBank) nr database. Next, MEGAN6 and the MicrobiomeAnalyst webserver were used to visualize the effect of two environmental factors (drainage, pre-incubation period) on functional gene expression.

A PCoA plot was used to differentiate between the effect of incubation period and drainage on functional gene expression profiles. The mRNA datasets from flooded soils were clustered together and they were distant from the drained soils, suggesting that the drainage had a stronger effect on the functional gene expression than the incubation period (**Figure 3.13**). The differential clustering of the mRNA datasets in the PCoA plot was explained by a heatmap showing KEGG level 2 functional categories (**Figure 3.14**). Transcripts related to functional categories such as "Membrane transport", "Cell motility" and "Energy metabolism" were enriched in flooded soils (7-day or 28-day pre-incubation) (**Figure 3.14**). Transcripts related to functional categories such as "Lipid metabolism" and "Metabolism of Polyketides and Trepenoids" were enriched in drained soils (after 7-day or 28-day pre-incubation). Drained soil samples after 7-day pre-incubation were enriched in transcripts involved in translation and transcription.

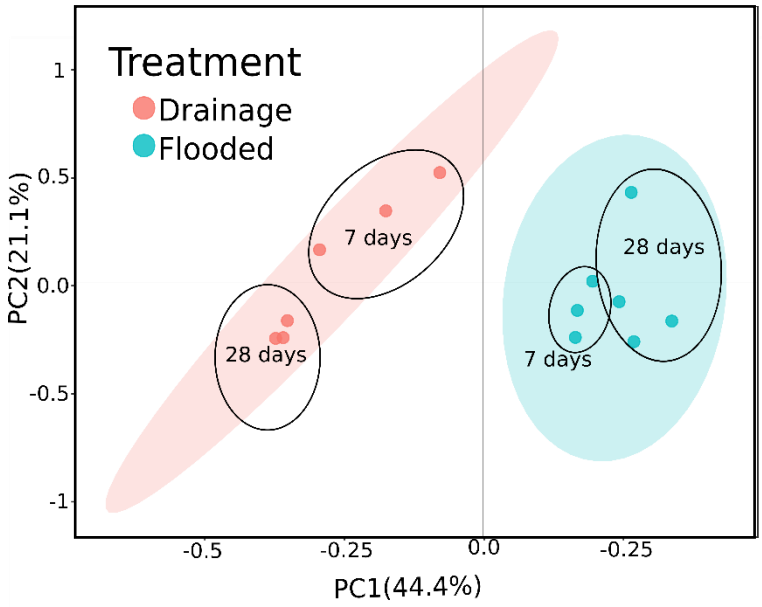

Figure 3.13: PCoA plot of mRNA datasets from flooded and drained soils after 7-day or 28-day pre-incubation period.
The PCoA plot was derived from the Bray–Curtis dissimilarity matrices based on the functional annotation of the mRNA transcripts (KEGG level 2). Data was normalized using the cumulative sum scaling method.

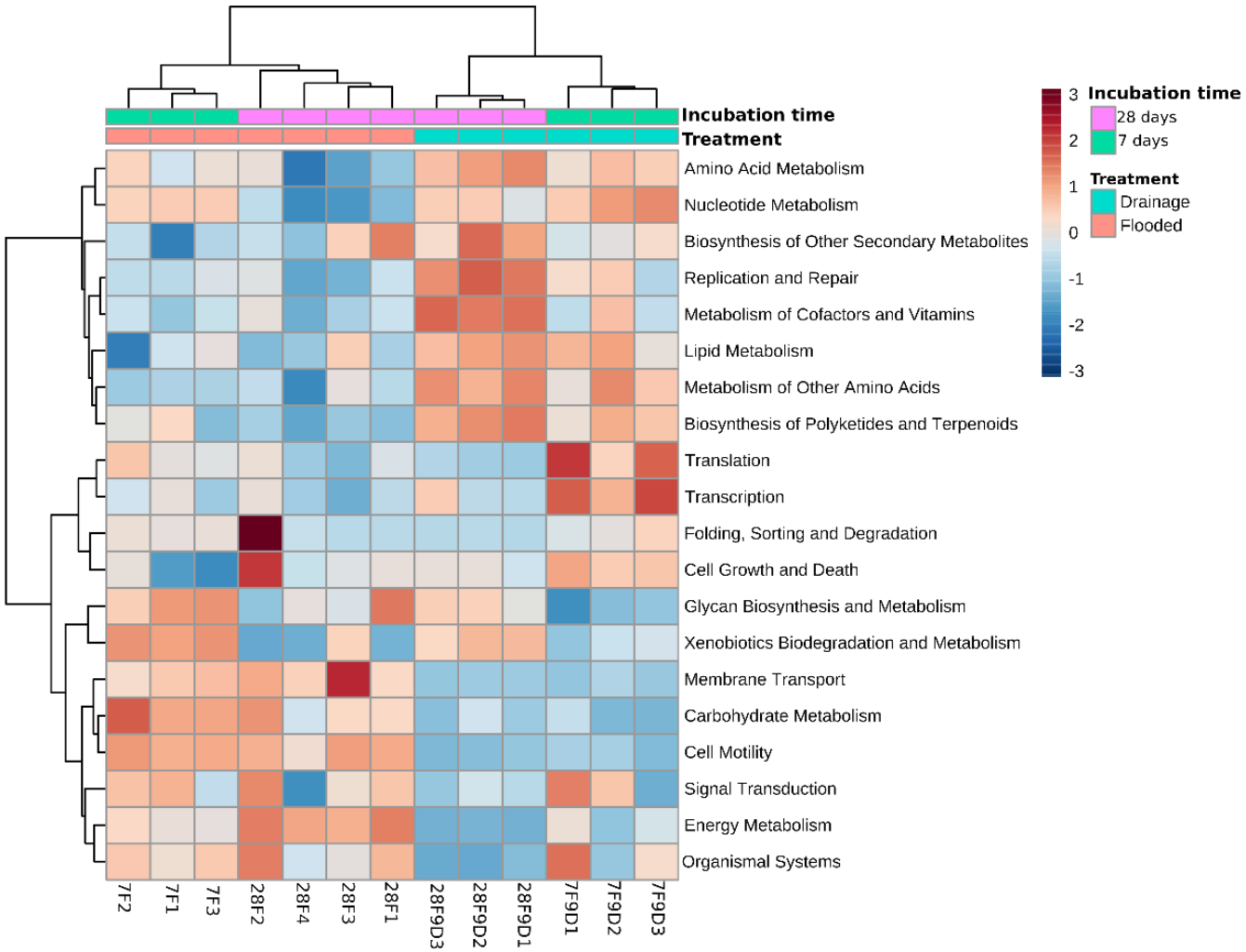

Figure 3.14: Heat-map of mRNA datasets showing the differential gene expression profiles from flooded and drained soils after 7-day or 28-day pre-incubation period.
The heat-map shows drainage-induced changes in mRNA expression on KEGG levels 2 categories. The heatmap was generated based on Euclidean distance matrix of mRNA transcripts raw counts by MicrobiomeAnalyst webpage. Data was normalized using the cumulative sum scaling method.

When the two data-sets (7-day pre-incubation and 28-day pre-incubation) were compared separately. Relative to the flooded soil, mRNA transcripts affiliated with nucleotide metabolism, DNA repair and recombination, transcription, translation, and fatty biosynthesis were significantly enriched (P [FDR] ≤ 0.05) in drained soil after 28-day pre-incubation. They were also enriched after 7-day pre-incubation, but this was not backed up with statistical significance (**Figure 3.15**). Vice versa, mRNA transcripts affiliated with methanogenesis were significantly underrepresented in drained soil after 28-day pre-incubation, but not after 7-day pre-incubation (**Figure 3.15**). By contrast, mRNA transcripts of a few ROS genes (i.e., catalase-peroxidase, superoxide dismutase Cu-Zn family) were significantly enriched in drained soil

after 7-day pre-incubation period, but not after 28-day pre-incubation (**Figure 3.16**).

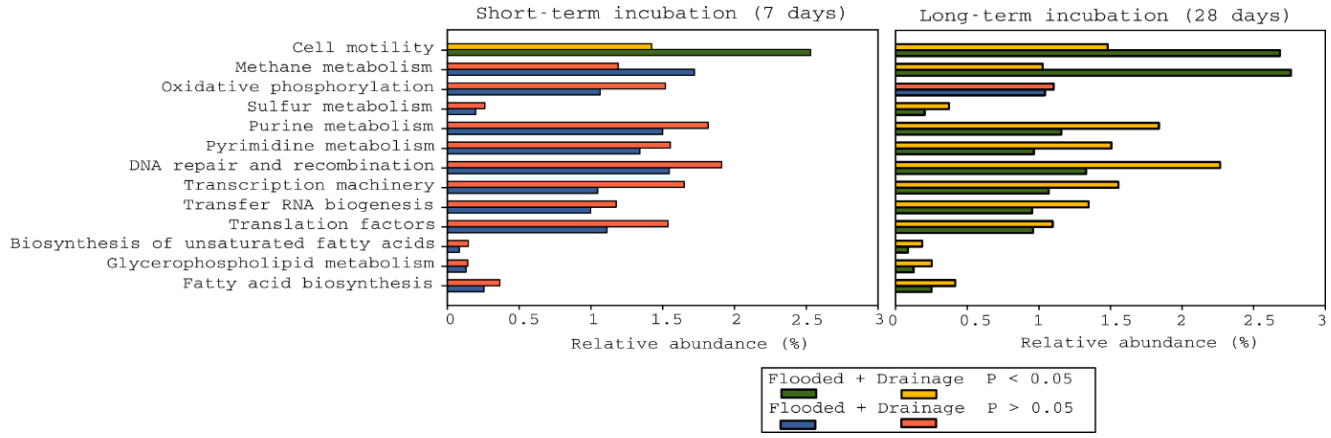

Figure 3.15: Differential effect of drainage on functional gene expression (KEGG levels 2/3).
The bar graphs show drainage-induced changes in mRNA expression on KEGG levels 2 (cell motility) and 3 (all other categories). Green and yellow bars indicate a statistical difference (P [FDR] ≤ 0.05) between flooded and drained conditions.

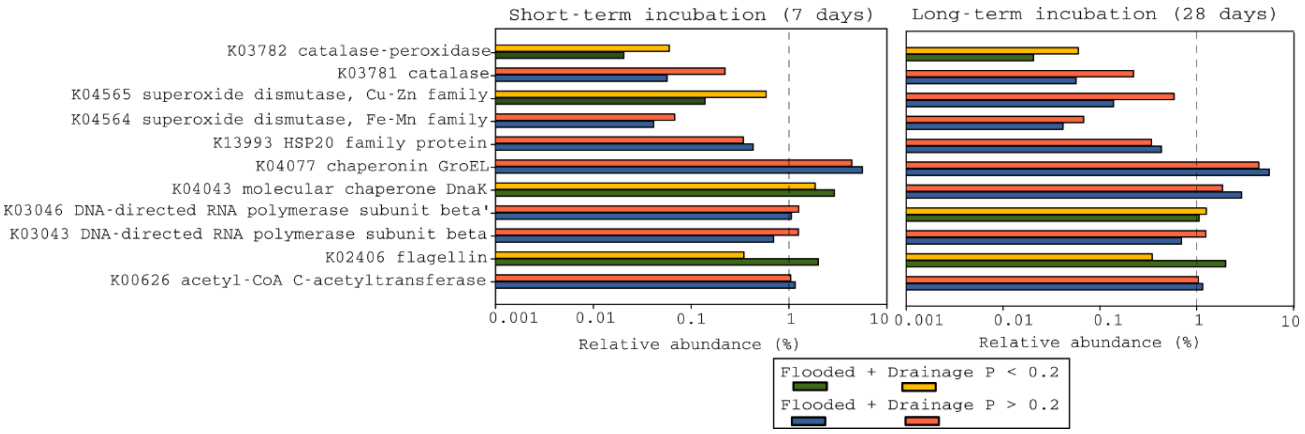

Figure 3.16: Differential effect of drainage on the expression of stress-responsive, motility, and general metabolism-related genes (KEGG level 4).
The bar graphs show drainage-induced changes in mRNA expression on KEGG level 4. Green and yellow bars indicate a statistical difference (P [FDR] ≤ 0.2) between flooded and drained conditions.

The mRNA datasets from flooded soils of both pre-incubation periods were merged to a single dataset. Likewise, the two mRNA datasets from the drained soils were merged to a single dataset. The DESeq2 R package was used to identify the mRNA transcripts that, regardless of pre-incubation period, were differently abundant between flooded and drained soils. On KEGG level 4, a total of 163 genes were significantly under- or over-represented in the mRNA datasets from drained soils, relative to those from flooded soils. For example, transcripts involved in cell motility, sporulation, and degradation of bio-polymer (e.g., cellulose) were underrepresented, while those involved in oxidative phosphorylation, phospholipid cleavage,

protein degradation and glycogen metabolism were overrepresented in drained soils (**Table 3.10** [selected list] and **Table S10** [full list of transcripts].

We also tested for a drainage effect on the expression of genes involved in osmotic stress response; however, transcripts of only a few genes were slightly overrepresented in the mRNA datasets from drained soils (**Table 3.11**). These genes were involved in proline utilization and trehalose transport and metabolism (**Table 3.11**). The $\log_2$ fold change was between 1.5 and 2.1. This log-fold change was not supported by FDR-corrected *P* value.

Table 3.10: *Transcript species that are significantly overrepresented within the combined flooded and drained data-sets*

KEGG Genes (level 4)	***Log2 fold change flooded /drainage*** [1]	***P value*** [2]	***Function***	***Over-represented in***
K00402 methyl-coenzyme m reductase gamma subunit [ec:2.8.4.1]	2.1	0.01	Methanogenesis	Flooded
K07406 alpha-galactosidase [ec:3.2.1.22]	2.2	0.01	Degradation of bio-polymer	Flooded
K02392 flagellar basal-body rod protein flgg	2.2	0.01	Cell motility	Flooded
K03421 methyl-coenzyme m reductase subunit c	2.2	0.01	Degradation of bio-polymer	Flooded
K01179 endoglucanase [ec:3.2.1.4]	2.4	0.00	Degradation of bio-polymer	Flooded
K03422 methyl-coenzyme m reductase subunit d	2.6	0.00	Methanogenesis	Flooded
K15531 oligosaccharide reducing-end xylanase	2.6	0.03	Degradation of bio-polymer	Flooded
K02406 flagellin	3.1	0.00	Cell motility	Flooded
K00702 cellobiose phosphorylase [ec:2.4.1.20]	3.3	0.00	Degradation of bio-polymer	Flooded
K01181 endo-1.4-beta-xylanase [ec:3.2.1.8]	3.4	0.00	Degradation of bio-polymer	Flooded
K01225 cellulose 1.4-beta-cellobiosidase [ec:3.2.1.91]	5.0	0.00	Degradation of cellulose	Flooded
K03235 elongation factor 3	-3.7	0.00	Fungal ribosomal protein	Drained
K03891 ubiquinol-cytochrome c reductase cytochrome b subunit	-3.6	0.00	Oxidative phosphorylation	Drained
K03379 cyclohexanone monooxygenase [ec:1.14.13.22]	-3.4	0.00	Degradation of aromatic compounds	Drained
K00982 adenylyltransferase / [glutamine synthetase]-adenylyl-l-tyrosine phosphorylase	-3.1	0.00	Peptide fermentation	Drained
K13571 proteasome accessory factor a [ec:6.3.1.19]	-2.8	0.04	Degradation of proteins	Drained
K01414 oligopeptidase a [ec:3.4.24.70]	-2.7	0.04	Hydrolysis of oligopeptides	Drained
K01114 phospholipase c [ec:3.1.4.3]	-2.2	0.00	Cleave phospholipids	Drained
K02301 protoheme ix farnesyltransferase [ec:2.5.1.-]	-2.1	0.02	Oxidative phosphorylation	Drained
K19302 undecaprenyl-diphosphatase [ec:3.6.1.27]	-2.1	0.03	Peptidoglycan biosynthesis	Drained
K02438 glycogen debranching enzyme [ec:3.2.1.196]	-2.0	0.00	Glycogen metabolism	Drained

[1] log2 foldchange between flooded and drained soil, blue colour (positive value) indicates a transcript that is enriched in flooded soils, while dark pink colour (negative value) indicates a transcript that is enriched in drained soils.
[2] FDR corrected *P* values

***Table 3.11*:** *Transcripts involved in compatible solute transport or trehalose metabolism in drained soils*

KEGG Genes (level 4)	***Log_2 fold change Flooded/drainage*** [1]	***P value***	***P value*** [2]	***Function***
K01259 proline iminopeptidase [ec:3.4.11.5]	-2.1	0.00	0.1	Proline utilization
K13821 proline dehydrogenase	-1.9	0.00	0.0	Proline utilization
K06044 trey; (1->4)-alpha-d-glucan 1-alpha-d-glucosylmutase [ec:5.4.99.15] [rn:r01824]	-1.5	0.003	0.09	Trehalose metabolism
K00697 trehalose 6-phosphate synthase [ec:2.4.1.15]	-1.5	0.004	0.1	Trehalose transport

[1] log2 foldchange between flooded and drained soil, blue colour (positive value) indicates a transcript that is enriched in flooded soils, while dark pink colour (negative value) indicates a transcript that is enriched in drained soils.
[2] FDR corrected *P* values

4 Discussion

Agricultural practices, mainly rice farming and livestock rearing, are considered to be the primary anthropogenic sources of methane emissions (IPCC, 2013). Rice farming alone contributes 10% to the total methane emitted to the atmosphere (Conrad, 2009). This is why paddy soil is frequently used as a model system to study methane emission, methanogenesis, and methanotrophy (Conrad and Frenzel, 2002). It represents an ideal system to study the structure-function relationships of microbial communities and how they adapt to the environmental conditions occurring in different soil compartments: bulk soil, surface soil, rhizosphere soil. Paddy soil has also been used as a model system to understand microbial plant bio-polymer breakdown (Glissmann and Conrad, 2002; Glissmann et al., 2005; Wegner and Liesack, 2016). Because rice field soil goes through alternating flooding and drainage periods, paddy soil represents a suitable system to study the effects of drought on microbial communities in soil. Previous studies on the effects of drainage (desiccation) and oxygenation, however, have mostly focused on particular functional guilds – namely, methanogens and methanotrophs (Henckel et al., 2000; Ma and Lu, 2011; Ma et al., 2012, 2013). Other studies have been methodologically limited to using PCR gene-based approaches (SSU rRNA, *pmoA*, and *mcrA*) to assess the effect of environmental variables on bacterial and archaeal communities in paddy soils (Henckel et al., 2000; Ma and Lu, 2011; Ma et al., 2012, 2013; Breidenbach et al., 2015; Breidenbach and Conrad, 2015; Reim et al., 2017).

The major objective of my PhD research was to elucidate how soil oxygenation and drying through drainage shapes the active bacterial, archaeal, and microeukaryotic communities in paddy soils. My research involved community-wide analysis of the total rRNA and mRNA via random-primed cDNA synthesis, which allowed me to link structural (rRNA) responses to drainage with functional (mRNA) ones. The mRNA analysis involved both taxonomic profiling and functional annotation. The functional gene expression analysis was focused particularly on CAZyme transcripts to achieve insights into the degradation of plant bio-polymers in both flooded and drained soils. The breakdown of plant bio-polymer is an important process in flooded paddy soil (Wegner and Liesack, 2016), yet the degradation of bio-polymer in drained paddy soil is poorly studied.

4.1 Effects of drainage on soil physical and chemical parameters

At a depth of 2 cm, the flooded soil was characterised by suboxic conditions. In preceding microcosms studied, no oxygen was detectable at this depth (Noll et al., 2005; Shrestha et al., 2007). The suboxic conditions were most likely caused by the soil being incubated under alternating day and night cycles (Frenzel et al., 1992). Drainage altered the flooded soil into a dry and oxic soil system. The gravimetric moisture content decreased during drainage to about 11%. This moisture content resembles field conditions in dry seasons, with 10% or less moisture (Soontranon et al., 2014). We anticipated that the corresponding change in water potential (-0.875±0.150 MPa) would decrease the relative abundance of gram-negative bacteria and soft-body soil fauna (Griffin, 1981; Manzoni et al., 2012) but, relatively favour the proliferation of gram-positive bacteria, actinomycetes, and some fungi. These latter groups are known to demonstrate optimal growth at -1 MPa and tolerate up to -15 MPa (Griffin, 1981).

4.2 Effects of drainage on absolute abundance of *Bacteria, Archaea,* and *Fungi*

The aim of my PhD research was not only to elucidate the relative changes in abundance that occur in response to drainage but also to quantify how drainage affects the microbial community. Therefore, absolute changes in abundance of the bacterial, archaeal, and fungal SSU rRNA genes and transcripts were determined before and after drainage.

With drainage, the bacterial SSU rRNA gene copy numbers decreased tenfold ($P = 0.017$); see **Figure 3.2**, **Table S1**. The gene copy numbers were used as a proxy for cell biomass. Generally, bacterial biomass has been found to decrease with drying and desiccation in other soil systems (Hueso et al., 2012; Alster et al., 2013; Naylor and Coleman-Derr, 2018). This agrees well with our results; however, SSU rRNA operon number per genome of the most abundant bacterial phyla in the flooded and drained soils may also have contributed to the drainage-induced decrease in bacterial SSU rRNA gene copy numbers. For example, *Proteobacteria* and *Actinobacteria* are known to have around 3 SSU rRNA copies per genome, while the phylum *Firmicutes* has on average about 5.8 (Vetrovsky and Baldrian, 2013). Interestingly, the bacterial SSU rRNA transcript numbers did not decrease with drainage. The increase in ratio between rRNA transcripts and rRNA gene copy numbers provides the first strong evidence for a metabolically active bacterial community after drainage (**Table S1**).

Methanogens are the most dominant archaeal group in paddy soil. Since methanogens are sensitive to oxygen and desiccation (Fetzer et al., 1993; Yuan et al., 2009), one would assume

that both archaeal SSU rRNA gene and transcript numbers will decrease during drainage; however, drainage had no significant effect on the SSU rRNA transcript numbers. Other studies have reported the same phenomenon (Watanabe et al., 2009; Ma and Lu, 2011; Ma et al., 2012; Breidenbach and Conrad, 2015). By contrast, both *mcrA* gene copy numbers and the potential for methane production decreased significantly during drainage, with the potential being zero in drained soil. In conclusion, the methanogenic community becomes dormant during drainage but maintains a high cellular rRNA level. This may be part of their ecological strategy. It may allow methanogens to rapidly respond with activity to more favourable environmental conditions.

The environmental scenario is different for fungi. Little is known about fungi in paddy soil, with only a small group of filamentous fungi identified (Choi, 2003; Tonouchi, 2009). Fungi are mostly aerobes. The penetration of oxygen during drainage induced fungal activity and led to an increase in fungal SSU rRNA gene and transcript numbers in our soil system and in other paddy soil research (Pan et al., 2016). The anoxic or suboxic nature of the flooded soil could be inhibitory to most fungal activity.

4.3 The use of a 'double RNA approach' – Illumina RNA sequencing (RNA-Seq) and computational analysis

In our research, I analysed total RNA rather than specifically enriching mRNA by subtractive hybridisation of ribosomal RNA. Such an enrichment would not only have made it impossible to analyse the effects of drainage on community structure (due to removal of rRNA) but would also have introduced bias in the mRNA composition (van Dijk et al., 2014). It is also important to note that Illumina RNA-Seq produced reads ranging from 180 bp to 480 bp in length. Read lengths greater than 150 bp are expected to increase annotation efficiency (Wommack et al., 2008). Additionally, the proportion of annotated reads increased from 0.36 to 0.52 for reads between 300 and 500 bp (Shrestha et al., 2009). Even though there is a difference in the number of raw reads obtained for flooded and drained soil samples, the datasets of taxonomically and functionally annotated mRNA reads were in the same size range for all samples (except for sample 28F1). Hence, no further sequencing effort was needed.

Stringent quality check procedures were applied to the metatranscriptomic datasets in order to remove all ambiguous, low-quality reads. This included removal of reads with low sequence

complexity and ambiguous nucleotide positions. Additionally, length cut-offs of 250 bp for SSU rRNA and 180 bp for mRNA were applied to ensure accurate and high-resolution annotation (Wommack et al., 2008).

4.4 The development of drainage-specific microbial communities in paddy soil

Microbial diversity is usually linked in soil microbiome studies with higher metabolic potential of the microbial community. The higher potential can facilitate nutrient decomposition and mineralisation (Naylor and Coleman-Derr, 2018). In upland agriculture and desert soils, drought has been seen to have minimal impact on the microbial alpha-diversity (Acosta-Martinez et al., 2014; Armstrong et al., 2016; Naylor and Coleman-Derr, 2018). Similarly, in our research, drainage slightly decreased alpha-diversity. The OTUs used for diversity analyses were derived from random regions of the SSU rRNA due to random-primed cDNA synthesis. This led to higher alpha-diversity indices compared to those in previous amplicon-based studies.

The composition of the active bacterial, archaeal, and fungal communities significantly changed with drainage (**Figure 3.5, Figure 3.6**). These changes were detected on the SSU rRNA level and, in most cases, were supported by taxonomic profiling of mRNA. As in previous drought studies, significant drainage-induced shifts were detected on the phylum level (Barnard et al., 2013; Bouskill et al., 2013; Acosta-Martinez et al., 2014; Evans et al., 2014). In addition, I also discuss the effects of drainage at the family (SSU rRNA and mRNA) and genus (only SSU rRNA) levels.

Bacteria. Families of the phylum *Firmicutes*, such as *Ruminococcaceae, Lachnospiraceae,* and *Clostridiaceae*, were prevalent in flooded soil. This finding is consistent with their anaerobic lifestyle (Cotta and Forster, 2006; Wiegel et al., 2006; Rainey, 2015). When drainage was applied, *Clostridiaceae* appeared to be more persistent than *Ruminococcaceae* and *Lachnospiraceae* at the SSU rRNA level. This persistence may be explained by the ability of *Clostridiaceae* to detoxify reactive oxygen species (ROS), as demonstrated for *Clostridium acetobutylicum* (Kawasaki et al., 2009).

Drainage enriched *Proteobacteria* and *Actinobacteria* on both SSU rRNA and mRNA levels. This finding is in agreement with previous studies, which revealed that drought led to an increase in abundance of *Proteobacteria*, *Planctomycetes*, and *Actinobacteria* in grasslands,

semiarid shortgrass steppe, forest soil, and agricultural soil (Barnard et al., 2013; Bouskill et al., 2013; Acosta-Martinez et al., 2014; Evans et al., 2014). Among *Proteobacteria*, the family *Comamonadaceae* exhibited the highest relative abundance in drained soil. This family has been reported to be one of the most active populations in oxygenated Vercelli rhizosphere soil (Lu et al., 2006). The two major actinobacterial families in drained soil were *Nocardioidaceae* and *Streptomycetaceae*. Notably, particular genera within *Nocardioidaceae*, such as *Marmoricola* was not detectable in the flooded soil.

In rice field soil, methanotrophs play a crucial role in methane cycling. Drainage increased their relative abundance. Moreover, drainage favoured Type I methanotrophs over Type II methanotrophs. This finding concurs with those from previous studies (Henckel et al., 2000; Ma et al., 2013); however, methanotrophs were inactive under drained conditions, as concluded from the low abundance of their pMMO transcripts. This may be due to the soil's low moisture content, which was below the level (20% v/v) favourable for methanotrophy (Jackel et al., 2001; Ho et al., 2016).

Planctomycetes are known inhabitants of paddy soil (Derakshani et al. 2001; Wegner & Liesack 2016). Their relative abundance on the SSU rRNA level (not supported with statistical significance) and mRNA level (P [FDR] ≤ 0.01) increased with drainage (**Figure 3.6**). A similar finding has been made for grasslands. There, the SSU rRNA abundance of *Planctomycetes* increased under extreme desiccation (Barnard et al., 2013).

Overall, it was apparent that the bacterial community responded to drainage by reviving dormant and rare groups within the *Proteobacteria*, *Actinobacteria*, and *Planctomycetes*.

Archaea. Relative and absolute abundances of the *archaea* were not affected by drainage, on either the SSU rRNA gene or the SSU rRNA transcript levels. Previous studies that specifically examined how drainage affects methanogen abundance in rice field soil also arrived at the same finding (Watanabe et al., 2009; Breidenbach and Conrad, 2015). The abundance of methanogen mRNA, however, significantly decreased with drainage, from 7% to 1.4%, in metatranscriptomic datasets (see Section 4.7, 'Drainage-induced changes in functional gene expression', for further details).

In our study, the methanogenic community's composition slightly changed with drainage. *Methanosarcinales* were favoured over *Methanocellales* (**Figure 3.6**). Conflicting results have

previously been reported for the effect of drainage or desiccation on the methanogenic community. Some studies did not observe any effect on methanogens community's composition (Watanabe et al., 2009; Ma and Lu, 2011). Other studies demonstrated a community shift towards an increase in abundance of the *Methanosarcinales* (Itoh et al., 2013; Breidenbach et al., 2015). Even though both *Methanosarcinales* and *Methanocellales* are classified as oxygen-tolerant Type II methanogens (Lyu and Lu, 2018), *Methanosarcinales* have been found to be more abundant than *Methanocellales* in arid environments (Angel et al., 2012). In our flooded samples, while *Euryarchaeota* (mostly methanogens) were the most abundant archaeal phylum, members of the new phylum *Candidatus Bathyarchaeota* represented 6% of the total archaeal SSU rRNA in flooded soil. This largely unexplored Candidatus phylum may harbour methanogens or anaerobic methane oxidisers (Evans et al., 2015; Zhou et al., 2018). Furthermore, members of this phylum were recently reported to thrive in paddy soil (Lee et al., 2015; Bai et al., 2017; Vaksmaa et al., 2017)

The discrepancy in methanogen response to drainage or desiccation is difficult to explain. It may be due to physical and chemical soil parameters being different among the studies. Among these parameters, the moisture content of soil may be the most decisive factor. For example, soil moisture content was 45% or less in studies where shifts occurred in the methanogenic community's composition; see **Table 4.1** (Itoh et al., 2013; Breidenbach et al., 2015). By contrast, drainage studies with no change in the methanogenic community's composition had a soil moisture content higher than 45%; see **Table 4.1** (Watanabe et al., 2009; Ma and Lu, 2011).

Remarkably, archaeal diversity increased with drainage. In particular, the abundance of non-methanogenic taxa, such as *Halobacteriaceae* and *Nitrososphaerales*, significantly increased. This increase in abundance was primarily detectable on the mRNA level. *Nitrososphaerales* are obligate aerobes that oxidise ammonia (Stieglmeier et al., 2014). Archaeal ammonia oxidisers (*Crenarchaeota* or *Thaumarchaeota*) have previously been reported to increase in abundance under crop rotation (Breidenbach et al., 2015). Nonetheless, the proliferation of *Halobacteriaceae* under drained and oxic paddy-soil conditions was unexpected. The increase in abundance of non-methanogenic archaea under drainage suggests that the response of bacterial and archaeal communities to environmental change follows the same principles – namely, adaptation by reviving dormant groups.

Table 4.1*: Literature describing the response of methanogens to drainage or desiccation, or both*

Papers where change occurring in the methanogenic community after drainage/desiccation **was** documented	SSU rRNA gene	SSU rRNA transcript	mRNA	Moisture content
Breidenbach *et al.* 2015	√	√	NA	32 to 36 (w/w)%
Itoh *et al.* 2013	√	√	NA	40 (v/v)%
This study	√	√	√	11.5 (w/w)%
Papers where change occurring in the methanogenic community after drainage/desiccation was not documented	**SSU rRNA gene**	**SSU rRNA transcript**	**mRNA**	**Moisture content**
Watanabe *et al.* 2009	√	√	NA	58 (w/w)%
Ma & Lu 2011	√	NA	NA	70 to 80 (w/w)%

(v/v) = volumetric water content
(w/w) = gravimetric water content

Eukarya. *Cercozoa* and *Acanthamoeba* were the most prominent taxa in flooded soil. In Vercelli paddy soil, both *Cercozoa* and *Acanthamoeba* have previously been found to graze on the bacterial community (Murase et al., 2006; Murase and Frenzel, 2008).

Drainage had a significant impact on the abundance of *Ascomycota* and *Basidiomycota*. As previously mentioned, substrate availability (rice straw) and oxygen penetration may explain the increase in abundance of these fungal groups (Pan et al., 2016). *Ascomycota* and *Basidiomycota* contain saprotrophic members with the ability to degrade lignocellulosic biomass and decaying organic matter (Hibbett et al., 2014; Maharachchikumbura et al., 2015).

Under flooded soil conditions, plant-related (*Archaeplastida*) sequences contributed most to the eukarya mRNA but not to eukarya SSU rRNA. Most likely, this discrepancy in the taxonomic affiliation of eukarya SSU rRNA and mRNA is due to a database bias towards *Archaeplastida*. Given that, protists (*Cercozoa*, or the SAR super-group) were the most abundant eukaryotes in flooded soil. Members of the SAR super-group are poorly represented in public genome databases. This phenomenon has also been observed in a peatland study by Ivanova et al. (2016).

4.5 SSU rRNA dynamics versus mRNA turnover

Our study revealed that in response to environmental change, mRNA turnover is more pronounced than rRNA dynamics. This result agrees with previous observations (Peng et al.,

2017). Moreover, it agrees with existing knowledge in the literature, which suggests that rRNA degradation occurs only under extreme conditions such as extended starvation (Deutscher, 2003). By contrast, mRNA degradation occurs within minutes for bacteria and within minutes to hours for archaea (Evguenieva-Hackenberg and Klug, 2009; Peterson et al., 2016). Therefore, taxonomic profiling of mRNA reveals compositional shifts in response to environmental change with greater statistical significance than SSU rRNA analysis does, for both the bacterial and archaeal communities.

Dormant microbial cells are known to maintain a large number of SSU rRNA transcripts. The maintenance level of cellular rRNA under stress or dormancy is taxon-specific and related to the ecological life strategy of each microbial group (Blazewicz et al., 2013). For this reason, the use of SSU rRNA as a proxy for microbial activity has serious limitations (Blazewicz et al., 2013). In our study, this is most obvious for the *Clostridiaceae* and methanogenic community. While their SSU rRNA abundance was nearly unaffected by drainage, the mRNA profiles made it evident that despite a stable SSU rRNA abundance, the metabolic activity of *Clostridiaceae* and methanogens was significantly inhibited by drainage. Therefore, taxonomic mRNA profiling is highly recommended for studying the responses of bacterial and archaeal communities to environmental change. The situation may be different for microeukaryotic communities due to their poor representation in public genome databases. Thus, studies that intend to assess community response across all three domains of life have to perform taxonomic profiling of both SSU rRNA and mRNA.

4.6 Environmental factors driving drainage-induced community change

One major objective of our research was to understand which of the two key factors, oxygen and desiccation, contributes most to the observed effects of drainage on the microbial community in soil. The drained soil had a water potential of about -0.87 MPa. It was previously shown that high water potential (-0.5 MPa or higher) correlates with the increased abundance of *Firmicutes* (Evans et al., 2014; McHugh et al., 2014). Therefore, desiccation may have had a major effect on the decrease in abundance of *Firmicutes*.

Similarly, in grassland soil, *Proteobacteria* were found to be less abundant in soil adjusted to a water potential of -0.5 or -1.0 MPa than in soil adjusted to -0.1 MPa (Evans et al., 2014). However, in our study, *Proteobacteria* were enriched during drainage, with *Ramlibacter* (family: *Comamonadaceae*) being the most abundant genus. *Ramlibacter* is an aerobic, Gram-

negative cyst-forming bacterium that was found in the Tataouine desert and is known to tolerate arid conditions (De Luca et al., 2011). Such an increase in phylum-level abundance based only one or two resident members in soil has previously been reported (Naylor and Coleman-Derr, 2018).

Actinobacteria was the second most abundant phylum in drained paddy soil. Its members are known to thrive in arid soils with a water potential of up to -10 MPa (Manzoni et al., 2012). A soil water potential of -1.5 MPa led to an increase in actinobacterial abundance, compared with soil with a higher water potential (Evans et al., 2014).

In our study, a firm conclusion on how oxygen and desiccation contributed to the drainage-induced dynamics of *Firmicutes*, *Proteobacteria*, and *Actinobacteria* cannot be drawn. Several factors could have been involved in the relative abundance changes occuring to these phyla, such as (i) oligotrophy (in the case of *Actinobacteria*), (ii) the physiological capability to tolerate desiccation (in the case of *Ramlibacter*), and (iii) the change from favourable anoxic to unfavourable oxic conditions (in the case of *Firmicutes*). However, most likely, oxygen was the main driver of proliferation of the aerobic microorganisms, with desiccation as a factor that selected for bacteria well-adapted to tolerate a water potential of around 1 MPa.

Among the archaea, drainage completely inhibited methanogenic activity. Methane production was nearly negligible at a water potential of -1.5 MPa (Rath et al., 1999); however, we obtained rRNA- and mRNA-based evidence that methanogens can persist in a viable state during drainage. This agrees with previous results showing that methanogens remain viable under desiccation and oxygen stress, while methane production drastically decreases (Fetzer et al., 1993; Rath et al., 1999; Watanabe et al., 2009; Anderson et al., 2012). This also concurs with findings about the ability of methanogens to recover after rewetting (Reim et al., 2017). In a pure culture study of *Methanosarcina* sp. strain MVF4, it was demonstrated that although oxygen inhibited methane production, 100% of the cells remained viable. On the contrary, desiccation decreased cell viability of methanogens to 10% and less than 5% under anoxic and oxic conditions, respectively (Fetzer et al., 1993). Thus, we assume that desiccation had a stronger effect than oxygen on the decrease of methanogens' mRNA. The drainage-induced proliferation of *Haloarchaea* can be attributed to their known tolerance to desiccation stress (Stan-Lotter and Fendrihan, 2013).

Within the eukaryotic community, fungi are mostly aerobes and known to tolerate desiccation

and a water potential as low as -60 MPa (Manzoni et al., 2012). In straw-amended Chinese paddy soil, fungal biomass was found to increase in response to oxygen intrusion (Pan et al. 2016). However, fungal LSU rRNA and biomass did not change significantly in upland soil (grassland) under an extreme desiccation and rewetting regime (Gordon et al., 2008; Barnard et al., 2013; Fuchslueger et al., 2016). These previous results suggest that the drainage-induced increase in oxygen availability is the most likely factor favouring proliferation of fungi in drained paddy soil.

On the other hand, desiccation is the most likely driver of the decrease in abundance of protists in drained paddy soil. The most negative water potential that these microeukaryotes can tolerate is -0.15 MPa (Alabouvette et al., 1981; Stefana et al., 2014). *Cercozoa* were the most abundant protists in flooded soil and exhibited a rapid response to the decrease in water availability in soil (Stefana et al., 2014).

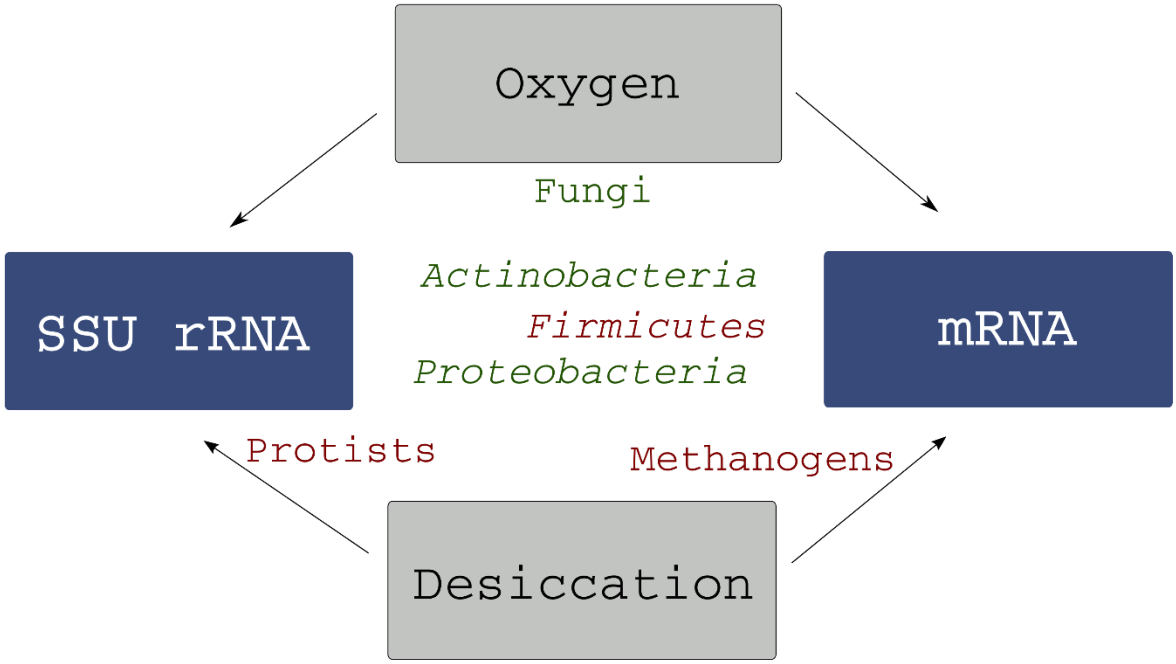

Figure 4.1: The effect of oxygen and desiccation on microbial community dynamics. Methanogens are near the mRNA box, because the effects of drainage were observed only on the mRNA level. The relative taxon abundance either increased (green) or decreased (red) with drainage.

4.7 Drainage-induced changes in functional gene expression

The analysis of the mRNA content in flooded and drained soils provides us with greater insight into microbial community activity under contrasting soil conditions. The proportion of mRNA in total RNA has been proposed to be a useful proxy for the short-term effects of environmental change on community-wide gene expression and metabolic activity (Peng et al., 2017). Interestingly, 9-day drainage did not have a significant effect on the proportion of mRNA in total RNA (**Table 3.4**). This observation, combined with stable bacterial and archaeal SSU rRNA abundances, indicates that the decrease in soil moisture and increase in oxygen concentration had no detrimental effect on functional gene expression. In addition to concurring with the taxonomic profiles of SSU rRNA, the mRNA datasets allowed us to understand the differential effect of drainage on functional gene expression. The next sections discuss this differential effect for particular functional categories.

4.7.1 Cellular processes: Decrease in cell motility but increase in transcription and translation

Maintenance metabolism such as 'energy metabolism' had, relative to other functional categories, a stable gene-expression level in both flooded and drained soils. This has also commonly been observed in other ecosystems, including ocean surface water and Rotböll sand-dune soil (Frias-Lopez et al., 2008; Urich et al., 2008). The drainage-induced decrease in 'cell motility' transcripts is related to the change in the water status of soil. In dry soil, other microbial movements are used, such as gliding, twitching, sliding, and swarming (Or et al., 2007).

After drainage, the increase in relative abundance of transcripts involved in genetic information processing such as transcription and translation, including *rpoB*, point towards an actively growing and newly developing bacterial community. In particular, *Proteobacteria* and *Actinobacteria* were the phyla expressing these transcripts. Specifically, *rpoB* transcripts are thought to be a reliable proxy for microbial activity (Barnard et al., 2013). Similarly, the increase in abundance of the phylum *Actinobacteria*, whose members have the ability to utilise hydrocarbons and lipids and to produce terpenoids and polyketides (Coleman et al., 2011; Kimbrel et al., 2013; Song et al., 2016), can be related to the increase in the KEGG level 2 functional categories 'xenobiotic degradation', 'lipid metabolism', and 'metabolism of terpenoids and polyketides'.

Reactive oxygen species (ROS), such as the superoxide anion radical (O_2^-), hydroxyl radicals (·OH), and hydrogen peroxide (H_2O_2), are generated continuously in cells grown aerobically (Fu et al., 2015). Thus, aeration of the soil through drainage is expected to induce the production of ROS enzymes; however, the relative abundance of ROS transcripts did not significantly differ between flooded and drained soils. This may be explained by the increased generation of endogenous ROS in anaerobes and facultative anaerobes due to the suboxic conditions measured in flooded soil after the 28-day pre-incubation period. Other reasons could be the presence of exogenous ROS generated (i) photochemically, (ii) by some bacteria for competitive advantage, or (iii) through the oxidation of reduced metals (Mishra and Imlay, 2012).

4.7.2 Decrease in methanogenesis-related transcripts

Drainage induced a nearly 300-fold decrease in *mcrA* transcripts in good agreement with previous results on the response of methanogens to oxygen and desiccation stress (Watanabe et al., 2009; Ma et al., 2012). In our study, this 300-fold decrease in *mcrA* transcript copies corresponds perfectly to the fact that the expression of nearly all the genes involved in the methane metabolism pathway was significantly reduced and, as a consequence, the potential for methane production was zero in dry soil. However, given the zero potential for methane production (**Table 3.1**), it remains unclear why *mcrA* transcription was not completely downregulated under desiccation and oxygen stress. It may be that methanogens maintain a minimum expression level of *mcrA* in dry paddy soil to allow for a rapid re-initiation of methanogenesis whenever the environment returns to providing favourable conditions (Watanabe et al., 2009). This would also explain the high maintenance level of their SSU rRNA. Rapid initiation of methanogenesis has been seen to occur in dryland environments within 7–14 days of incubation under anoxic conditions (Angel et al., 2012) and also in paddy soil (Reim et al., 2017).

4.7.3 Drainage-induced effects on bio-polymer degradation

The CAZyme dbCAN database was used to unravel the mechanisms by which microbial communities in paddy soil degrade bio-polymers in flooded and drained soils. Interestingly, the relative expression level of total CAZyme transcripts did not change between flooded and drained soils, indicating that the potential for bio-polymer degradation remains stable under the two contrasting soil conditions. However, the expression level of different CAZyme classes

changed with drainage. For example, upon drainage, there was a significant decrease in abundance of the CBM transcripts but an increase in the GT transcripts. The two main glycosyltransferases were GT2 and GT4. This increase in abundance of GT2 and GT4 can be linked to the revival of dormant bacterial and fungal groups. Both GT2 and GT4 are considered major glycosyltransferase families (Henrissat et al., 2008). Furthermore, GT2 is involved in the biosynthesis of disaccharides, oligosaccharides, and polysaccharides, while GT4 is involved in cell-wall peptidoglycan synthesis (Henrissat et al., 2008).

With regard to rice straw degradation, drainage had a minor effect on the relative abundance of transcripts encoding GHs and CEs involved in degrading the hemicellulose constituents of rice straw, especially with regard to endo-b-1,4-xylanase (GH5), a-galactosidase (GH36), and acetyl xylan esterase (CE4). By contrast, the relative abundance of CAZyme transcripts involved in cellulose degradation significantly decreased with drainage. This may be explained by complex cellulase systems (cellulosomes) being present only under anoxic conditions (Lynd et al. 2002; Schwarz 2001). As discussed above, the taxa involved in cellulose and hemicellulose degradation in flooded soil were *Firmicutes* (*Clostridia* and *Bacilli*) and, to a lesser extent, *Actinobacteria* and *Bacteroidetes* (Wegner and Liesack, 2016). In drained soil, the taxonomic sources of CAZymes involved in cellulose and hemicellulose degradation were mostly *Actinobacteria* and *Proteobacteria*. This finding is in accordance with the taxonomic profiles of SSU rRNA and total mRNA. Members of these phyla are well-known for their ability to degrade lignocellulose (Lynd et al., 2002; Cragg et al., 2015). The functional gene expression profiles suggest that after drainage, eukarya played a stronger role in plant bio-polymer degradation than that in flooded soil, albeit transcripts encoding the glycoside hydrolase family 7 (GH7) were not detected. GH7 encompasses only fungal cellobiohydrolases (Wilson, 2011). These transcripts not being detected suggests that in drained paddy soil, fungi used GH families other than GH7 for cellulose degradation (Berlemont, 2017). The two major fungal classes involved in plant bio-polymer degradation in drained paddy soil are *Saccharomycetes* and *Sordariomycetes*, which have the genetic potential for cellulose and xylan degradation (Berlemont, 2017).

Lignin is one of the recalcitrant components of rice straw. The significant increase in abundance of CAZyme transcripts involved in lignin degradation (AA family) agrees well with the fact that the well-known lignin-degradation processes are based on oxygen-dependent enzymes (Brown and Chang, 2014). *Actinobacteria* and *Proteobacteria* were the main players in lignin

degradation in paddy soil. Bacterial lignin degraders such as *Streptomyces*, *Sphingomonas*, *Pseudomonas*, and *Burkholderia* are all members of the phyla *Actinobacteria* and *Proteobacteria* (Bugg et al., 2011). The significant increase in abundance of the KEGG level 2 category 'xenobiotic biodegradation' in drained paddy soil can be linked to the boost in lignin degradation transcripts. Lignin degradation produces a pool of mixed aromatic compounds, which can be metabolised by a variety of organisms (Cragg et al., 2015).

Chitin is an important component of the fungal cell wall. In agreement with previous research (Wegner and Liesack, 2016), chitinase transcripts (GH19 and CBM 37, CBM 50) were enriched in flooded paddy soil. *Clostridia* contributed the most to the CAZyme transcript pool involved in chitin degradation. Within the class *Clostridia*, *Clostridium phytofermentans* was shown to hydrolyse fungal cells while growing on cellulose (Tolonen et al., 2015). In our study, the number of fungal SSU rRNA genes per gram dry weight of flooded soil were as high as 10^6 gene copies. Therefore, we support the conclusion that during cellulose degradation, members of the class *Clostridia* concomitantly feed on fungi during the degradation of cellulose (Tolonen et al., 2015; Wegner and Liesack, 2016). The decrease in *Clostridia* mRNA could be why the relative expression level of transcripts involved in cellulose and chitin degradation concomitantly decreased with drainage.

Remarkably, drainage led to the enrichment of transcripts affiliated with GHs involved in the degradation of other substrates such as GH23 family. The GH23 family contains lysozymes that catalyse the lysis of the peptidoglycan component of bacterial cell walls (Lombard et al., 2014). Also, CAZymes of the GH13 family and the accompanying CBM48 family were significantly (P [FDR] ≤ 0.1) enriched in drained soil. Both GH13 and CBM48 are involved in glycogen breakdown (Lombard et al., 2014). This suggests that during drainage, the microbial community utilises substrates released from dead and lysed cells and their own storage molecules. Similar phenomena were detected in forest soil, where the microbial community switched to utilising storage compounds under unfavourable nutrient-limiting winter conditions (Zifcakova et al., 2017).

The abundance of CAZyme transcripts expressed by *Planctomycetes* significantly increased with drainage. *Planctomycetes* are inhabitants of different terrestrial and aquatic ecosystems and are known to be slow degraders of plant bio-polymers. Recently, it was demonstrated that *Planctomycetes* play an important role in bio-polymer breakdown in peatlands (Ivanova et al.,

2016, 2017). The increase in CAZyme expression by *Planctomycetes* is related to the increase in their abundance on both SSU rRNA and mRNA levels and their ability to adapt to dry and oxic conditions (Barnard et al., 2013). The level of cyanobacterial SSU rRNA and mRNA did not change with drainage; however, their contribution to the CAZyme transcript pool significantly increased. This was mainly attributed to the increased expression of glycosyltransferases. *Cyanobacteria* were shown to be involved in the production of extracellular polysaccharides (EPS) in arid environments (Mager and Thomas, 2011). The high cyanobacterial GT transcript level suggests that drainage triggered EPS production to increase their drought tolerance. The EPS also may have been a carbon source used by various microorganisms during drainage (Rossi and De Philippis, 2015).

4.8 The pre-incubation period and its impact on drainage-induced community effects

The main aim of my thesis was to understand how microbial communities in paddy soil respond to drainage. The analysis involved both taxonomic and functional profiling. In addition, we decided that it was also important to know whether the pre-incubation period under flooded conditions has an effect on this response. As discussed in the Introduction (section 1), drainage can be applied either during the rice-growing season (e.g. mid-season drainage) or after harvest. Here, we compared the potential effects of short-term (7-day) and long-term (28-day) pre-incubation under flooded conditions on the microbial community that responds to drainage. Seven-day pre-incubation resembles mid-season drainage, while 28-day pre-incubation resembles long-term water-saturated paddy soil. First, we assessed the changes in taxonomic composition and functional gene expression between flooded and drained soils after either a 7-day or a 28-day pre-incubation period. Next, we compared the taxonomic and functional community composition of the two drained soils using the DESeq2 package. This is an R package that estimates variance-mean dependence in count data from high-throughput sequencing and checks for differential expression based on a model using the negative binomial distribution (Love et al., 2014).

4.8.1 Pre-incubation period effects on the drainage-induced changes in taxonomic composition

Regardless of the duration of pre-incubation, the alpha diversity of the microbial communities slightly decreased with drainage. This agrees with the results of previous research (Naylor and Coleman-Derr, 2018). The PCoA plot revealed that the duration of pre-incubation had a major

impact on the microbial community in flooded soil; however, this impact was clearly less pronounced in drained soils. The microbial communities in drained soils clustered closely together, most probably due to the similar environmental conditions in these soils (**Table 3.1**, **Table S11**). The duration effect on the microbial communities in flooded soil can be attributed to the different nutrient statuses after 7 or 28 days of pre-incubation (Noll et al., 2005; Wegner and Liesack, 2016).

In general, the outcome of the DESeq2 analysis agrees well with the results presented in section 3.6. Members of the phyla *Firmicutes*, *Proteobacteria*, and *Actinobacteria* and the kingdom fungi had the greatest number of OTUs, the relative normalised abundance of which significantly differed between flooded and drained soils. Aside from supporting the taxonomic profiles of SSU rRNA and mRNA, the DESeq2 analysis allowed us to detect members of the rare communities that were differentially abundant between flooded and drained soils. An example is the aerobic chemoheterotrophic members of the phylum *Armatimonadetes*, which may be involved in carbon fixation (Tamaki et al., 2011). Other examples are aerobic members of the *Firmicutes* and chemoheterotrophic *Bacteroidetes*, which significantly increased in abundance with drainage (Kwon et al., 2007; Garcia-Fraile et al., 2008).

As evidenced by the DESeq2 diagnostic plot, the microbial communities of the two drained soils differed only in a few characteristic OTUs. This finding relates to the fact that the two communities clustered closely together in the PCoA. Fungi of the order *Mucorales* (*Mucor* and other as-yet-uncharacterised fungi) were mainly detected in drained soil after 7-day pre-incubation. Members of these groups are known to be saprobic fungi that degrade lignocellulosic biomass (Hoffmann et al., 2013). They are also known to be *r*-strategists, which may explain why they are only present in drained soil after 7-day pre-incubation (Richardson, 2002; Veresoglou et al., 2018). In contrast, OTUs affiliated with *Bacteroidetes* were mainly detected in drained soil after 28-day pre-incubation. These OTUs may be indicative of *K*-strategists. Members of the *Bacteroidetes* play a major role in bio-polymer degradation in flooded, straw-amended paddy soil during the later incubation stages (Wegner and Liesack, 2016). Type I methanotrophs (genus: *Methylomonas*) were mainly present in drained soil after 28-day pre-incubation. This corresponds well with the detection of Type I methanotrophs in the oxic zone of flooded paddy soil in late-succession communities (Noll et al., 2005). *Methylomonas*, in particular, has been shown to increase after drainage events (Ma et al., 2013).

4.8.2 Pre-incubation period effects on the drainage-induced changes in functional gene expression

We also assessed how the duration of pre-incubation affected drainage-induced changes in functional gene expression. As observed for the taxonomic composition, the mRNA of the microbial communities in drained soils clustered together in the PCoA plot, indicating that differences in duration of the pre-incubation period had no major effect on functional gene expression after drainage. Drainage after 7-day and 28-day pre-incubation periods enriched for transcripts involved in biosynthesis of secondary metabolites, polyketides, and terpenoids, and lipid metabolism. In the heatmap, the highest value for transcripts involved in transcription and translation were detected in the drained soil samples after 7-day pre-incubation. Moreover, drained soil after a 7-day pre-incubation period had the highest mRNA in total RNA ratio (approximately 3.4%), indicating high metabolic activity. The presence of easily degradable organic matter in the drained soils after 7-day pre-incubation is the most likely cause for this high activity (Glissmann and Conrad, 2002). Collectively, our results unambiguously demonstrated that drainage induces the proliferation of a microbial community well-adapted to oxic and dry soil conditions. The microbial community in drained soil (after 7 or 28 days of pre-incubation) exhibited higher metabolic activity compared to that demonstrated by the microbial communities in flooded soils.

Even though the microbial communities in 7-day and 28-day flooded soils exhibited different functional profiles, both communities shared mRNA transcripts that were differentially expressed in response to drainage. In particular, these were transcripts encoding subunits of the methyl-coenzyme M reductase (MCR). Transcripts encoding cellulase, cellobiosidase, and endoglucanase were also over-represented in the two flooded soils. This suggests that regardless of the incubation period, cellulose degradation is more favoured by flooded soil conditions. Conversely, transcripts involved in the degradation of proteins, phospholipids, and oligopeptides were enriched in the metatranscriptome datasets from drained soils, suggesting that the newly developing communities are well-adapted to utilising storage compounds (e.g. glycogen) and proteins from decaying cells. In addition, the microbial communities in drained soils were characterised by increased numbers of transcripts encoding fungal ribosomal proteins. This implies that drainage induced fungal growth, as also evidenced by the quantitation of fungal SSU rRNA.

In addition to oxygen, desiccation is the second key variable affecting microbial communities in paddy soil. Bacteria are well-known to secrete exo-polysaccharides and exhibit an uptake or synthesise of compatible solutes to combat desiccation stress (Esbelin et al., 2018). Therefore, we surveyed our metatranscriptome datasets for the differential expression of genes involved in any of these pathways. The majority of transcripts involved in trehalose, glycine betaine, proline, and ectoine metabolism demonstrated a less than $\log_2$-fold change in their transcript level, and the corresponding FDR-corrected *P* values were higher than 0.05. We identified only a single transcript species involved in trehalose transport and two transcript species involved in proline utilisation or degradation that were upregulated during drainage (not supported with *P* [FDR] ≤ 0.05). Proline accumulation is expected to increase in response to stressful conditions (Liang et al., 2013). Therefore, during stress response, proline biosynthesis is expected to increase, while proline utilisation or degradation is expected to decrease (Liang et al., 2013). The near absence of differential expression of genes involved in synthesis or uptake of compatible solutes provides further evidence that the decrease in gravimetric moisture content of soil to about 11% during drainage did not have a detrimental effect on microbial community activity.

5 Conclusion and outlook

Our study revealed that the microbial communities (archaeal, bacterial, and eukaryotic) responded to drainage by reviving dormant microbial groups. These groups were well-adapted to oxic and dry soil conditions. Drainage did not have a detrimental effect on microbial activity in paddy soil. Moreover, it did not affect the absolute (RT-qPCR) SSU rRNA abundance of *Bacteria* and *Archaea* but significantly changed their community composition. Drainage also significantly changed the CAZyme profile (mRNA transcripts) of the microbial community in paddy soil and hence their substrate preference. In our study, the use of a metatranscriptomic approach allowed us to study the active microbial community by examining their SSU rRNA reads and the mRNA transcripts –'the double RNA approach'. Concurrently, it allowed us to decipher the metabolic potential of the paddy-soil microbial community in drained soils, which had not previously been explored. Our study has laid the foundation for research on how drainage affects the microbial community in paddy soil. However, the results presented here represent only a first insight. Our study was performed in engineered microcosms. Its results should be challenged by performing research based on a similar experimental design in planted rice fields, although the microcosms in this study were designed to mimic field conditions.

Our study demonstrated how drainage affected the paddy-soil microbial community on the taxonomic and functional levels after a single drainage event. During rice farming, rice fields are exposed to repeated wet and dry cycles. To relate to field conditions, future work should focus on examining whether the effect of drainage we present here is stochastic or determinative. Previous research has demonstrated that the microbial community in paddy soil does not return to its original community composition (initial incubation) after one drainage and one re-flooding event each (Hernandez et al., 2017; Reim et al., 2017). It would be of value to know if the second or the third drainage event results in the same taxonomic and functional changes that we observe here.

The observation that the microbial community in dry paddy soil had a higher potential to degrade storage molecules (e.g. glycogen) and peptidoglycan is interesting and should be studied in greater detail by specifically providing these substrates to the microbial communities in paddy soil under both flooded and drained conditions. The capability of the microbial community in dry paddy soil to degrade specific substrates such as cellulose, xylan, and chitin

should also be addressed in more detailed studies. Moreover, it would be interesting to discover the CAZyme expression profile in unamended, drained paddy soils to know whether the ability of the microbial community to degrade substrates released from dead cells is more pronounced. Unamended, flooded paddy soils are known to be nutrient-poor (Wegner and Liesack, 2016). Such studies will allow us to understand in greater detail the substrate preference of the microbial communities in drained paddy soil.

The findings presented in my PhD thesis highlight that high-throughput sequencing approaches such as metatranscriptomics can generate new hypotheses (Jansson, 2013). However, these approaches are strongly impaired by low assignment efficiencies of the mRNA datasets. (In this work, on average, 47% of the flooded soil mRNA and 67% of the drained soil mRNA had at least one hit in the nr database.) Moreover, assignment of mRNA, especially, could be biased towards publicly available genomes. This could be clearly seen in my study in the case of protists and *Archaeplastida*. Therefore, improved isolation is needed, especially for phyla that are poorly covered in public databases (e.g. protists, *Acidobacteria*, and *Verrucomicrobia*).

Altogether, drainage (oxygen and desiccation) is an environmental condition that shapes the taxonomy and functionality but not the activity of the microbial community in paddy soil. Drainage is highly relevant to global climate change as it a mitigation strategy for the high level of methane emissions produced by rice farming. Other experimental setups under field conditions are required to further research some of the findings presented in my PhD thesis. Likewise, efforts should be made to culture and isolate new microbes as they are crucial for complementing the exponential growth of high-throughput sequencing data.

6 References

Acosta-Martinez, V., Cotton, J., Gardner, T., Moore-Kucera, J., Zak, J., Wester, D., Cox, S., 2014. Predominant bacterial and fungal assemblages in agricultural soils during a record drought/heat wave and linkages to enzyme activities of biogeochemical cycling. Applied Soil Ecology 84, 69-82.

Alabouvette, C., Coûteaux, M., Old, K., Pussard, M., Reisinger, O., Toutain, F., 1981. Les protozoaires du sol: aspects écologiques et méthodologiques. Année biol 20, 255-303.

Alster, C.J., German, D.P., Lu, Y., Allison, S.D., 2013. Microbial enzymatic responses to drought and to nitrogen addition in a southern California grassland. Soil Biology & Biochemistry 64, 68-79.

Anderson, K.L., Apolinario, E.E., Sowers, K.R., 2012. Desiccation as a Long-Term Survival Mechanism for the Archaeon Methanosarcina barkeri. Applied and Environmental Microbiology 78, 1473-1479.

Angel, R., Claus, P., Conrad, R., 2012. Methanogenic archaea are globally ubiquitous in aerated soils and become active under wet anoxic conditions. ISME J 6, 847-862.

Angel, R., Matthies, D., Conrad, R., 2011. Activation of methanogenesis in arid biological soil crusts despite the presence of oxygen. PLoS One 6, e20453.

Armstrong, A., Valverde, A., Ramond, J.B., Makhalanyane, T.P., Jansson, J.K., Hopkins, D.W., Aspray, T.J., Seely, M., Trindade, M.I., Cowan, D.A., 2016. Temporal dynamics of hot desert microbial communities reveal structural and functional responses to water input. Scientific Reports 6.

Aronesty, E., 2011. ea-utils : Command-line tools for processing biological sequencing data.

Bai, R., Wang, J.T., Deng, Y., He, J.Z., Feng, K., Zhang, L.M., 2017. Microbial Community and Functional Structure Significantly Varied among Distinct Types of Paddy Soils But Responded Differently along Gradients of Soil Depth Layers. Frontiers in Microbiology 8.

Bapiri, A., Baath, E., Rousk, J., 2010. Drying-Rewetting Cycles Affect Fungal and Bacterial Growth Differently in an Arable Soil. Microbial Ecology 60, 419-428.

Barnard, R.L., Osborne, C.A., Firestone, M.K., 2013. Responses of soil bacterial and fungal communities to extreme desiccation and rewetting. ISME J 7, 2229-2241.

Berlemont, R., 2017. Distribution and diversity of enzymes for polysaccharide degradation in fungi. Scientific Reports 7.

Blazewicz, S.J., Barnard, R.L., Daly, R.A., Firestone, M.K., 2013. Evaluating rRNA as an indicator of microbial activity in environmental communities: limitations and uses. Isme Journal 7, 2061-2068.

Bouskill, N.J., Lim, H.C., Borglin, S., Salve, R., Wood, T.E., Silver, W.L., Brodie, E.L., 2013. Pre-exposure to drought increases the resistance of tropical forest soil bacterial communities to extended drought. Isme Journal 7, 384-394.

Breidenbach, B., Blaser, M.B., Klose, M., Conrad, R., 2015. Crop rotation of flooded rice with upland maize impacts the resident and active methanogenic microbial community. Environmental Microbiology

Breidenbach, B., Conrad, R., 2014. Seasonal dynamics of bacterial and archaeal methanogenic communities in flooded rice fields and effect of drainage. Frontiers in Microbiology 5.

Breidenbach, B., Conrad, R., 2015. Seasonal dynamics of bacterial and archaeal methanogenic communities in flooded rice fields and effect of drainage. Frontiers in Microbiology 5.

Brown, M.E., Chang, M.C., 2014. Exploring bacterial lignin degradation. Curr Opin Chem Biol 19, 1-7.

Bugg, T.D.H., Ahmad, M., Hardiman, E.M., Singh, R., 2011. The emerging role for bacteria in lignin degradation and bio-product formation. Current Opinion in Biotechnology 22, 394-400.

Cantarel, B.L., Coutinho, P.M., Rancurel, C., Bernard, T., Lombard, V., Henrissat, B., 2009. The Carbohydrate-Active EnZymes database (CAZy): an expert resource for Glycogenomics. Nucleic acids research 37, D233-D238.

Caporaso, J.G., Kuczynski, J., Stombaugh, J., Bittinger, K., Bushman, F.D., Costello, E.K., Fierer, N., Pena, A.G., Goodrich, J.K., Gordon, J.I., Huttley, G.A., Kelley, S.T., Knights, D., Koenig, J.E., Ley, R.E., Lozupone, C.A., McDonald, D., Muegge, B.D., Pirrung, M., Reeder, J., Sevinsky, J.R., Tumbaugh, P.J., Walters, W.A., Widmann, J., Yatsunenko, T., Zaneveld, J., Knight, R., 2010. QIIME allows analysis of high-throughput community sequencing data. Nature Methods 7, 335-336.

Chidthaisong, A., Conrad, R., 2000a. Specificity of chloroform, 2-bromoethanesulfonate and fluoroacetate to inhibit methanogenesis and other anaerobic processes in anoxic rice field soil. Soil Biology & Biochemistry 32, 977-988.

Chidthaisong, A., Conrad, R., 2000b. Turnover of glucose and acetate coupled to reduction of nitrate, ferric iron and sulfate and to methanogenesis in anoxic rice field soil.

Chin, K.J., Conrad, R., 1995. Intermediary Metabolism in Methanogenic Paddy Soil and the Influence of Temperature. FEMS microbiology ecology 18, 85-102.

Chin, K.J., Rainey, F.A., Janssen, P.H., Conrad, R., 1998. Methanogenic degradation of polysaccharides and the characterization of polysaccharolytic clostridia from anoxic rice field soil. Systematic and Applied Microbiology 21, 185-200.

Chodak, M., Golebiewski, M., Morawska-Ploskonka, J., Kuduk, K., Niklinska, M., 2015. Soil chemical properties affect the reaction of forest soil bacteria to drought and rewetting stress. Annals of Microbiology 65, 1627-1637.

Choi, S.-Y., 2003. Distribution of Alcohol-tolerant Microfungi in Paddy Field Soils. Mycobiology 31, 191.

Christensen, B.T., 1986. Barley Straw Decomposition under Field Conditions - Effect of Placement and Initial Nitrogen-Content on Weight-Loss and Nitrogen Dynamics. Soil Biology & Biochemistry 18, 523-529.

Coleman, N.V., Wilson, N.L., Barry, K., Brettin, T.S., Bruce, D.C., Copeland, A., Dalin, E., Detter, J.C., Del Rio, T.G., Goodwin, L.A., Hammon, N.M., Han, S., Hauser, L.J., Israni, S., Kim, E., Kyrpides, N., Land, M.L., Lapidus, A., Larimer, F.W., Lucas, S., Pitluck, S., Richardson, P., Schmutz, J., Tapia, R., Thompson, S., Tice, H.N., Spain, J.C., Gossett, J.G., Mattes, T.E., 2011. Genome Sequence of the ethene- and vinyl chloride-oxidizing actinomycete Nocardioides sp. strain JS614. J Bacteriol 193, 3399-3400.

Conrad, R., 2007. Microbial ecology of methanogens and methanotrophs. Advances in Agronomy, Vol 96 96, 1-63.

Conrad, R., 2009. The global methane cycle: recent advances in understanding the microbial processes involved. Environ Microbiol Rep 1, 285-292.

Conrad, R., Frenzel, P., 2002. Flooded Soils. Encyclopedia of Environmental Microbiology.

Conrad, R., Ji, Y., Noll, M., Klose, M., Claus, P., Enrich-Prast, A., 2014. Response of the methanogenic microbial communities in Amazonian oxbow lake sediments to desiccation stress. Environmental microbiology 16, 1682-1694.

Conrad, R., Klose, M., 1999. How specific is the inhibition by methyl fluoride of acetoclastic methanogenesis in anoxic rice field soil? FEMS microbiology ecology 30, 47-56.

Cotta, M., Forster, R., 2006. The Family Lachnospiraceae, Including the Genera Butyrivibrio, Lachnospira and Roseburia. Prokaryotes: A Handbook on the Biology of Bacteria, Vol 4, Third Edition, 1002-1021.

Cragg, S.M., Beckham, G.T., Bruce, N.C., Bugg, T.D.H., Distel, D.L., Dupree, P., Etxabe, A.G., Goodell, B.S., Jellison, J., McGeehan, J.E., McQueen-Mason, S.J., Schnorr, K., Walton, P.H., Watts, J.E.M., Zimmer, M., 2015. Lignocellulose degradation mechanisms across the Tree of Life. Current Opinion in Chemical Biology 29, 108-119.

Croucher, N.J., Thomson, N.R., 2010. Studying bacterial transcriptomes using RNA-seq. Current opinion in microbiology 13, 619-624.

De Luca, G., Barakat, M., Ortet, P., Fochesato, S., Jourlin-Castelli, C., Ansaldi, M., Py, B., Fichant, G., Coutinho, P.M., Voulhoux, R., Bastien, O., Marechal, E., Henrissat, B., Quentin, Y., Noirot, P., Filloux, A., Mejean, V., DuBow, M.S., Barras, F., Barbe, V.,

Weissenbach, J., Mihalcescu, I., Vermeglio, A., Achouak, W., Heulin, T., 2011. The Cyst-Dividing Bacterium Ramlibacter tataouinensis TTB310 Genome Reveals a Well-Stocked Toolbox for Adaptation to a Desert Environment. Plos One 6.

Deutscher, M.P., 2003. Degradation of stable RNA in bacteria. Journal of Biological Chemistry 278, 45041-45044.

Dhariwal, A., Chong, J., Habib, S., King, I.L., Agellon, L.B., Xia, J., 2017. MicrobiomeAnalyst: a web-based tool for comprehensive statistical, visual and meta-analysis of microbiome data. Nucleic acids research 45, W180-W188.

Dunfield, P.F., Yuryev, A., Senin, P., Smirnova, A.V., Stott, M.B., Hou, S., Ly, B., Saw, J.H., Zhou, Z., Ren, Y., Wang, J., Mountain, B.W., Crowe, M.A., Weatherby, T.M., Bodelier, P.L., Liesack, W., Feng, L., Wang, L., Alam, M., 2007. Methane oxidation by an extremely acidophilic bacterium of the phylum Verrucomicrobia. Nature 450, 879-882.

Edgar, R.C., 2010. Search and clustering orders of magnitude faster than BLAST. Bioinformatics 26, 2460-2461.

Erkel, C., Kube, M., Reinhardt, R., Liesack, W., 2006. Genome of Rice Cluster I archaea—the key methane producers in the rice rhizosphere. Science 313, 370-372.

Esbelin, J., Santos, T., Hebraud, M., 2018. Desiccation: An environmental and food industry stress that bacteria commonly face. Food Microbiology 69, 82-88.

Evans, P.N., Parks, D.H., Chadwick, G.L., Robbins, S.J., Orphan, V.J., Golding, S.D., Tyson, G.W., 2015. Methane metabolism in the archaeal phylum Bathyarchaeota revealed by genome-centric metagenomics. Science 350, 434-438.

Evans, S.E., Byrne, K.M., Lauenroth, W.K., Burke, I.C., 2011. Defining the limit to resistance in a drought-tolerant grassland: long-term severe drought significantly reduces the dominant species and increases ruderals. Journal of Ecology 99, 1500-1507.

Evans, S.E., Wallenstein, M.D., Burke, I.C., 2014. Is bacterial moisture niche a good predictor of shifts in community composition under long-term drought? Ecology 95, 110-122.

Evguenieva-Hackenberg, E., Klug, G., 2009. RNA degradation in Archaea and Gram-negative bacteria different from Escherichia coli. Prog Mol Biol Transl Sci 85, 275-317.

Fazli, P., Man, H.C., Shah, U.K.M., Idris, A., 2013. Characteristics of Methanogens and Methanotrophs in Rice Fields: A Review. Asia-Pacific Journal of Molecular Biology and Biotechnology 21, 3-17.

Fetzer, S., Bak, F., Conrad, R., 1993. Sensitivity of methanogenic bacteria from paddy soil to oxygen and desiccation. FEMS microbiology ecology 12, 107-115.

Fierer, N., Schimel, J.P., 2002. Effects of drying-rewetting frequency on soil carbon and nitrogen transformations. Soil Biology & Biochemistry 34, 777-787.

Frenzel, P., Rothfuss, F., Conrad, R., 1992. Oxygen Profiles and Methane Turnover in a Flooded Rice Microcosm. Biology and Fertility of Soils 14, 84-89.

Frias-Lopez, J., Shi, Y., Tyson, G.W., Coleman, M.L., Schuster, S.C., Chisholm, S.W., DeLong, E.F., 2008. Microbial community gene expression in ocean surface waters. Proceedings of the National Academy of Sciences of the United States of America 105, 3805-3810.

Fu, H., Yuan, J., Gao, H., 2015. Microbial oxidative stress response: Novel insights from environmental facultative anaerobic bacteria. Arch Biochem Biophys 584, 28-35.

Fuchslueger, L., Bahn, M., Hasibeder, R., Kienzl, S., Fritz, K., Schmitt, M., Watzka, M., Richter, A., 2016. Drought history affects grassland plant and microbial carbon turnover during and after a subsequent drought event. Journal of Ecology 104, 1453-1465.

Gan, Y., Qiu, Q., Liu, P., Rui, J., Lu, Y., 2012. Syntrophic oxidation of propionate in rice field soil at 15 and 30 C under methanogenic conditions. Applied and Environmental Microbiology 78, 4923-4932.

Garcia-Fraile, P., Velazquez, E., Mateos, P.F., Martinez-Molina, E., Rivas, R., 2008. Cohnella phaseoli sp. nov., isolated from root nodules of Phaseolus coccineus in Spain, and emended description of the genus Cohnella. Int J Syst Evol Microbiol 58, 1855-1859.

Glissmann, K., Conrad, R., 2000. Fermentation pattern of methanogenic degradation of rice straw in anoxic paddy soil. FEMS microbiology ecology 31, 117-126.

Glissmann, K., Conrad, R., 2002. Saccharolytic activity and its role as a limiting step in methane formation during the anaerobic degradation of rice straw in rice paddy soil. Biology and Fertility of Soils 35, 62-67.

Glissmann, K., Hammer, E., Conrad, R., 2005. Production of aromatic compounds during methanogenic degradation of straw in rice field soil. FEMS microbiology ecology 52, 43-48.

Gordon, H., Haygarth, P.M., Bardgett, R.D., 2008. Drying and rewetting effects on soil microbial community composition and nutrient leaching. Soil Biology & Biochemistry 40, 302-311.

Griffin, D.M., 1981. Water and Microbial Stress. Advances in Microbial Ecology 5, 91-136.

Griffiths, R.I., Whiteley, A.S., O'Donnell, A.G., Bailey, M.J., 2003. Physiological and community responses of established grassland bacterial populations to water stress. Applied and Environmental Microbiology 69, 6961-6968.

Grosskopf, R., Janssen, P.H., Liesack, W., 1998. Diversity and structure of the methanogenic community in anoxic rice paddy soil microcosms as examined by cultivation and

direct 16S rRNA gene sequence retrieval. Applied and Environmental Microbiology 64, 960-969.

Hartmann, M., Brunner, I., Hagedorn, F., Bardgett, R.D., Stierli, B., Herzog, C., Chen, X.M., Zingg, A., Graf-Pannatier, E., Rigling, A., Frey, B., 2017. A decade of irrigation transforms the soil microbiome of a semi-arid pine forest. Molecular Ecology 26, 1190-1206.

He, Y., Li, M., Perumal, V., Feng, X., Fang, J., Xie, J., Sievert, S.M., Wang, F., 2016. Genomic and enzymatic evidence for acetogenesis among multiple lineages of the archaeal phylum Bathyarchaeota widespread in marine sediments. Nature Microbiology 1.

Henckel, T., Jäckel, U., Conrad, R., 2001. Vertical distribution of the methanotrophic community after drainage of rice field soil. FEMS microbiology ecology 34, 279-291.

Henckel, T., Roslev, P., Conrad, R., 2000. Effects of O2 and CH4 on presence and activity of the indigenous methanotrophic community in rice field soil. Environmental Microbiology 2, 666- 679.

Henrissat, B., Sulzenbacher, G., Bourne, Y., 2008. Glycosyltransferases, glycoside hydrolases: surprise, surprise! Current Opinion in Structural Biology 18, 527-533.

Hernandez, M., Conrad, R., Klose, M., Ma, K., Lu, Y.H., 2017. Structure and function of methanogenic microbial communities in soils from flooded rice and upland soybean fields from Sanjiang plain, NE China. Soil Biology & Biochemistry 105, 81-91.

Hibbett, D.S., Bauer, R., Binder, M., Giachini, A.J., Hosaka, K., Justo, A., Larsson, E., Larsson, K.-H., Lawrey, J.D., Miettinen, O., 2014. 14 Agaricomycetes, Systematics and evolution. Springer, pp. 373-429.

Ho, A., Luke, C., Reim, A., Frenzel, P., 2016. Resilience of (seed bank) aerobic methanotrophs and methanotrophic activity to desiccation and heat stress. Soil Biology & Biochemistry 101, 130-138.

Hoffmann, K., Pawlowska, J., Walther, G., Wrzosek, M., de Hoog, G.S., Benny, G.L., Kirk, P.M., Voigt, K., 2013. The family structure of the Mucorales: a synoptic revision based on comprehensive multigene-genealogies. Persoonia 30, 57-76.

Hoh, C.Y., Cord-Ruwisch, R., 1996. A practical kinetic model that considers endproduct inhibition in anaerobic digestion processes by including the equilibrium constant. Biotechnology and Bioengineering 51, 597- 604.

Hori, T., Muller, A., Igarashi, Y., Conrad, R., Friedrich, M.W., 2010. Identification of iron-reducing microorganisms in anoxic rice paddy soil by C-13-acetate probing. Isme Journal 4, 267-278.

Hueso, S., Garcia, C., Hernandez, T., 2012. Severe drought conditions modify the microbial community structure, size and activity in amended and unamended soils. Soil Biology & Biochemistry 50, 167-173.

Huson, D.H., Beier, S., Flade, I., Gorska, A., El-Hadidi, M., Mitra, S., Ruscheweyh, H.J., Tappu, R., 2016. MEGAN Community Edition - Interactive Exploration and Analysis of Large-Scale Microbiome Sequencing Data. PLOS Computational Biology 12, e1004957.

Hussain, S., Peng, S.B., Fahad, S., Khaliq, A., Huang, J.L., Cui, K.H., Nie, L.X., 2015. Rice management interventions to mitigate greenhouse gas emissions: a review. Environmental Science and Pollution Research 22, 3342-3360.

Ikenaga, M., Asakawa, S., Muraoka, Y., Kimura, M., 2003. Bacterial communities associated with nodal roots of rice plants along with the growth stages: Estimation by PCR-DGGE and sequence analyses. Soil Science and Plant Nutrition 49, 591-602.

IPCC, 2007. Climate change 2007: The physical science basis, Contribution working Group I to the Fourth Assessment Report of the Intergovernmental Panel on Climate Change.

IPCC, 2013. Summary for Policymakers. In: Climate Change 2013: The Physical Science Basis, In: T.F. Stocker, Qin, D., Plattner, G.-K., Tignor, M., Allen, S.K., Boschung, J., Nauels, A., Xia, Y., Bex, V., Midgley, P.M. (Eds.), Contribution of Working Group I to the Fifth Assessment Report of the Intergovernmental Panel on Climate Change, Cambridge University Press, Cambridge, United Kingdom and New York, NY, USA.

Itoh, H., Ishii, S., Shiratori, Y., Oshima, K., Otsuka, S., Hattori, M., Senoo, K., 2013. Seasonal Transition of Active Bacterial and Archaeal Communities in Relation to Water Management in Paddy Soils. Microbes and Environments 28, 370-380.

Ivanova, A.A., Wegner, C.E., Kim, Y., Liesack, W., Dedysh, S.N., 2016. Identification of microbial populations driving biopolymer degradation in acidic peatlands by metatranscriptomic analysis. Mol Ecol 25, 4818-4835.

Ivanova, A.A., Wegner, C.E., Kim, Y., Liesack, W., Dedysh, S.N., 2017. Metatranscriptomics reveals the hydrolytic potential of peat-inhabiting Planctomycetes. Antonie Van Leeuwenhoek.

Jackel, U., Schnell, S., Conrad, R., 2001. Effect of moisture, texture and aggregate size of paddy soil on production and consumption of CH4. Soil Biology & Biochemistry 33, 965-971.

Jansson, J.K., 2013. FORUM: Microbiology The life beneath our feet. Nature 494, 40-41.

Jasso-Chavez, R., Santiago-Martinez, M.G., Lira-Silva, E., Pineda, E., Zepeda-Rodriguez, A., Belmont-Diaz, J., Encalada, R., Saavedra, E., Moreno-Sanchez, R., 2015. Air-adapted Methanosarcina acetivorans shows high methane production and develops resistance against oxygen stress. PLoS One 10, e0117331.

Kawasaki, S., Sakai, Y., Takahashi, T., Suzuki, I., Niimura, Y., 2009. O2 and reactive oxygen species detoxification complex, composed of O2-responsive NADH:rubredoxin oxidoreductase-flavoprotein A2-desulfoferrodoxin operon enzymes, rubperoxin, and rubredoxin, in Clostridium acetobutylicum. Appl Environ Microbiol 75, 1021-1029.

Ke, X., Angel, R., Lu, Y., Conrad, R., 2013. Niche differentiation of ammonia oxidizers and nitrite oxidizers in rice paddy soil. Environ Microbiol 15, 2275-2292.

Kemnitz, D., Kolb, S., Conrad, R., 2005. Phenotypic characterization of Rice Cluster III archaea without prior isolation by applying quantitative polymerase chain reaction to an enrichment culture. Environmental Microbiology 7, 553-565.

Kim, Y., Liesack, W., 2015. Differential assemblage of functional units in paddy soil microbiomes. PLoS One 10, e0122221.

Kimbrel, J.A., Chang, J., Arp, D.J., Sayavedra-Soto, L.A., 2013. The Draft Genome Sequence of Nocardioides sp. Strain CF8 Reveals the Scope of Its Metabolic Capabilities. Genome Announc 1.

Klemm, D., Heublein, B., Fink, H.P., Bohn, A., 2005. Cellulose: Fascinating biopolymer and sustainable raw material. Angewandte Chemie-International Edition 44, 3358-3393.

Kogel-Knabner, I., Amelung, W., Cao, Z.H., Fiedler, S., Frenzel, P., Jahn, R., Kalbitz, K., Kolbl, A., Schloter, M., 2010. Biogeochemistry of paddy soils. Geoderma 157, 1-14.

Kopylova, E., Noe, L., Touzet, H., 2012. SortMeRNA: fast and accurate filtering of ribosomal RNAs in metatranscriptomic data. Bioinformatics 28, 3211-3217.

Krause, S., Luke, C., Frenzel, P., 2010. Succession of methanotrophs in oxygen-methane counter-gradients of flooded rice paddies. Isme Journal 4, 1603-1607.

Krylova, N.I., Janssen, P.H., Conrad, R., 1997. Turnover of propionate in methanogenic paddy soil. FEMS microbiology ecology 23, 107-117.

Kwon, K.K., Yang, S.J., Lee, H.S., Cho, J.C., Kim, S.J., 2007. Sufflavibacter maritimus gen. nov., sp. nov., novel Flavobacteriaceae bacteria isolated from marine environments. J Microbiol Biotechnol 17, 1379-1384.

Ladha, J.K., Reddy, P.M., 2003. Nitrogen fixation in rice systems: state of knowledge and future prospects. Plant and Soil 252, 151-167.

Le Mer, J., Roger, P., 2001. Production, oxidation, emission and consumption of methane by soils: A review. European Journal of Soil Biology 37, 25-50.

Lee, H.J., Jeong, S.E., Kim, P.J., Madsen, E.L., Jeon, C.O., 2015. High resolution depth distribution of Bacteria, Archaea, methanotrophs, and methanogens in the bulk and rhizosphere soils of a flooded rice paddy. Frontiers in Microbiology 6, 639.

Leff, B., Ramankutty, N., Foley, J.A., 2004. Geographic distribution of major crops across the world. Global Biogeochemical Cycles 18.

Lelieveld, J., Crutzen, P.J., Bruhl, C., 1993. Climate Effects of Atmospheric Methane. Chemosphere 26, 739-768.

Leon, A., Kohyama, K., Yagi, K., Takata, Y., Obara, H., 2017. The effects of current water management practices on methane emissions in Japanese rice cultivation. Mitigation and Adaptation Strategies for Global Change 22, 85-98.

Liang, X.W., Zhang, L., Natarajan, S.K., Becker, D.F., 2013. Proline Mechanisms of Stress Survival. Antioxidants & Redox Signaling 19, 998-1011.

Liesack, W., Schnell, S., Revsbech, N.P., 2000. Microbiology of flooded rice paddies. FEMS Microbiology Reviews 24, 625-645.

Liu, P.F., Conrad, R., 2017. Syntrophobacteraceae-affiliated species are major propionate-degrading sulfate reducers in paddy soil. Environmental Microbiology 19, 1669-1686.

Lombard, V., Ramulu, H.G., Drula, E., Coutinho, P.M., Henrissat, B., 2014. The carbohydrate-active enzymes database (CAZy) in 2013. Nucleic acids research 42, D490-D495.

Love, M.I., Huber, W., Anders, S., 2014. Moderated estimation of fold change and dispersion for RNA-seq data with DESeq2. Genome Biology 15.

Lu, Y., Rosencrantz, D., Liesack, W., Conrad, R., 2006. Structure and activity of bacterial community inhabiting rice roots and the rhizosphere. Environmental Microbiology 8, 1351-1360.

Lu, Y.H., Lueders, T., Friedrich, M.W., Conrad, R., 2005. Detecting active methanogenic populations on rice roots using stable isotope probing. Environmental Microbiology 7, 326-336.

Lu, Y.H., Wassmann, R., Neue, H.U., Huang, C.Y., 2000. Dynamics of dissolved organic carbon and methane emissions in a flooded rice soil. Soil Science Society of America Journal 64, 2011-2017.

Lü, Z., Lu, Y., 2012. Complete genome sequence of a thermophilic methanogen, Methanocella conradii HZ254, isolated from Chinese rice field soil. Journal of bacteriology 194, 2398-2399.

Lüdemann, H., Arth, I., Liesack, W., 2000. Spatial changes in the bacterial community structure along a vertical oxygen gradient in flooded paddy soil cores. Applied and Environmental Microbiology 66, 754-762.

Lueders, T., Friedrich, M., 2000. Archaeal population dynamics during sequential reduction processes in rice field soil. Applied and Environmental Microbiology 66, 2732-2742.

Lynd, L.R., Weimer, P.J., van Zyl, W.H., Pretorius, I.S., 2002. Microbial cellulose utilization: Fundamentals and biotechnology. Microbiology and Molecular Biology Reviews 66, 506-+.

Lyu, Z., Lu, Y.H., 2018. Metabolic shift at the class level sheds light on adaptation of methanogens to oxidative environments. Isme Journal 12, 411-423.

Ma, K., Conrad, R., Lu, Y., 2012. Responses of methanogen mcrA genes and their transcripts to an alternate dry/wet cycle of paddy field soil. Applied and Environmental Microbiology 78, 445-454.

Ma, K., Conrad, R., Lu, Y., 2013. Dry/wet cycles change the activity and population dynamics of methanotrophs in rice field soil. Applied and Environmental Microbiology 79, 4932-4939.

Ma, K., Lu, Y., 2011. Regulation of microbial methane production and oxidation by intermittent drainage in rice field soil. FEMS microbiology ecology 75, 446-456.

Maeder, D.L., Anderson, I., Brettin, T.S., Bruce, D.C., Gilna, P., Han, C.S., Lapidus, A., Metcalf, W.W., Saunders, E., Tapia, R., 2006. The Methanosarcina barkeri genome: comparative analysis with Methanosarcina acetivorans and Methanosarcina mazei reveals extensive rearrangement within methanosarcinal genomes. Journal of bacteriology 188, 7922-7931.

Mager, D.M., Thomas, A.D., 2011. Extracellular polysaccharides from cyanobacterial soil crusts A review of their role in dryland soil processes. Journal of Arid Environments 75, 91-97.

Maharachchikumbura, S.S.N., Hyde, K.D., Jones, E.B.G., McKenzie, E.H.C., Huang, S.K., Abdel-Wahab, M.A., Daranagama, D.A., Dayarathne, M., D'souza, M.J., Goonasekara, I.D., Hongsanan, S., Jayawardena, R.S., Kirk, P.M., Konta, S., Liu, J.K., Liu, Z.Y., Norphanphoun, C., Pang, K.L., Perera, R.H., Senanayake, I.C., Shang, Q.J., Shenoy, B.D., Xiao, Y.P., Bahkali, A.H., Kang, J.C., Somrothipol, S., Suetrong, S., Wen, T.C., Xu, J.C., 2015. Towards a natural classification and backbone tree for Sordariomycetes. Fungal Diversity 72, 199-301.

Manzoni, S., Schimel, J.P., Porporato, A., 2012. Responses of soil microbial communities to water stress: results from a meta-analysis. Ecology 93, 930-938.

Mayumi, D., Yoshimoto, T., Uchiyama, H., Nomura, N., Nakajima-Kambe, T., 2010. Seasonal change in methanotrophic diversity and populations in a rice field soil assessed by DNA-stable isotope probing and quantitative real-time PCR. Microbes and environments 25, 156-163.

McHugh, T.A., Koch, G.W., Schwartz, E., 2014. Minor Changes in Soil Bacterial and Fungal Community Composition Occur in Response to Monsoon Precipitation in a Semiarid Grassland. Microbial Ecology 68, 370-378.

Mettel, C., Kim, Y., Shrestha, P.M., Liesack, W., 2010. Extraction of mRNA from soil. Appl Environ Microbiol 76, 5995-6000.

Mishra, S., Imlay, J., 2012. Why do bacteria use so many enzymes to scavenge hydrogen peroxide? Archives of Biochemistry and Biophysics 525, 145-160.

Moran, M.A., 2010. Metatranscriptomics: eavesdropping on complex microbial communities. Issues.

Murase, J., Frenzel, P., 2008. Selective grazing of methanotrophs by protozoa in a rice field soil. FEMS microbiology ecology 65, 408-414.

Murase, J., Noll, M., Frenzel, P., 2006. Impact of protists on the activity and structure of the bacterial community in a rice field soil. Applied and Environmental Microbiology 72, 5436-5444.

Muthayya, S., Sugimoto, J.D., Montgomery, S., Maberly, G.F., 2014. An overview of global rice production, supply, trade, and consumption. Ann N Y Acad Sci 1324, 7-14.

Naylor, D., Coleman-Derr, D., 2018. Drought Stress and Root-Associated Bacterial Communities. Frontiers in Plant Science 8.

Nisbet, E.G., Dlugokencky, E.J., Bousquet, P., 2014. Atmospheric science. Methane on the rise--again. Science 343, 493-495.

Noll, M., Matthies, D., Frenzel, P., Derakshani, M., Liesack, W., 2005. Succession of bacterial community structure and diversity in a paddy soil oxygen gradient. Environmental Microbiology 7, 382-395.

Or, D., Smets, B.F., Wraith, J.M., Dechesne, A., Friedman, S.P., 2007. Physical constraints affecting bacterial habitats and activity in unsaturated porous media - a review. Advances in Water Resources 30, 1505-1527.

Pan, F.X., Li, Y.Y., Chapman, S.J., Yao, H.Y., 2016. Effect of rice straw application on microbial community and activity in paddy soil under different water status. Environmental Science and Pollution Research 23, 5941-5948.

Peng, J.J., Wegner, C.E., Liesack, W., 2017. Short- Term Exposure of Paddy Soil Microbial Communities to Salt Stress Triggers Different Transcriptional Responses of Key Taxonomic Groups. Frontiers in Microbiology 8.

Peterson, J.R., Thor, S., Kohler, L., Kohler, P.R., Metcalf, W.W., Luthey-Schulten, Z., 2016. Genome-wide gene expression and RNA half-life measurements allow predictions of regulation and metabolic behavior in Methanosarcina acetivorans. BMC Genomics 17, 924.

Pump, J., Conrad, R., 2014. Rice biomass production and carbon cycling in (CO2)-C-13 pulse-labeled microcosms with different soils under submerged conditions. Plant and Soil 384, 213-229.

Quast, C., Pruesse, E., Yilmaz, P., Gerken, J., Schweer, T., Yarza, P., Peplies, J., Glockner, F.O., 2013. The SILVA ribosomal RNA gene database project: improved data processing and web-based tools. Nucleic acids research 41, D590-596.

Rainey, F.A., 2015. Ruminococcaceae fam. nov, Bergey's Manual of Systematics of Archaea and Bacteria. John Wiley & Sons.

Ramakrishnan, B., Lueders, T., Dunfield, P.F., Conrad, R., Friedrich, M.W., 2001. Archaeal community structures in rice soils from different geographical regions before and after initiation of methane production.

Ratering, S., Schnell, S., 2001. Nitrate-dependent iron (II) oxidation in paddy soil. Environmental Microbiology 3, 100-109.

Rath, A.K., Mohanty, S.R., Mishra, S., Kumaraswamy, S., Ramakrishnan, B., Sethunathan, N., 1999. Methane production in unamended and rice-straw-amended soil at different moisture levels. Biology and Fertility of Soils 28, 145-149.

Ray, D.K., Mueller, N.D., West, P.C., Foley, J.A., 2013. Yield Trends Are Insufficient to Double Global Crop Production by 2050. PLoS One 8, e66428.

Reim, A., Hernandez, M., Klose, M., Chidthaisong, A., Yuttitham, M., Conrad, R., 2017. Response of Methanogenic Microbial Communities to Desiccation Stress in Flooded and Rain-Fed Paddy Soil from Thailand. Frontiers in Microbiology 8, 785.

Reim, A., Lüke, C., Krause, S., Pratscher, J., Frenzel, P., 2012. One millimetre makes the difference: high-resolution analysis of methane-oxidizing bacteria and their specific activity at the oxic–anoxic interface in a flooded paddy soil. The ISME journal 6, 2128-2139.

Richardson, M.J., 2002. The coprophilous succession. Fungal Diversity 10, 101-111.

Rosencrantz, D., Rainey, F.A., Janssen, P.H., 1999. Culturable populations of Sporomusa spp. and Desulfovibrio spp. in the anoxic bulk soil of flooded rice microcosms. Applied and Environmental Microbiology 65, 3526-3533.

Roslev, P., King, G.M., 1994. Survival and recovery of methanotrophic bacteria starved under oxic and anoxic conditions. Applied and Environmental Microbiology 60, 2602-2608.

Rossi, F., De Philippis, R., 2015. Role of cyanobacterial exopolysaccharides in phototrophic biofilms and in complex microbial mats. Life (Basel) 5, 1218-1238.

Rotthauwe, J.-H., Witzel, K.-P., Liesack, W., 1997. The ammonia monooxygenase structural gene amoA as a functional marker: molecular fine-scale analysis of natural ammonia-oxidizing populations. Applied and Environmental Microbiology 63, 4704-4712.

Rui, J., Peng, J., Lu, Y., 2009. Succession of bacterial populations during plant residue decomposition in rice field soil. Appl Environ Microbiol 75, 4879-4886.

Saito, K., Muto, H., Takizama, Y., Kodama, M., 1994. Concentrations of Various Elements and Inorganic-Ions in Rice Straw and Ash. Toxicological and Environmental Chemistry 41, 15-20.

Sass, R., Fisher, F., Wang, Y., Turner, F., Jund, M., 1992. Methane emission from rice fields: the effect of floodwater management. Global Biogeochemical Cycles 6, 249-262.

Shrestha, M., Shrestha, P.M., Frenzel, P., Conrad, R., 2010. Effect of nitrogen fertilization on methane oxidation, abundance, community structure, and gene expression of methanotrophs in the rice rhizosphere. ISME J 4, 1545-1556.

Shrestha, P.M., Kube, M., Reinhardt, R., Liesack, W., 2009. Transcriptional activity of paddy soil bacterial communities. Environmental microbiology 11, 960-970.

Shrestha, P.M., Noll, M., Liesack, W., 2007. Phylogenetic identity, growth-response time and rRNA operon copy number of soil bacteria indicate different stages of community succession. Environmental microbiology 9, 2464-2474.

Song, J.Y., Yoo, Y.J., Lim, S.K., Cha, S.H., Kim, J.E., Roe, J.H., Kim, J.F., Yoon, Y.J., 2016. Complete genome sequence of Streptomyces venezuelae ATCC 15439, a promising cell factory for production of secondary metabolites. J Biotechnol 219, 57-58.

Soontranon, N., Tangpattanakul, P., Srestasathiern, P., Rakwatin, P., 2014. An Agricultural Monitoring System: Field Server Data Collection and Analysis on Paddy Field. 2014 14th International Symposium on Communications and Information Technologies (ISCIT), 597-601.

Stan-Lotter, H., Fendrihan, S., 2013. Survival strategies of halophilic oligotrophic and desiccation resistant prokaryotes, Polyextremophiles. Springer, pp. 233-248.

Stefana, G., Cornelia, B., Jorg, R., Michael, B., 2014. Soil water availability strongly alters the community composition of soil protists. Pedobiologia 57, 205-213.

Steinberg, L.M., Regan, J.M., 2009. mcrA-targeted real-time quantitative PCR method to examine methanogen communities. Applied and Environmental Microbiology 75, 4435-4442.

Stieglmeier, M., Klingl, A., Alves, R.J., Rittmann, S.K., Melcher, M., Leisch, N., Schleper, C., 2014. Nitrososphaera viennensis gen. nov., sp. nov., an aerobic and mesophilic, ammonia-oxidizing archaeon from soil and a member of the archaeal phylum Thaumarchaeota. Int J Syst Evol Microbiol 64, 2738-2752.

Stubner, S., 2004. Quantification of Gram-negative sulphate-reducing bacteria in rice field soil by 16S rRNA gene-targeted real-time PCR. J Microbiol Methods 57, 219-230.

Sun, R.C., Tomkinson, J., Ma, P.L., Liang, S.F., 2000. Comparative study of hemicelluloses from rice straw by alkali and hydrogen peroxide treatments. Carbohydrate Polymers 42, 111-122.

Tamaki, H., Tanaka, Y., Matsuzawa, H., Muramatsu, M., Meng, X.Y., Hanada, S., Mori, K., Kamagata, Y., 2011. Armatimonas rosea gen. nov., sp nov., of a novel bacterial phylum, Armatimonadetes phyl. nov., formally called the candidate phylum OP10. International Journal of Systematic and Evolutionary Microbiology 61, 1442-1447.

Thauer, R.K., Kaster, A.K., Seedorf, H., Buckel, W., Hedderich, R., 2008. Methanogenic archaea: ecologically relevant differences in energy conservation. Nature reviews Microbiology 6, 579-591.

Tolonen, A.C., Cerisy, T., El-Sayyed, H., Boutard, M., Salanoubat, M., Church, G.M., 2015. Fungal lysis by a soil bacterium fermenting cellulose. Environmental Microbiology 17, 2618-2627.

Tonouchi, A., 2009. Isolation and characterization of a novel facultative anaerobic filamentous fungus from Japanese rice field soil. Int J Microbiol 2009, 571383.

Toth, Z., Tancsics, A., Kriszt, B., Kroel-Dulay, G., Onodi, G., Hornung, E., 2017. Extreme effects of drought on composition of the soil bacterial community and decomposition of plant tissue. European Journal of Soil Science 68, 504-513.

Towprayoon, S., Smakgahn, K., Poonkaew, S., 2005. Mitigation of methane and nitrous oxide emissions from drained irrigated rice fields. Chemosphere 59, 1547-1556.

Urich, T., Lanzen, A., Qi, J., Huson, D.H., Schleper, C., Schuster, S.C., 2008. Simultaneous Assessment of Soil Microbial Community Structure and Function through Analysis of the Meta-Transcriptome. Plos One 3.

Vainio, E.J., Hantula, J., 2000. Direct analysis of wood-inhabiting fungi using denaturing gradient gel electrophoresis of amplified ribosomal DNA. Mycological Research 104, 927-936.

Vaksmaa, A., van Alen, T.A., Ettwig, K.F., Lupotto, E., Vale, G., Jetten, M.S.M., Luke, C., 2017. Stratification of Diversity and Activity of Methanogenic and Methanotrophic Microorganisms in a Nitrogen-Fertilized Italian Paddy Soil. Frontiers in Microbiology 8, 2127.

van Dijk, E.L., Jaszczyszyn, Y., Thermes, C., 2014. Library preparation methods for next-generation sequencing: Tone down the bias. Experimental Cell Research 322, 12-20.

Van Elsas, J., Boersma, F., 2011. A review of molecular methods to study the microbiota of soil and the mycosphere. European Journal of Soil Biology 47, 77-87.

Vanwonterghem, I., Evans, P.N., Parks, D.H., Jensen, P.D., Woodcroft, B.J., Hugenholtz, P., Tyson, G.W., 2016. Methylotrophic methanogenesis discovered in the archaeal phylum Verstraetearchaeota. Nat Microbiol 1, 16170.

Veresoglou, S.D., Wang, D.W., Andrade-Linares, D.R., Hempel, S., Rillig, M.C., 2018. Fungal Decision to Exploit or Explore Depends on Growth Rate. Microbial Ecology 75, 289-292.

Verhoef, H.A., 1996. The role of soil microcosms in the study of ecosystem processes. Ecology, 685-690.

Vetrovsky, T., Baldrian, P., 2013. The variability of the 16S rRNA gene in bacterial genomes and its consequences for bacterial community analyses. PLoS One 8, e57923.

Wang, Q., Garrity, G.M., Tiedje, J.M., Cole, J.R., 2007. Naive Bayesian classifier for rapid assignment of rRNA sequences into the new bacterial taxonomy. Applied and Environmental Microbiology 73, 5261-5267.

Wang, Y., Zhu, G., Harhangi, H.R., Zhu, B., Jetten, M.S.M., Yin, C., Op den Camp, H.J.M., 2012. Co-occurrence and distribution of nitrite-dependent anaerobic ammonium and methane-oxidizing bacteria in a paddy soil. Fems Microbiology Letters 336, 79-88.

Watanabe, A., Katoh, K., Kimura, M., 1993. Effect of Rice Straw Application on Ch4 Emission from Paddy Fields .2. Contribution of Organic-Constituents in Rice Straw. Soil Science and Plant Nutrition 39, 707-712.

Watanabe, T., Kimura, M., Asakawa, S., 2009. Distinct members of a stable methanogenic archaeal community transcribe mcrA genes under flooded and drained conditions in Japanese paddy field soil. Soil Biology and Biochemistry 41, 276-285.

Wegner, C.E., Liesack, W., 2016. Microbial community dynamics during the early stages of plant polymer breakdown in paddy soil. Environmental Microbiology 18, 2825-2842.

Welch, B.L., 1947. The Generalization of Students Problem When Several Different Population Variances Are Involved. Biometrika 34, 28-35.

White, J.R., Nagarajan, N., Pop, M., 2009. Statistical Methods for Detecting Differentially Abundant Features in Clinical Metagenomic Samples. Plos Computational Biology 5.

Wichelns, D., 2016. Managing Water and Soils to Achieve Adaptation and Reduce Methane Emissions and Arsenic Contamination in Asian Rice Production. Water 8.

Wiegel, J., Tanner, R., Rainey, F.A., 2006. An Introduction to the Family Clostridiaceae. Prokaryotes: A Handbook on the Biology of Bacteria, Vol 4, Third Edition, 654-678.

Wilson, D.B., 2011. Microbial diversity of cellulose hydrolysis. Current Opinion in Microbiology 14, 259-263.

Wind, T., Conrad, R., 1995. Sulfur compounds, potential turnover of sulfate and thiosulfate, and numbers of sulfate-reducing bacteria in planted and unplanted paddy soil. FEMS microbiology ecology 18, 257-266.

Wind, T., Conrad, R., 1997. Localization of sulfate reduction in planted and unplanted rice field soil. Biogeochemistry 37, 253-278.

Wind, T., Stubner, S., Conrad, R., 1999. Sulfate-reducing Bacteria in Rice Field Soil and on Rice Roots. Systematic and Applied Microbiology 22, 269- 279.

Wommack, K.E., Bhavsar, J., Ravel, J., 2008. Metagenomics: Read length matters. Applied and Environmental Microbiology 74, 1453-1463.

Wu, X., Conrad, R., 2001. Functional and structural response of a cellulose-degrading methanogenic microbial community to multiple aeration stress at two different temperatures. Environmental microbiology 3, 355-362.

Yao, H., Conrad, R., Wassmann, R., Neue, H.U., 1999. Effect of soil characteristics on sequential reduction and methane production in sixteen rice paddy soils from China, the Philippines, and Italy. Biogeochemistry 47, 269-295.

Yuan, Y.L., Conrad, R., Lu, Y.H., 2009. Responses of methanogenic archaeal community to oxygen exposure in rice field soil. Environmental Microbiology Reports 1, 347-354.

Zhang, J., Kobert, K., Flouri, T., Stamatakis, A., 2014. PEAR: a fast and accurate Illumina Paired-End reAd mergeR. Bioinformatics 30, 614-620.

Zhou, W., Lv, T.F., Chen, Y., Westby, A.P., Ren, W.J., 2014. Soil Physicochemical and Biological Properties of Paddy-Upland Rotation: A Review. Scientific World Journal.

Zhou, Z., Pan, J., Wang, F., Gu, J.D., Li, M., 2018. Bathyarchaeota: globally distributed metabolic generalists in anoxic environments. FEMS Microbiology Reviews.

Zhu, G.B., Wang, S.Y., Wang, Y., Wang, C.X., Risgaard-Petersen, N., Jetten, M.S.M., Yin, C.Q., 2011. Anaerobic ammonia oxidation in a fertilized paddy soil. Isme Journal 5, 1905-1912.

Zifcakova, L., Vetrovsky, T., Lombard, V., Henrissat, B., Howe, A., Baldrian, P., 2017. Feed in summer, rest in winter: microbial carbon utilization in forest topsoil. Microbiome 5, 122.

7 Supporting information

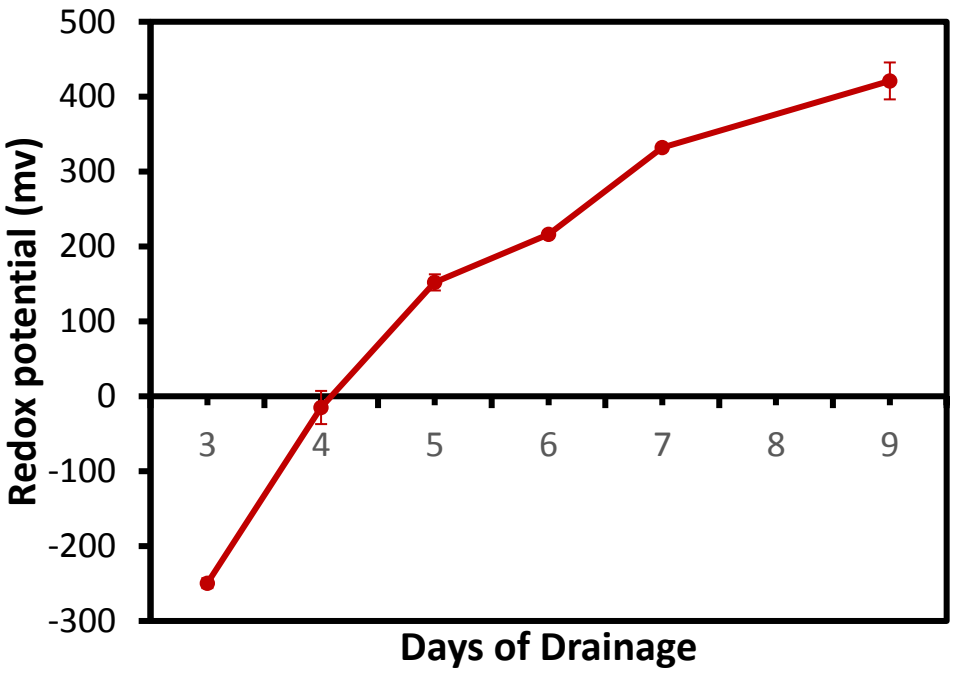

Figure S1 Redox potential profile**.**
The graph shows the redox potential of the soil after 9 days of drainage. Standard deviation is based on 3 biological replicas.

	16S rRNA			mRNA		
Phylum	Flooded	Drainage	*P* values	Flooded	Drainage	*P* values
Bacteria;Verrucomicrobia	0.93	1.33		0.94	0.68	
Bacteria;Proteobacteria	20.38	30.70	*	14.68	29.12	***
Bacteria;Planctomycetes	2.77	3.65		1.35	2.80	***
Bacteria;Firmicutes	38.99	21.10	**	28.20	6.52	***
Bacteria;Fibrobacteres	1.45	0.24		0.43	0.00	*
Bacteria;Cyanobacteria	1.97	1.26		0.91	1.00	
Bacteria;Chloroflexi	4.42	4.76		3.10	2.54	
Bacteria;Chlorobi/Ignavibacteriae	1.79	1.12		1.08	0.33	**
Bacteria;Bacteroidetes	2.64	3.23		5.08	3.94	
Bacteria;Armatimonadetes	1.06	0.93		0.30	0.21	
Bacteria;Actinobacteria	4.55	12.63	*	4.28	20.27	***
Bacteria;Acidobacteria	3.39	4.72		3.21	4.12	
Archaea; Euryarchaeota	4.20	3.89		7.03	1.41	***
Bacteria;Unclassfied †	0.19	0.17		0.26	0.37	*
Eukaryota;Archaeplastida	0.18	0.30		2.12	0.56	*
Eukaryota;Opisthokonta	0.18	1.97		1.79	2.05	
Eukaryota;SAR	1.54	1.15		0.421	0.502	

Fig S2 Detailed taxonomic analysis phylum level (bacteria and archaea) and super-group level (eukarya).

Relative abundance is shown in relation to the total number of SSU rRNA reads. Archaeal, bacterial phyla and eukarya super-groups > 1 % are shown. Asterisks * ($P \leq 0.1$), ** ($P \leq 0.05$) and *** ($P \leq 0.01$) indicate significant difference between flooded and drained soils. *P* values are FDR corrected. The sign † indicates that this phyla was not presented in Figure 3.5.

	16S rRNA			mRNA		
	Flooded	Drainage	*P* values	Flooded	Drainage	*P* values
Bacteria (Family)						
Proteobacteria;Sphingomonadaceae	0.42	1.27	*	0.51	2.01	**
Proteobacteria;Comamonadaceae	0.86	5.52	*	0.42	2.93	***
Proteobacteria;Alcaligenaceae†	0.05	0.11	*	0.98	2.05	***
Proteobacteria;Bradyrhizobiaceae†	2.04	0.79		2.33	2.66	
Proteobacteria;Burkholderiaceae†	0.05	0.05		0.85	2.15	***
Proteobacteria;Rhodospirillaceae†	2.63	3.55		1.42	2.02	
Firmicutes;Ruminococcaceae	10.21	1.55	*	8.17	0.79	**
Firmicutes;Lachnospiraceae	3.48	0.95	*	2.52	0.26	**
Firmicutes;Clostridiaceae	14.90	14.04		11.63	2.83	**
Firmicutes;Bacillaceae	3.58	2.11		3.48	1.02	**
Firmicutes;Sporomusaceae†	NA	NA		5.64	0.69	**
Actinobacteria;Nocardioidaceae	0.90	5.55	**	0.25	3.51	***
Actinobacteria;Streptomycetaceae	0.21	0.89	*	1.24	4.83	***
Actinobacteria;Mycobacteriaceae†	0.13	0.29	*	2.16	6.92	***
Acidobacteria;Solibacteraceae†	NA	NA		1.66	2.12	
Planctomycetes;Planctomycetaceae†	2.28	3.29		0.56	0.87	*
Chloroflexi;Anaerolineaceae†	2.40	2.14		1.92	0.57	
Archaea (Order)						
Thaumarchaeota; Nitrososphaerales	0.10	0.14		0.0	9.7	***
Euryarchaeota;Methanosarcinales	56.13	67.12	*	31.3	46.6	*
Euryarchaeota;Methanocellales	17.82	13.96	*	35.2	24.6	*
Euryarchaeota;Methanobacteriales	10.34	3.72		16.0	2.7	*
Euryarchaeota;Methanomassiliicoccales†	2.48	2.34		1.7	0.0	**
Euryarchaeota;Methanomicrobiales†	2.50	3.03		3.5	4.6	
Euryarchaeota;Halobacteriaceae†	0.30	0.17		0.0	2.6	*
Candidatus Bathyarchaeota	5.76	3.54		11.6	9.3	
Unclassfied archaea†	0.25	0.13		0.7	0.0	
Eukarya (Phylum)						
Cercozoa	42.4	14.7	*	NA	NA	
Ascomycota	2.7	34.8	*	11.18	29.19	**
Basidiomycota	0.5	4.0		1.23	6.70	**
Chloroplastida†	8.2	8.0		51.99	16.31	**
Ciliophora†	7.0	7.8		1.40	0.69	
Amoebozoa†	24.5	14.0	*	8.00	5.79	
Apicomplexa†	0.0	0.0		4.00	4.74	
Arthropoda†	0.5	0.1		6.32	7.32	

Figure S3 Detailed Taxonomic analysis of bacteria (family level), archaea (order level), and eukarya (phylum level).
Relative abundance is shown in relation to each domain. Bacterial families, archaeal orders, eukaryotic phylum > 1% are shown. Asterisks * ($P \leq 0.1$), ** ($P \leq 0.05$) and *** ($P \leq 0.01$) indicate significant difference between flooded and drained soils. *P* values are FDR corrected. The sign † indicates that this phyla was not presented in Figure 3.6.

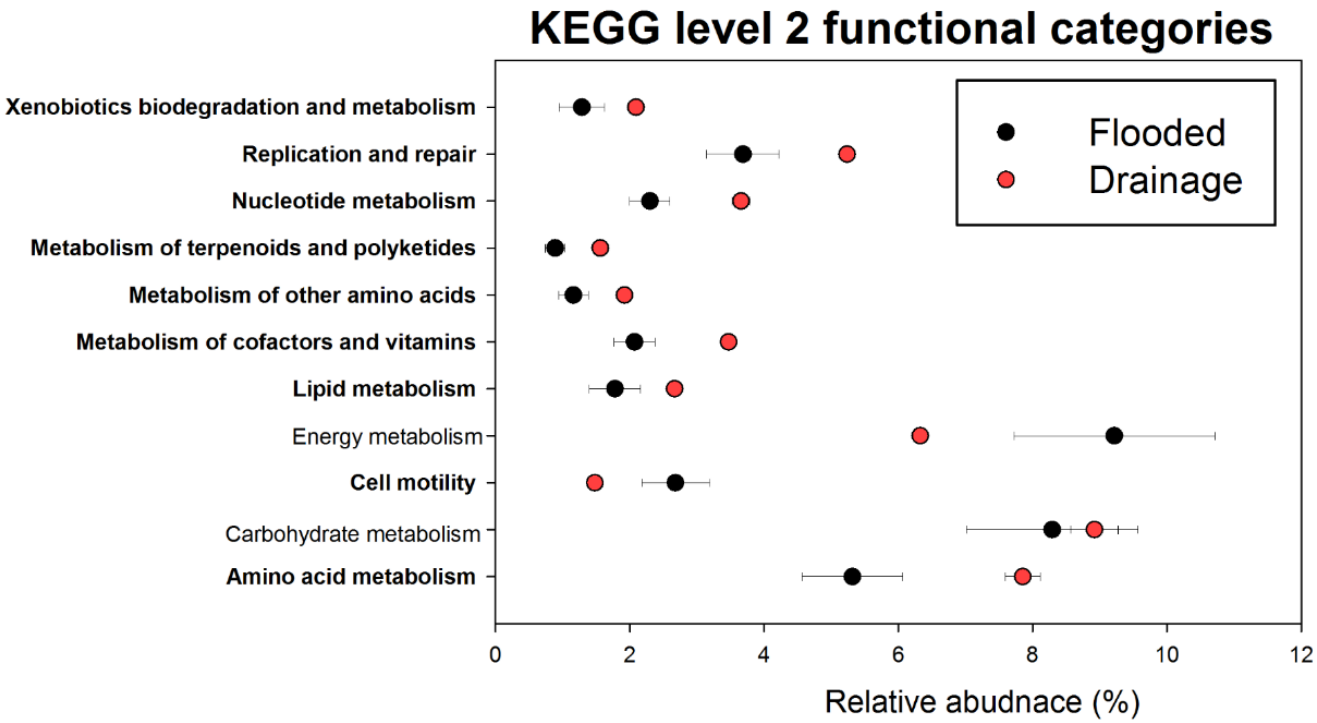

Figure S4 KEGG level 2 assigned transcripts under flooded and drained soils. Relative mRNA transcripts abundance is shown on the X-axis. Functional categories in bold indicate corrected *P* [FDR] ≤ 0.05.

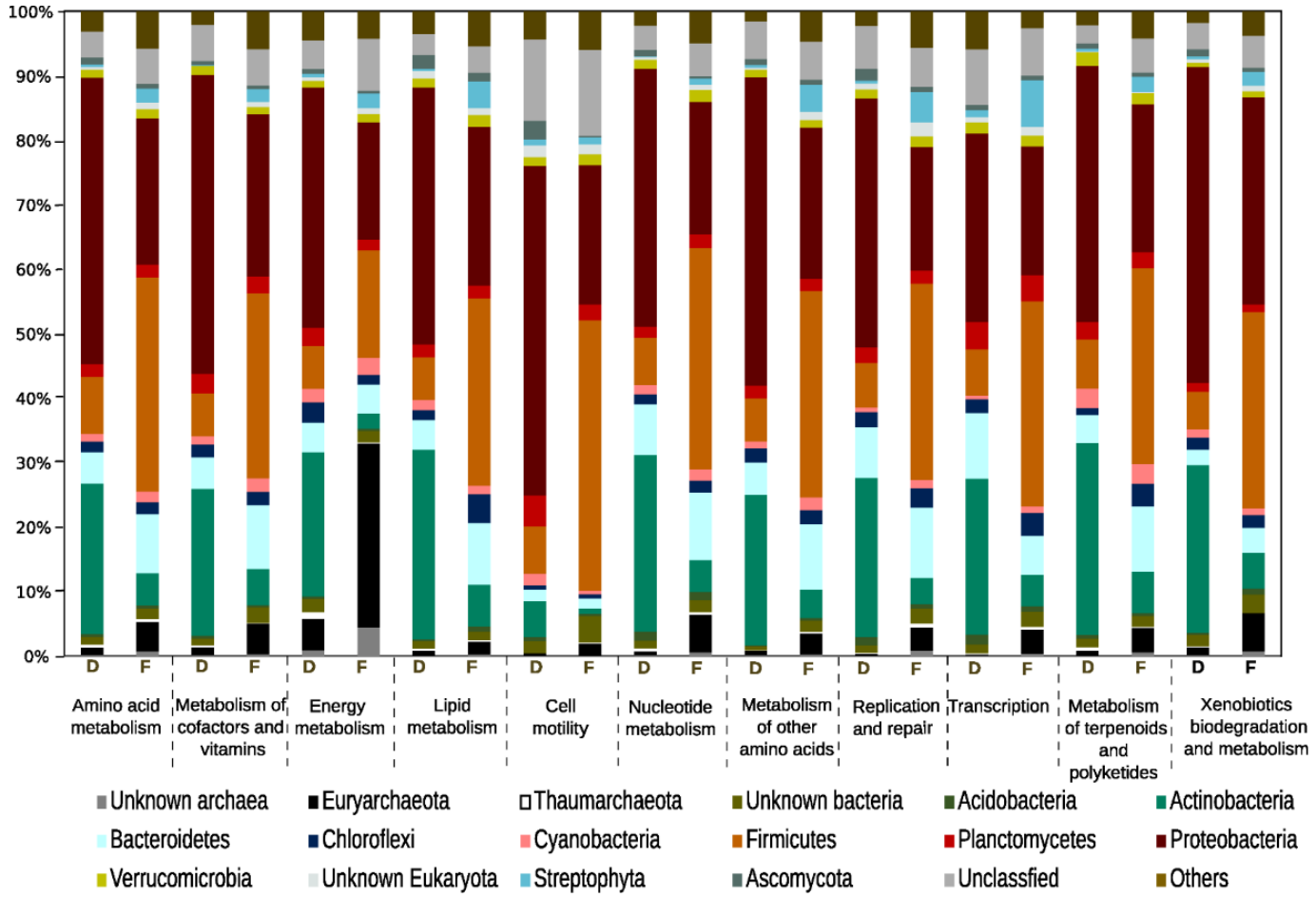

Figure S5 Taxonomic classification of mRNA transcripts assigned to KEGG level 2 categories. Relative mRNA transcripts abundance is shown on the Y-axis. D = Drainage, F = Flooded.

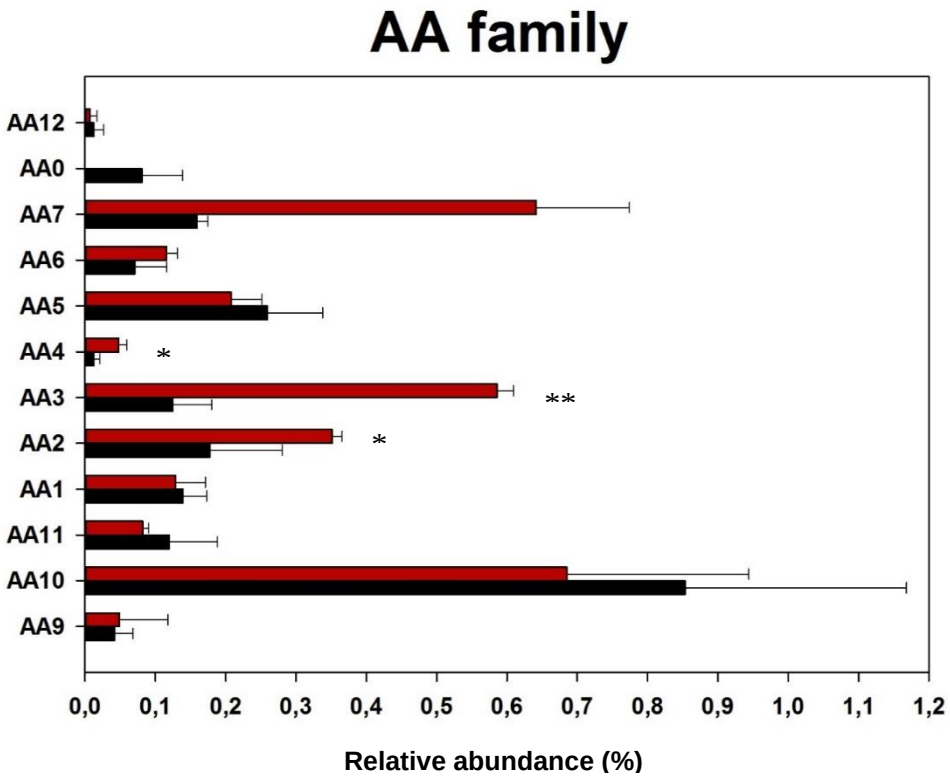

Figure S6 Transcripts assigned to CAZymes family Auxiliary activity (AA) in flooded and drained soils. Graph shows the relative abundance of transcripts encoding carbohydrate-active enzymes belonging to the AA family in flooded and drained soils. Asterisks * $P \leq 0.1$, ** $P \leq 0.05$, *** $P \leq 0.01$ indicate significant difference between flooded and drained soils. P values are FDR corrected. Black bars = flooded, red bars = drainage.

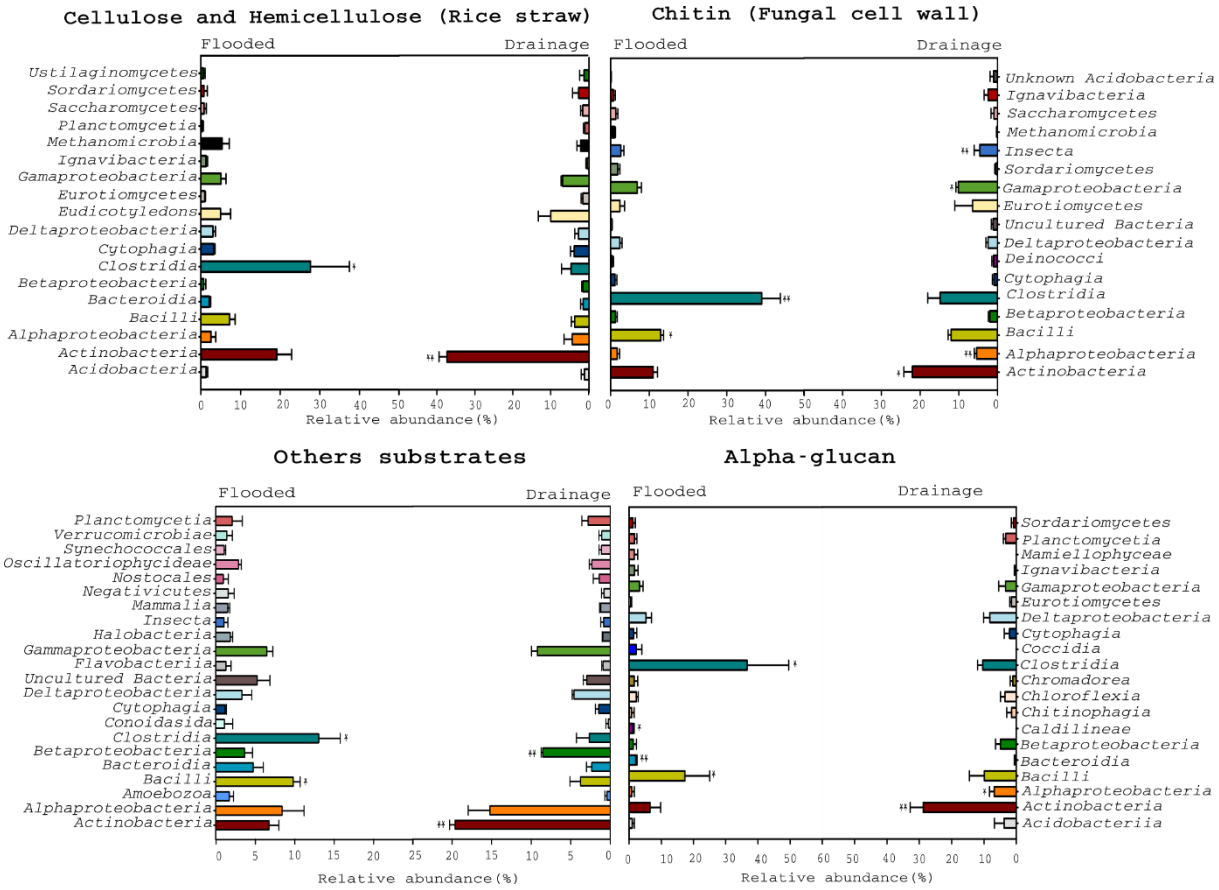

Fig S7 Taxonomic classification of CAZymes mRNA transcripts on class level. The graph shows the taxonomic classification of transcripts encoding carbohydrate-active enzymes involved in the degradation of cellulose, hemicellulose, alpha-glucans and other substrates. Asterisks * $P \leq 0.1$, ** $P \leq 0.05$, *** $P \leq 0.01$ indicate significant difference between flooded and drained soils.

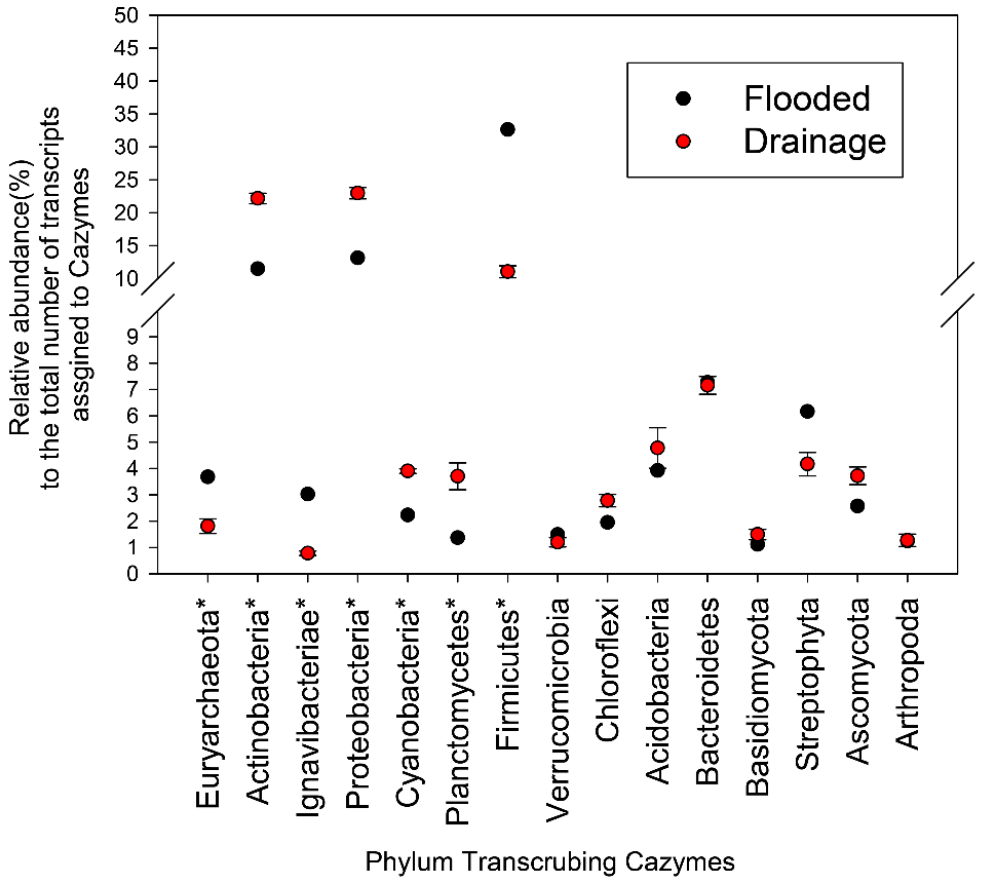

Figure S8 Taxonomic classification of CAZymes mRNA transcripts on phylum level. The graph shows the taxonomic on phylum level of transcripts encoding carbohydrate-active enzymes. Asterisk * indicates corrected *P* [FDR] ≤ 0.05.

Table S1 *SSU rRNA gene and transcript numbers of bacteria, archaea and fungi and mcrA transcript numbers*

	Archaea			Bacteria			Fungi		
	Flooded	Drainage	*P* value [2]	Flooded	Drainage	*P* value [2]	Flooded	Drainage	*P* value [2]
SSU rRNA gene numbers[1]	5.14E+08	9.22E+08	0.009	3.77E+10	1.17E+09	0.004	5.10E+06	2.25E+08	0.017
SSU rRNA transcript numbers[1]	4.77E+09	3.62E+09	0.7	3.61E+12	1.29E+12	0.2	8.59E+06	4.54E+08	0.06
SSU rRNA transcripts/gene ratio	5.8	3.4		59.9	714.5		4.2	1.1	
mcrA transcript numbers[1]	5.79E+06	1.52E+04	0.04						

[1] copy number per g dry weight
[2] Uncorrected *P* values

Table S2 *Relative abundance* (%) *of the methanotrophic community* [1]

	SSU rRNA		mRNA	
	Flooded	**Drainage**	**Flooded**	**Drainage**
Methylocystaceae	1.4±1.6%	0.63±0.01%	0.3±03%	0.2±01%
Crenotrichaceae	0.2±0.3%	0.4±0.3%	NA	NA
Methylococcaceae	0.7±0.9%	1.8±0.9%	1±1.2%	0.5±0.03%
Other uncultured *Methylococcales* [2]	0.3%	0.4%	NA	NA
Sum [2]	2.6%	3.2%	1.3%	0.7%

[1] Relative abundance within the bacterial community, *P* [FDR] ≥ 0.1, therefore not shown
[2] sum of different taxonomic groups

Table S3 *Relative abundance (%) of the most abundant (>1) bacterial species in flooded and drained soils based on SSU rRNA*

Phylum	*Family*	*Species*	*Flooded* [1]	*Drainage* [1]	*P-value* [2]
Actinobacteria	*Nocardioidaceae*	*Marmoricola* sp.	0.2	1.6	0.00
Actinobacteria	*Nocardioidaceae*	unassigned	0.4	2.2	0.00
Planctomycetes	*Planctomycetaceae*	unassigned	0.8	1.0	0.37
Proteobacteria	*Comamonadaceae*	*Ramlibacter* sp.	0.1	1.1	0.07
Proteobacteria	*Comamonadaceae*	unassigned	0.2	1.6	0.04
Proteobacteria	*Haliangiaceae*	unassigned	1.1	1.2	0.74
Fibrobacteres	*Fibrobacterales (order)*	unassigned	1.2	0.2	0.09
Firmicutes	*Bacillaceae*	*Bacillus* sp.	1.1	0.4	0.34
Firmicutes	*Bacillaceae*	*Bacillus* sp.	2.3	1.6	0.51
Firmicutes	*Christensenellaceae R-7 group*	unassigned	1.5	0.6	0.06
Firmicutes	*Clostridiaceae*	*Clostridium sensu stricto 10* (sp.)	3.1	4.0	0.25
Firmicutes	*Clostridiaceae*	*Clostridium sensu stricto 1* (sp.)	2.6	2.3	0.70
Firmicutes	*Clostridiaceae*	*Clostridium sensu stricto 1*(sp.)	1.7	1.0	0.15
Firmicutes	*Clostridiaceae*	C*lostridium sensu stricto* (sp.)	1.1	0.8	0.07
Firmicutes	*Clostridiaceae*		1.2	1.1	0.79
Firmicutes	*Lachnospiraceae*	*Mobilitalea* sp.	1.0	0.3	0.02
Firmicutes	*Ruminococcaceae*	*Pseudobacteroides* sp.	1.1	0.0	0.31
Firmicutes	*Ruminococcaceae*	*Ruminiclostridium* sp.	1.5	0.3	0.01
Firmicutes	*Ruminococcaceae*	*Ruminiclostridium* sp.	2.1	0.3	0.02
Firmicutes	*Ruminococcaceae*	unassigned	1.1	0.2	0.02
Firmicutes	*Ruminococcaceae*	unassigned	1.6	0.2	0.08
Firmicutes	*OPB54*	unassigned	3.2	0.2	0.03

[1] Percentage to the eukarya SSU rRNA reads
[2] Uncorrected *P* values
Green highlight indicates taxa that significantly increased ($P \leq 0.05$) with drainage
Red highlight indicates taxa that significantly decreased ($P \leq 0.05$) with drainage

Table S4 *Relative abundance (%) of the most abundant (>1) archaeal species in flooded and drained soils based on SSU rRNA*

Phylum	***Order***	***Species***	***Flooded*** [1]	***Drainage*** [1]	***P-value*** [2]
Euryarchaeota	*Methanobacteriales*	*Methanobacterium* sp.	1.5	0.7	0.22
Euryarchaeota	*Methanobacteriales*	*Methanobacterium* sp.	2.0	0.6	0.19
Euryarchaeota	*Methanobacteriales*	*Methanobacterium* sp.	8.2	2.4	0.18
Euryarchaeota	*Methanocellales*	*Methanocella* sp.	5.1	5.1	0.91
Euryarchaeota	*Methanocellales*	*Methanocella* sp.	1.1	1.4	0.23
Euryarchaeota	*Methanocellales*	Unassigned Rice Cluster I	6.7	4.4	0.02
Euryarchaeota	*Methanocellales*	Unassigned Rice Cluster I	5.1	2.9	0.02
Euryarchaeota	*Methanomicrobiales*	WCHA2-08	0.8	1.0	0.17
Euryarchaeota	*Methanomicrobiales*	WCHA2-09	1.1	1.6	0.10
	Methanosarcinales	*Methanosaeta* sp.	3.3	4.7	0.25
Euryarchaeota	*Methanosarcinales*	*Methanosarcina* sp	27.9	36.3	0.04
Euryarchaeota	*Methanosarcinales*	*Methanosarcina* sp.	1.0	0.5	0.02
Euryarchaeota	*Methanosarcinales*	*Methanosarcina* sp.	5.9	5.4	0.80
Euryarchaeota	*Methanosarcinales*	*Methanosarcina* sp.	15.4	18.5	0.04
Euryarchaeota	*Thermoplasmatales*	*Methanomassiliicoccus* sp.	1.8	2.0	0.52
Candidatus *Bathyarchaeota*	NA	unassigned	6.7	4.1	0.08
Soil Crenarchaeotic Group(SCG)	NA	unassigned	0.8	1.6	0.06
Soil Crenarchaeotic Group(SCG)	NA	unassigned	0.6	1.0	0.16
Soil Crenarchaeotic Group(SCG)	NA	unassigned	1.2	2.2	0.07

[1] Percentage to the eukarya SSU rRNA reads
[2] Uncorrected *P* values
Green highlight indicates taxa that significantly increased ($P \leq 0.05$) with drainage
Red highlight indicates taxa that significantly decreased ($P \leq 0.05$) with drainage

Table S5 *Relative abundance (%) of the most abundant (>1) lower taxonomic ranks of Eukarya in flooded and drained soils based on SSU rRNA*

Super-group	*Phylum*	*Lower taxonomic levels*	*Flooded* [1]	*Drainage* [1]	*P values* [2]
NA	*Amoebozoa*	MPE1-14	3.1	1.7	0.39
NA	*Amoebozoa*	unassigned *Vannellida*	2.0	0.4	0.47
NA	*Amoebozoa*	unassigned *Acanthamoeba*	5.1	2.0	0.35
NA	*Amoebozoa*	unassigned *Filamoeba*	2.7	2.4	0.75
NA	*Amoebozoa*	unassigned soil amoeba AND16	1.0	0.4	0.42
NA	*Amoebozoa*	unassigned *Telaepolella tubasferens*	0.7	1.2	0.51
NA	*Amoebozoa*	unassigned LKM74	2.2	0.6	0.32
NA	*Amoebozoa*	unassigned *Schizoplasmodiida*	2.0	2.1	0.96
NA	*Archaeplastida*	unassigned *Chlamydomonadales*	1.4	1.3	0.67
NA	*Archaeplastida*	unassigned *Chlorophyceae*	4.3	3.4	0.72
NA	*Archaeplastida*	unassigned *Trebouxiophyceae*	0.5	1.2	0.17
NA	*Centrohelida*	unassigned	3.9	2.3	0.35
Incertae Sedis	*Breviatea*	unassigned *Breviata*	1.6	0.7	0.37
Opisthokonta	*Chytridiomycota*	unassigned *Monoblepharidomycetes*	0.2	1.2	0.14
Opisthokonta	*Ascomycota*	unassigned *Pezizomycotina*	2.7	35.5	0.06
Opisthokonta	*Basidiomycota*	unassigned *Agaricomycotina*	0.5	4.0	0.11
RT5iin2	NA	unassigned uncultured *Eimeriidae*	0.4	1.7	0.03
SAR	*Ciliophora*	unassigned *Colpodea*	2.6	1.1	0.36
SAR	*Ciliophora*	unassigned *Nassophorea*	1.0	0.3	0.47
SAR	*Ciliophora*	unassigned *Hypotrichia*	2.1	4.3	0.17
SAR	*Ciliophora*	unassigned *Spirotrichea*	0.1	1.0	0.14
SAR	*Cercozoa*	*Cercomonas* sp. ATCC 50367	1.2	0.3	0.21
SAR	*Cercozoa*	unassigned *Cercomonas*	2.2	0.5	0.24
SAR	*Cercozoa*	unassigned *Cercomonas*	12.4	3.2	0.08
SAR	*Cercozoa*	unassigned *Pseudopirsonia*	1.2	0.4	0.32
SAR	*Cercozoa*	uncultured marine eukaryote	3.3	1.0	0.22
SAR	*Cercozoa*	unassigned Novel Clade 12	7.5	2.5	0.22
SAR	*Cercozoa*	unassigned *Cercozoa*	6.6	2.3	0.01
SAR	*Ochrophyta*	unassigned *Tribonematales*	0.4	1.4	0.12
unassigned	unassigned	unassigned	0.7	0.5	0.43

[1] Percentage to the eukarya SSU rRNA reads
[2] Uncorrected *P* values
Green highlight indicates taxa that significantly increased ($P \leq 0.05$) with drainage
Red highlight indicates taxa that significantly decreased ($P \leq 0.05$) with drainage

Table S6 *Relative abundance (%) of the top transcripts assigned to KEGG genes (> 0, 1) (KEGG level 4) in flooded and drained soils*

***KEGG genes* (level 4)**	***Flooded*** [1]	***Drainage*** [1]	***P value*** [2]
K00001 alcohol dehydrogenase [EC:1.1.1.1]	0.14	0.21	0.07
K00012 UDPglucose 6-dehydrogenase [EC:1.1.1.22]	0.12	0.12	0.86
K00024 malate dehydrogenase [EC:1.1.1.37]	0.43	0.26	0.31
K00031 isocitrate dehydrogenase [EC:1.1.1.42]	0.15	0.19	0.26
K00052 3-isopropylmalate dehydrogenase [EC:1.1.1.85]	0.07	0.09	0.39
K00053 ketol-acid reductoisomerase [EC:1.1.1.86]	0.15	0.08	0.04
K00058 D-3-phosphoglycerate dehydrogenase [EC:1.1.1.95]	0.22	0.21	0.72
K00059 3-oxoacyl-[acyl-carrier protein] reductase [EC:1.1.1.100]	0.34	0.53	0.02
K00074 3-hydroxybutyryl-CoA dehydrogenase [EC:1.1.1.157]	0.11	0.10	0.69
K00088 IMP dehydrogenase [EC:1.1.1.205]	0.16	0.20	0.47
K00114 alcohol dehydrogenase (cytochrome c) [EC:1.1.2.8]	0.06	0.10	0.00
K00121 S-(hydroxymethyl)glutathione dehydrogenase / alcohol dehydrogenase [EC:1.1.1.284 1.1.1.1]	0.12	0.25	0.06
K00123 formate dehydrogenase major subunit [EC:1.2.1.2]	0.33	0.20	0.13
K00128 aldehyde dehydrogenase (NAD+) [EC:1.2.1.3]	0.26	0.63	0.01
K00133 aspartate-semialdehyde dehydrogenase [EC:1.2.1.11]	0.17	0.11	0.03
K00134 glyceraldehyde 3-phosphate dehydrogenase [EC:1.2.1.12]	0.97	0.47	0.00
K00135 succinate-semialdehyde dehydrogenase / glutarate-semialdehyde dehydrogenase [EC:1.2.1.16 1.2.1.79 1.2.1.20]	0.05	0.19	0.00
K00140 malonate-semialdehyde dehydrogenase (acetylating) / methylmalonate-semialdehyde dehydrogenase [EC:1.2.1.18 1.2.1.27]	0.04	0.11	0.03
K00161 pyruvate dehydrogenase E1 component alpha subunit [EC:1.2.4.1]	0.11	0.21	0.05
K00162 pyruvate dehydrogenase E1 component beta subunit [EC:1.2.4.1]	0.12	0.19	0.13
K00163 pyruvate dehydrogenase E1 component [EC:1.2.4.1]	0.04	0.15	0.00
K00164 2-oxoglutarate dehydrogenase E1 component [EC:1.2.4.2]	0.08	0.26	0.02
K00169 pyruvate ferredoxin oxidoreductase alpha subunit [EC:1.2.7.1]	0.15	0.05	0.04
K00170 pyruvate ferredoxin oxidoreductase beta subunit [EC:1.2.7.1]	0.11	0.06	0.39
K00174 2-oxoglutarate/2-oxoacid ferredoxin oxidoreductase subunit alpha [EC:1.2.7.3 1.2.7.11]	0.29	0.26	0.44
K00175 2-oxoglutarate/2-oxoacid ferredoxin oxidoreductase subunit beta [EC:1.2.7.3 1.2.7.11]	0.17	0.13	0.20
K00197 acetyl-CoA decarbonylase/synthase complex subunit gamma [EC:2.1.1.245]	0.10	0.02	0.02
K00239 succinate dehydrogenase / fumarate reductase, flavoprotein subunit [EC:1.3.5.1 1.3.5.4]	0.13	0.23	0.03
K00248 butyryl-CoA dehydrogenase [EC:1.3.8.1]	0.12	0.08	0.09
K00249 acyl-CoA dehydrogenase [EC:1.3.8.7]	0.07	0.40	0.00
K00257 E1.3.99.- [EC:1.3.99.-]	0.06	0.13	0.00
K00261 glutamate dehydrogenase (NAD(P)+) [EC:1.4.1.3]	0.20	0.08	0.12
K00262 glutamate dehydrogenase (NADP+) [EC:1.4.1.4]	0.22	0.02	0.00
K00265 glutamate synthase (NADPH/NADH) large chain [EC:1.4.1.13 1.4.1.14]	0.06	0.18	0.00
K00266 glutamate synthase (NADPH/NADH) small chain [EC:1.4.1.13 1.4.1.14]	0.12	0.11	0.72

K00320 5,10-methylenetetrahydromethanopterin reductase [EC:1.5.98.2]	0.16	0.01	0.02
K00335 NADH-quinone oxidoreductase subunit F [EC:1.6.5.3]	0.11	0.06	0.02
K00382 dihydrolipoamide dehydrogenase [EC:1.8.1.4]	0.21	0.45	0.00
K00383 glutathione reductase (NADPH) [EC:1.8.1.7]	0.01	0.01	0.36
K00384 thioredoxin reductase (NADPH) [EC:1.8.1.9]	0.09	0.17	0.02
K00399 methyl-coenzyme M reductase alpha subunit [EC:2.8.4.1]	0.81	0.11	0.02
K00401 methyl-coenzyme M reductase beta subunit [EC:2.8.4.1]	0.62	0.05	0.01
K00402 methyl-coenzyme M reductase gamma subunit [EC:2.8.4.1]	0.49	0.03	0.01
K00507 stearoyl-CoA desaturase (Delta-9 desaturase) [EC:1.14.19.1]	0.02	0.19	0.05
K00517 E1.14.-.- [EC:1.14.-.-]	0.01	0.13	0.02
K00525 ribonucleoside-diphosphate reductase alpha chain [EC:1.17.4.1]	0.16	0.21	0.16
K00540 E1.-.-.- [EC:1.-.-.-]	0.05	0.11	0.01
K00548 5-methyltetrahydrofolate--homocysteine methyltransferase [EC:2.1.1.13]	0.21	0.25	0.33
K00584 tetrahydromethanopterin S-methyltransferase subunit H [EC:2.1.1.86]	0.13	0.01	0.02
K00600 glycine hydroxymethyltransferase [EC:2.1.2.1]	0.20	0.22	0.59
K00615 transketolase [EC:2.2.1.1]	0.29	0.40	0.12
K00626 acetyl-CoA C-acetyltransferase [EC:2.3.1.9]	1.09	1.10	0.99
K00627 pyruvate dehydrogenase E2 component (dihydrolipoamide acetyltransferase) [EC:2.3.1.12]	0.11	0.17	0.02
K00632 acetyl-CoA acyltransferase [EC:2.3.1.16]	0.14	0.18	0.41
K00658 2-oxoglutarate dehydrogenase E2 component (dihydrolipoamide succinyltransferase) [EC:2.3.1.61]	0.10	0.18	0.05
K00666 fatty-acyl-CoA synthase [EC:6.2.1.-]	0.04	0.12	0.00
K00681 gamma-glutamyltranspeptidase / glutathione hydrolase [EC:2.3.2.2 3.4.19.13]	0.09	0.14	0.48
K00688 starch phosphorylase [EC:2.4.1.1]	0.15	0.16	0.88
K00790 UDP-N-acetylglucosamine 1-carboxyvinyltransferase [EC:2.5.1.7]	0.13	0.08	0.39
K00799 glutathione S-transferase [EC:2.5.1.18]	0.05	0.18	0.03
K00812 aspartate aminotransferase [EC:2.6.1.1]	0.25	0.28	0.52
K00817 histidinol-phosphate aminotransferase [EC:2.6.1.9]	0.06	0.12	0.01
K00820 glucosamine--fructose-6-phosphate aminotransferase (isomerizing) [EC:2.6.1.16]	0.17	0.23	0.22
K00826 branched-chain amino acid aminotransferase [EC:2.6.1.42]	0.17	0.22	0.29
K00831 phosphoserine aminotransferase [EC:2.6.1.52]	0.18	0.07	0.02
K00845 glucokinase [EC:2.7.1.2]	0.15	0.15	0.93
K00850 6-phosphofructokinase 1 [EC:2.7.1.11]	0.62	0.31	0.03
K00864 glycerol kinase [EC:2.7.1.30]	0.20	0.09	0.08
K00873 pyruvate kinase [EC:2.7.1.40]	0.16	0.27	0.01
K00925 acetate kinase [EC:2.7.2.1]	0.16	0.06	0.01
K00927 phosphoglycerate kinase [EC:2.7.2.3]	0.24	0.16	0.15
K00928 aspartate kinase [EC:2.7.2.4]	0.14	0.12	0.65
K00936 E2.7.3.- [EC:2.7.3.-]	0.08	0.16	0.00
K00948 ribose-phosphate pyrophosphokinase [EC:2.7.6.1]	0.08	0.13	0.08
K00962 polyribonucleotide nucleotidyltransferase [EC:2.7.7.8]	0.34	0.51	0.01
K01006 pyruvate, orthophosphate dikinase [EC:2.7.9.1]	0.70	0.21	0.00

K01007	pyruvate, water dikinase [EC:2.7.9.2]	0.12	0.10	0.51
K01053	gluconolactonase [EC:3.1.1.17]	0.04	0.11	0.02
K01179	endoglucanase [EC:3.2.1.4]	0.22	0.05	0.00
K01181	endo-1,4-beta-xylanase [EC:3.2.1.8]	0.15	0.01	0.00
K01225	cellulose 1,4-beta-cellobiosidase [EC:3.2.1.91]	0.10	0.00	0.02
K01251	adenosylhomocysteinase [EC:3.3.1.1]	0.13	0.22	0.04
K01338	ATP-dependent Lon protease [EC:3.4.21.53]	0.26	0.36	0.07
K01358	ATP-dependent Clp protease, protease subunit [EC:3.4.21.92]	0.18	0.17	0.76
K01362	ovochymase [EC:3.4.21.-]	0.13	0.17	0.52
K01365	cathepsin L [EC:3.4.22.15]	0.14	0.13	0.73
K01426	amidase [EC:3.5.1.4]	0.04	0.17	0.01
K01448	N-acetylmuramoyl-L-alanine amidase [EC:3.5.1.28]	0.17	0.06	0.00
K01593	aromatic-L-amino-acid decarboxylase [EC:4.1.1.28]	0.02	0.12	0.00
K01596	phosphoenolpyruvate carboxykinase (GTP) [EC:4.1.1.32]	0.42	0.39	0.83
K01610	phosphoenolpyruvate carboxykinase (ATP) [EC:4.1.1.49]	0.11	0.12	0.81
K01624	fructose-bisphosphate aldolase, class II [EC:4.1.2.13]	0.36	0.13	0.01
K01647	citrate synthase [EC:2.3.3.1]	0.20	0.24	0.30
K01649	2-isopropylmalate synthase [EC:2.3.3.13]	0.13	0.15	0.40
K01652	acetolactate synthase I/II/III large subunit [EC:2.2.1.6]	0.20	0.45	0.03
K01679	fumarate hydratase, class II [EC:4.2.1.2]	0.04	0.13	0.00
K01681	aconitate hydratase [EC:4.2.1.3]	0.25	0.37	0.09
K01687	dihydroxy-acid dehydratase [EC:4.2.1.9]	0.11	0.16	0.11
K01689	enolase [EC:4.2.1.11]	0.60	0.28	0.02
K01692	enoyl-CoA hydratase [EC:4.2.1.17]	0.10	0.33	0.02
K01703	3-isopropylmalate/(R)-2-methylmalate dehydratase large subunit [EC:4.2.1.33 4.2.1.35]	0.08	0.16	0.03
K01710	dTDP-glucose 4,6-dehydratase [EC:4.2.1.46]	0.09	0.11	0.13
K01714	4-hydroxy-tetrahydrodipicolinate synthase [EC:4.3.3.7]	0.10	0.09	0.68
K01738	cysteine synthase A [EC:2.5.1.47]	0.10	0.18	0.02
K01768	adenylate cyclase [EC:4.6.1.1]	0.04	0.25	0.01
K01782	3-hydroxyacyl-CoA dehydrogenase / enoyl-CoA hydratase / 3-hydroxybutyryl-CoA epimerase [EC:1.1.1.35 4.2.1.17 5.1.2.3]	0.05	0.18	0.07
K01784	UDP-glucose 4-epimerase [EC:5.1.3.2]	0.07	0.12	0.01
K01803	triosephosphate isomerase (TIM) [EC:5.3.1.1]	0.16	0.13	0.40
K01810	glucose-6-phosphate isomerase [EC:5.3.1.9]	0.11	0.11	0.98
K01847	methylmalonyl-CoA mutase [EC:5.4.99.2]	0.05	0.11	0.12
K01848	methylmalonyl-CoA mutase, N-terminal domain [EC:5.4.99.2]	0.09	0.13	0.23
K01854	UDP-galactopyranose mutase [EC:5.4.99.9]	0.02	0.18	0.05
K01868	threonyl-tRNA synthetase [EC:6.1.1.3]	0.11	0.17	0.10
K01869	leucyl-tRNA synthetase [EC:6.1.1.4]	0.13	0.12	0.81
K01870	isoleucyl-tRNA synthetase [EC:6.1.1.5]	0.10	0.14	0.21
K01872	alanyl-tRNA synthetase [EC:6.1.1.7]	0.08	0.15	0.01
K01873	valyl-tRNA synthetase [EC:6.1.1.9]	0.09	0.14	0.02
K01874	methionyl-tRNA synthetase [EC:6.1.1.10]	0.07	0.13	0.08
K01876	aspartyl-tRNA synthetase [EC:6.1.1.12]	0.11	0.09	0.39
K01885	glutamyl-tRNA synthetase [EC:6.1.1.17]	0.07	0.10	0.49
K01895	acetyl-CoA synthetase [EC:6.2.1.1]	0.52	0.52	0.94

K01897	long-chain acyl-CoA synthetase [EC:6.2.1.3]	0.40	0.65	0.01
K01903	succinyl-CoA synthetase beta subunit [EC:6.2.1.5]	0.09	0.16	0.20
K01915	glutamine synthetase [EC:6.3.1.2]	0.60	0.63	0.62
K01953	asparagine synthase (glutamine-hydrolysing) [EC:6.3.5.4]	0.09	0.16	0.07
K01955	carbamoyl-phosphate synthase large subunit [EC:6.3.5.5]	0.09	0.14	0.01
K01961	acetyl-CoA carboxylase, biotin carboxylase subunit [EC:6.4.1.2 6.3.4.14]	0.07	0.14	0.07
K01966	propionyl-CoA carboxylase beta chain [EC:6.4.1.3]	0.10	0.11	0.43
K01971	bifunctional non-homologous end joining protein LigD [EC:6.5.1.1]	0.03	0.13	0.00
K01972	DNA ligase (NAD+) [EC:6.5.1.2]	0.06	0.15	0.04
K01990	ABC-2 type transport system ATP-binding protein	0.09	0.10	0.42
K01999	branched-chain amino acid transport system substrate-binding protein	0.35	0.21	0.21
K02004	putative ABC transport system permease protein	0.09	0.10	0.15
K02014	iron complex outermembrane recepter protein	0.13	0.08	0.36
K02027	multiple sugar transport system substrate-binding protein	0.24	0.07	0.06
K02035	peptide/nickel transport system substrate-binding protein	0.45	0.19	0.11
K02040	phosphate transport system substrate-binding protein	0.11	0.18	0.04
K02058	simple sugar transport system substrate-binding protein	0.14	0.01	0.01
K02111	F-type H+-transporting ATPase subunit alpha [EC:3.6.3.14]	0.22	0.16	0.34
K02112	F-type H+-transporting ATPase subunit beta [EC:3.6.3.14]	0.15	0.16	0.71
K02183	calmodulin	0.13	0.02	0.01
K02274	cytochrome c oxidase subunit I [EC:1.9.3.1]	0.04	0.12	0.01
K02335	DNA polymerase I [EC:2.7.7.7]	0.11	0.27	0.00
K02337	DNA polymerase III subunit alpha [EC:2.7.7.7]	0.16	0.28	0.03
K02338	DNA polymerase III subunit beta [EC:2.7.7.7]	0.13	0.12	0.87
K02342	DNA polymerase III subunit epsilon [EC:2.7.7.7]	0.02	0.10	0.01
K02343	DNA polymerase III subunit gamma/tau [EC:2.7.7.7]	0.12	0.16	0.03
K02355	elongation factor G	0.33	0.38	0.33
K02358	elongation factor Tu	0.59	0.62	0.75
K02406	flagellin	1.18	0.06	0.00
K02469	DNA gyrase subunit A [EC:5.99.1.3]	0.12	0.15	0.18
K02470	DNA gyrase subunit B [EC:5.99.1.3]	0.10	0.14	0.02
K02519	translation initiation factor IF-2	0.19	0.30	0.02
K02520	translation initiation factor IF-3	0.07	0.11	0.06
K02650	type IV pilus assembly protein PilA	0.11	0.02	0.04
K02651	pilus assembly protein Flp/PilA	0.17	0.02	0.01
K02871	large subunit ribosomal protein L13	0.10	0.11	0.46
K02886	large subunit ribosomal protein L2	0.10	0.09	0.46
K02888	large subunit ribosomal protein L21	0.08	0.10	0.09
K02945	small subunit ribosomal protein S1	0.11	0.23	0.01
K02950	small subunit ribosomal protein S12	0.08	0.11	0.26
K02967	small subunit ribosomal protein S2	0.10	0.11	0.48
K02990	small subunit ribosomal protein S6	0.06	0.13	0.01
K03040	DNA-directed RNA polymerase subunit alpha [EC:2.7.7.6]	0.29	0.43	0.15
K03041	DNA-directed RNA polymerase subunit A' [EC:2.7.7.6]	0.05	0.02	0.10

K03043 DNA-directed RNA polymerase subunit beta [EC:2.7.7.6]	0.66	1.13	0.07
K03044 DNA-directed RNA polymerase subunit B' [EC:2.7.7.6]	0.02	0.00	0.06
K03046 DNA-directed RNA polymerase subunit beta' [EC:2.7.7.6]	0.61	1.28	0.05
K03070 preprotein translocase subunit SecA	0.14	0.20	0.05
K03076 preprotein translocase subunit SecY	0.15	0.14	0.65
K03086 RNA polymerase primary sigma factor	0.08	0.14	0.08
K03088 RNA polymerase sigma-70 factor, ECF subfamily	0.12	0.20	0.00
K03106 signal recognition particle subunit SRP54 [EC:3.6.5.4]	0.09	0.10	0.51
K03111 single-strand DNA-binding protein	0.21	0.19	0.68
K03168 DNA topoisomerase I [EC:5.99.1.2]	0.09	0.17	0.02
K03231 elongation factor 1-alpha	0.44	0.17	0.00
K03234 elongation factor 2	0.13	0.05	0.03
K03283 heat shock 70kDa protein 1/8	0.45	0.27	0.15
K03386 peroxiredoxin (alkyl hydroperoxide reductase subunit C) [EC:1.11.1.15]	0.12	0.12	0.82
K03388 heterodisulfide reductase subunit A [EC:1.8.98.1]	0.19	0.03	0.01
K03406 methyl-accepting chemotaxis protein	0.26	0.17	0.11
K03407 two-component system, chemotaxis family, sensor kinase CheA [EC:2.7.13.3]	0.13	0.19	0.02
K03520 aerobic carbon-monoxide dehydrogenase large subunit [EC:1.2.7.4]	0.05	0.28	0.02
K03530 DNA-binding protein HU-beta	0.40	0.11	0.02
K03531 cell division protein FtsZ	0.16	0.07	0.00
K03544 ATP-dependent Clp protease ATP-binding subunit ClpX	0.11	0.10	0.86
K03585 membrane fusion protein, multidrug efflux system	0.08	0.13	0.17
K03628 transcription termination factor Rho	0.08	0.11	0.24
K03657 DNA helicase II / ATP-dependent DNA helicase PcrA [EC:3.6.4.12]	0.08	0.19	0.00
K03695 ATP-dependent Clp protease ATP-binding subunit ClpB	0.22	0.17	0.70
K03696 ATP-dependent Clp protease ATP-binding subunit ClpC	0.15	0.17	0.57
K03704 cold shock protein (beta-ribbon, CspA family)	0.09	0.12	0.49
K03737 pyruvate-ferredoxin/flavodoxin oxidoreductase [EC:1.2.7.1 1.2.7.-]	0.76	0.23	0.00
K03738 aldehyde:ferredoxin oxidoreductase [EC:1.2.7.5]	0.21	0.03	0.04
K03781 catalase [EC:1.11.1.6]	0.18	0.24	0.41
K03797 carboxyl-terminal processing protease [EC:3.4.21.102]	0.11	0.17	0.10
K03798 cell division protease FtsH [EC:3.4.24.-]	0.23	0.43	0.01
K04043 molecular chaperone DnaK	2.57	1.73	0.56
K04072 acetaldehyde dehydrogenase / alcohol dehydrogenase [EC:1.2.1.10 1.1.1.1]	0.20	0.05	0.01
K04077 chaperonin GroEL	6.16	1.97	0.33
K04078 chaperonin GroES	0.25	0.11	0.40
K04079 molecular chaperone HtpG	0.78	0.28	0.09
K04392 Ras-related C3 botulinum toxin substrate 1	0.12	0.11	0.92
K04480 methanol---5-hydroxybenzimidazolylcobamide Co-methyltransferase [EC:2.1.1.90]	0.10	0.02	0.04
K04487 cysteine desulfurase [EC:2.8.1.7]	0.17	0.24	0.22
K04564 superoxide dismutase, Fe-Mn family [EC:1.15.1.1]	0.37	0.53	0.13

K04771	serine protease Do [EC:3.4.21.107]	0.20	0.21	0.98
K05349	beta-glucosidase [EC:3.2.1.21]	0.22	0.15	0.23
K05366	penicillin-binding protein 1A [EC:2.4.1.- 3.4.-.-]	0.10	0.25	0.00
K05592	ATP-dependent RNA helicase DeaD [EC:3.6.4.13]	0.06	0.11	0.05
K05692	actin beta/gamma 1	0.67	0.05	0.03
K05747	Wiskott-Aldrich syndrome protein	0.32	0.38	0.45
K06204	DnaK suppressor protein	0.05	0.12	0.07
K06236	collagen, type I, alpha	0.53	0.13	0.02
K06237	collagen, type IV, alpha	0.15	0.05	0.05
K06399	stage IV sporulation protein B [EC:3.4.21.116]	0.11	0.03	0.14
K07466	replication factor A1	0.10	0.01	0.01
K07516	3-hydroxyacyl-CoA dehydrogenase [EC:1.1.1.35]	0.20	0.08	0.16
K07646	two-component system, OmpR family, sensor histidine kinase KdpD [EC:2.7.13.3]	0.03	0.12	0.03
K07827	GTPase KRas	0.26	0.24	0.92
K08300	ribonuclease E [EC:3.1.26.12]	0.06	0.12	0.03
K08738	cytochrome c	0.21	0.30	0.23
K08884	serine/threonine protein kinase, bacterial [EC:2.7.11.1]	0.11	0.33	0.01
K09458	3-oxoacyl-[acyl-carrier-protein] synthase II [EC:2.3.1.179]	0.18	0.22	0.40
K10112	multiple sugar transport system ATP-binding protein	0.10	0.05	0.03
K10117	raffinose/stachyose/melibiose transport system substrate-binding protein	0.28	0.02	0.01
K10439	ribose transport system substrate-binding protein	0.54	0.07	0.06
K10540	methyl-galactoside transport system substrate-binding protein	0.15	0.00	0.01
K10543	D-xylose transport system substrate-binding protein	0.19	0.06	0.03
K10546	putative multiple sugar transport system substrate-binding protein	0.33	0.01	0.01
K11927	ATP-dependent RNA helicase RhlE [EC:3.6.4.13]	0.01	0.11	0.01
K12132	eukaryotic-like serine/threonine-protein kinase [EC:2.7.11.1]	0.05	0.12	0.02
K13171	serine/arginine repetitive matrix protein 1	0.08	0.26	0.00
K13525	transitional endoplasmic reticulum ATPase	0.12	0.07	0.09
K13924	two-component system, chemotaxis family, CheB/CheR fusion protein [EC:2.1.1.80 3.1.1.61]	0.16	0.32	0.01
K13953	alcohol dehydrogenase, propanol-preferring [EC:1.1.1.1]	0.05	0.18	0.00
K13993	HSP20 family protein	1.26	0.50	0.37
K15987	K(+)-stimulated pyrophosphate-energized sodium pump [EC:3.6.1.1]	0.19	0.09	0.00
K17318	putative aldouronate transport system substrate-binding protein	0.45	0.01	0.03
K18682	ribonucrease Y [EC:3.1.-.-]	0.13	0.05	0.01
K18698	beta-lactamase class A TEM [EC:3.5.2.6]	0.16	0.00	0.06

[1] Percentage to the total functionally annotated mRNA
[2] Uncorrected *P* values
Green highlight indicates transcripts that significantly increased ($P \leq 0.05$) with drainage
Red highlight indicates transcripts that significantly decreased ($P \leq 0.05$) with drainage

Table S7 Relative abundance (%) of transcripts assigned to particulate methane monooxygenase (KEGG level 4) in flooded and drained soils

KEGG genes **(**level 4)	***Flooded*** [1]	***Drainage*** [1]	***P values*** [2]
K16161 methane monooxygenase component C [EC:1.14.13.25]	0.002	0.002	0.861
K10944 methane/ammonia monooxygenase subunit A [EC:1.14.18.3 1.14.99.39]	0.033	0.007	0.268
K10945 methane/ammonia monooxygenase subunit B	0.077	0.031	0.331
K10946 methane/ammonia monooxygenase subunit C	0.088	0.053	0.366

[1] Percentage to the total functionally annotated mRNA
[2] Uncorrected *P values*

Table S8 Phylum level classification within each CAZymes family

Phylum	***Auxiliary Activities*** [1]		***Glycoside Hydrolase*** [1]		***Carbohydrate-Binding Module*** [1]		***Carbohydrate Esterase*** [1]		***Glycosyltransferase*** [1]	
	F	D	F	D	F	D	F	D	F	D
Euryarchaeota	0.2	1.7	1.9	0.8	3	1.2	3.3	1	4.3	1.6
Actinobacteria	23.2	27.6	11	17.6	15.7	26.2	9.3	18.1	17.7	25.8
Ignavibacteriae	0	0	1.9	0.9	3.4	0.8	14.3	3.8	0.5	0.3
Proteobacteria	25.8	40.3	12.1	22.7	10.4	18.8	14.7	28.8	21	31.7
Cyanobacteria	0.2	0.2	0.8	1	0.5	0.6	3.9	6	4.9	7.5
Planctomycetes	0	0.5	0.9	1.4	0.8	4.1	1.3	2.5	0.6	1.7
Firmicutes	6.1	2	30.4	12.1	44.3	21.8	31.7	10	17.7	8.7
Verrucomicrobia	0	0	1	0.6	0.4	0.5	0.2	0.2	0.3	0.3
Chloroflexi	0	0	1.4	1.8	1.5	2.5	0.9	1.2	1.7	2.1
Acidobacteria	0.3	0	2.5	2.5	2.8	1.4	1.2	2.5	1.1	3.1
Bacteroidetes	0.2	2.3	8.4	6.9	4.7	4.3	7.7	8.3	4	4.3
Basidiomycota	17.4	6.4	0.5	0.9	0.1	0.2	1.2	1.2	1.6	1.7
Streptophyta	7.2	0.5	6.7	4.5	2.2	2.4	1	0.3	4.1	1.1
Ascomycota	9.4	9.5	3.5	7.6	3.5	7.6	2.7	7	2.8	2.2
Others	9.9	8.9	17	18.8	6.6	7.6	6.5	9	17.7	8.1

[1] Data is shown in percentage (%) to the total number of transcripts annotated per CAZyme functional category
Green highlight indicates CAZymes family that significantly increased (*P* [FDR] ≤ 0.05) within a specified phyla after drainage
Red highlight indicates CAZymes family that significantly decreased (*P* [FDR] ≤ 0.05) within a specified phyla after drainage
F = Flooded, D= Drainage

Table S9 *Differentially abundant taxa between flooded and drained soils within the combined flooded and drained data-sets (7 + 28 days flooded, and 7 + 28 days drainage)*

OTU	Base Mean	log2 FoldChange	P [FDR]value	Domain/ Super-group	Phylum	Genus	Incubation time
denovo130614	22.0	3.4	0.0	Bacteria	Actinobacteria	Streptomyces	7
denovo697979	36.0	3.2	0.0	Bacteria	Actinobacteria	NA	7
Total number of OTUs within the phylum					**2**		7
denovo444227	72.3	5.0	0.0	Bacteria	Amoebozoa	NA	7
denovo79430	55.2	4.7	0.0	Bacteria	Amoebozoa	NA	7
denovo234356	28.8	4.0	0.0	Bacteria	Amoebozoa	Copromyxa protea	7
denovo575655	18.5	3.5	0.0	Bacteria	Amoebozoa	NA	7
Total number of OTUs within the phylum					4		7
denovo573974	18.1	3.2	0.0	Bacteria	Chlamydiae	NA	7
Total number of OTUs within the phylum				Bacteria	1		7
denovo827239	20.4	3.3	0.0	Bacteria	Cyanobacteria	NA	7
denovo821143	29.2	3.3	0.0	Bacteria	Cyanobacteria	NA	7
Total number of OTUs within the phylum					**2**		7
denovo90560	276.2	5.3	0.0	Bacteria	Firmicutes	Bacillus	7
denovo582448	80.7	4.7	0.0	Bacteria	Firmicutes	NA	7
denovo428689	69.4	4.5	0.0	Bacteria	Firmicutes	Bacillus	7
denovo779101	193.9	4.2	0.0	Bacteria	Firmicutes	NA	7
denovo228329	114.7	4.2	0.0	Bacteria	Firmicutes	Bacillus	7
denovo477339	46.6	4.2	0.0	Bacteria	Firmicutes	Bacillus	7
denovo716260	41.4	4.1	0.0	Bacteria	Firmicutes	Bacillus	7
denovo322365	100.1	4.0	0.0	Bacteria	Firmicutes	Bacillus	7
denovo176902	90.1	4.0	0.0	Bacteria	Firmicutes	Bacillus	7
denovo604890	143.0	4.0	0.0	Bacteria	Firmicutes	Bacillus	7
denovo229904	37.6	4.0	0.0	Bacteria	Firmicutes	Bacillus	7
denovo480766	36.9	4.0	0.0	Bacteria	Firmicutes	uncultured	7
denovo523520	66.0	3.9	0.0	Bacteria	Firmicutes	Bacillus	7
denovo679786	56.3	3.8	0.0	Bacteria	Firmicutes	NA	7
denovo347636	25.2	3.7	0.0	Bacteria	Firmicutes	Bacillus	7
denovo144121	60.6	3.7	0.0	Bacteria	Firmicutes	Bacillus	7
denovo358436	259.2	3.7	0.0	Bacteria	Firmicutes	Bacillus	7
denovo22612	75.9	3.6	0.0	Bacteria	Firmicutes	Clostridium sensu stricto 11	7
denovo797267	54.4	3.6	0.0	Bacteria	Firmicutes	Bacillus	7
denovo747418	132.3	3.6	0.0	Bacteria	Firmicutes	Bacillus	7
denovo328345	137.5	3.6	0.0	Bacteria	Firmicutes	NA	7
denovo191169	58.2	3.5	0.0	Bacteria	Firmicutes	Ruminiclostridium 5	7
denovo380018	23.4	3.5	0.0	Bacteria	Firmicutes	Bacillus	7
denovo412205	29.3	3.5	0.0	Bacteria	Firmicutes	NA	7
denovo153834	52.1	3.5	0.0	Bacteria	Firmicutes	Bacillus	7
denovo553143	50.9	3.4	0.0	Bacteria	Firmicutes	NA	7
denovo402848	31.2	3.4	0.0	Bacteria	Firmicutes	Bacillus	7
denovo667046	138.2	3.4	0.0	Bacteria	Firmicutes	Bacillus	7

denovo314428	80.9	3.4	0.0	Bacteria	Firmicutes	NA	7
denovo152124	38.3	3.4	0.0	Bacteria	Firmicutes	NA	7
denovo354722	107.4	3.4	0.0	Bacteria	Firmicutes	Bacillus	7
denovo201289	18.4	3.4	0.0	Bacteria	Firmicutes	NA	7
denovo205049	86.8	3.4	0.0	Bacteria	Firmicutes	NA	7
denovo514991	81.1	3.4	0.0	Bacteria	Firmicutes	Clostridium sensu stricto 12	7
denovo678646	17.0	3.4	0.0	Bacteria	Firmicutes	uncultured	7
denovo379447	16.2	3.4	0.0	Bacteria	Firmicutes	uncultured	7
denovo785771	71.0	3.4	0.0	Bacteria	Firmicutes	NA	7
denovo547750	52.9	3.3	0.0	Bacteria	Firmicutes	Ruminiclostridium 5	7
denovo600889	46.6	3.3	0.0	Bacteria	Firmicutes	Bacillus	7
denovo811073	15.1	3.3	0.0	Bacteria	Firmicutes	Bacillus	7
denovo297638	30.5	3.3	0.0	Bacteria	Firmicutes	Bacillus	7
denovo521885	20.7	3.3	0.0	Bacteria	Firmicutes	Bacillus	7
denovo61232	62.8	3.3	0.0	Bacteria	Firmicutes	uncultured	7
denovo753200	37.3	3.3	0.0	Bacteria	Firmicutes	Ruminiclostridium 5	7
denovo304232	48.2	3.3	0.0	Bacteria	Firmicutes	Cohnella	7
denovo766974	86.8	3.3	0.0	Bacteria	Firmicutes	Bacillus	7
denovo517422	64.2	3.3	0.0	Bacteria	Firmicutes	Bacillus	7
denovo93385	75.6	3.3	0.0	Bacteria	Firmicutes	Bacillus	7
denovo604553	35.4	3.3	0.0	Bacteria	Firmicutes	NA	7
denovo250202	205.4	3.2	0.0	Bacteria	Firmicutes	Clostridium sensu stricto 11	7
denovo443822	105.0	3.2	0.0	Bacteria	Firmicutes	Bacillus	7
denovo650348	265.6	3.2	0.0	Bacteria	Firmicutes	Bacillus	7
denovo286435	21.7	3.2	0.0	Bacteria	Firmicutes	Bacillus	7
denovo262300	40.1	3.2	0.0	Bacteria	Firmicutes	NA	7
denovo717763	16.4	3.2	0.0	Bacteria	Firmicutes	Bacillus	7
denovo501187	28.0	3.2	0.0	Bacteria	Firmicutes	Bacillus	7
denovo339622	26.1	3.2	0.0	Bacteria	Firmicutes	Bacillus	7
denovo769506	108.6	3.2	0.0	Bacteria	Firmicutes	Clostridium sensu stricto 11	7
denovo431786	132.8	3.2	0.0	Bacteria	Firmicutes	NA	7
denovo537539	30.2	3.2	0.0	Bacteria	Firmicutes	Ruminiclostridium 5	7
denovo277073	127.3	3.2	0.0	Bacteria	Firmicutes	Bacillus	7
denovo124500	13.3	3.2	0.0	Bacteria	Firmicutes	Bacillus	7
denovo685520	59.9	3.2	0.0	Bacteria	Firmicutes	Bacillus	7
denovo640582	28.3	3.2	0.0	Bacteria	Firmicutes	Bacillus	7
denovo76696	17.3	3.2	0.0	Bacteria	Firmicutes	Bacillus	7
denovo693900	64.5	3.2	0.0	Bacteria	Firmicutes	Bacillus	7
denovo29271	44.9	3.2	0.0	Bacteria	Firmicutes	NA	7
denovo214548	47.3	3.2	0.0	Bacteria	Firmicutes	Bacillus	7
denovo48314	29.6	3.1	0.0	Bacteria	Firmicutes	Bacillus	7
denovo128143	151.0	3.1	0.0	Bacteria	Firmicutes	NA	7
denovo250344	18.9	3.1	0.0	Bacteria	Firmicutes	NA	7

denovo666382	13.9	3.1	0.0	Bacteria	Firmicutes	Bacillus	7
denovo678410	65.3	3.1	0.0	Bacteria	Firmicutes	Bacillus	7
denovo738482	76.3	3.1	0.0	Bacteria	Firmicutes	Bacillus	7
denovo576382	14.1	3.1	0.0	Bacteria	Firmicutes	Bacillus	7
denovo500874	11.3	3.0	0.0	Bacteria	Firmicutes	Bacillus	7
denovo644131	169.4	3.0	0.0	Bacteria	Firmicutes	Bacillus	7
denovo243134	21.6	3.0	0.0	Bacteria	Firmicutes	Bacillus	7
denovo118695	30.3	3.0	0.0	Bacteria	Firmicutes	Bacillus	7
denovo312868	44.1	3.0	0.0	Bacteria	Firmicutes	Bacillus	7
denovo537457	32.9	3.0	0.0	Bacteria	Firmicutes	Bacillus	7
denovo57982	26.9	3.0	0.0	Bacteria	Firmicutes	Bacillus	7
denovo631329	26.3	2.9	0.0	Bacteria	Firmicutes	Bacillus	7
denovo739696	99.1	2.9	0.0	Bacteria	Firmicutes	Bacillus	7
denovo543107	24.2	2.9	0.0	Bacteria	Firmicutes	Bacillus	7
denovo291225	40.2	2.9	0.0	Bacteria	Firmicutes	Bacillus	7
denovo78063	24.8	2.9	0.0	Bacteria	Firmicutes	uncultured	7
denovo628231	21.9	2.9	0.0	Bacteria	Firmicutes	Bacillus	7
denovo702559	19.7	2.9	0.0	Bacteria	Firmicutes	Bacillus	7
denovo709008	86.5	2.9	0.0	Bacteria	Firmicutes	Bacillus	7
denovo662041	118.1	2.9	0.0	Bacteria	Firmicutes	Bacillus	7
denovo161106	40.0	2.8	0.0	Bacteria	Firmicutes	Bacillus	7
denovo461448	413.9	2.8	0.0	Bacteria	Firmicutes	NA	7
denovo369130	40.1	2.8	0.0	Bacteria	Firmicutes	Bacillus	7
denovo563849	64.7	2.8	0.0	Bacteria	Firmicutes	Bacillus	7
denovo629779	256.8	2.8	0.0	Bacteria	Firmicutes	Bacillus	7
denovo211467	55.7	2.7	0.0	Bacteria	Firmicutes	Bacillus	7
Total number of OTUs within the phylum					**97**	0.0	7
denovo386489	851.1	4.4	0.0	Opisthokonta (fungi)	Mucoromycotina	Mucor	7
denovo747896	452.5	4.4	0.0	Opisthokonta (fungi)	Mucoromycotina	NA	7
denovo33995	186.3	4.3	0.0	Opisthokonta (fungi)	Mucoromycotina	NA	7
denovo356427	314.5	4.2	0.0	Opisthokonta (fungi)	Mucoromycotina	Rhizopus	7
denovo565501	265.6	4.2	0.0	Opisthokonta (fungi)	Mucoromycotina	NA	7
denovo165159	115.3	4.1	0.0	Opisthokonta (fungi)	Mucoromycotina	NA	7
denovo669350	162.9	4.1	0.0	Opisthokonta (fungi)	Mucoromycotina	NA	7
denovo391969	57.7	4.1	0.0	Opisthokonta (fungi)	NA	NA	7
denovo766569	512.3	4.1	0.0	Opisthokonta (fungi)	Mucoromycotina	NA	7
denovo20284	117.4	4.1	0.0	Opisthokonta (fungi)	Mucoromycotina	NA	7
denovo782460	136.5	4.0	0.0	Opisthokonta (fungi)	Mucoromycotina	NA	7
denovo515465	120.9	3.9	0.0	Opisthokonta (fungi)	Mucoromycotina	NA	7

denovo551553	237.0	3.9	0.0	Opisthokonta (fungi)	Mucoromycotina	NA	7
denovo490486	43.6	3.9	0.0	Opisthokonta (fungi)	Ascomycota	NA	7
denovo785135	244.1	3.9	0.0	Opisthokonta (fungi)	Mucoromycotina	NA	7
denovo772279	112.8	3.8	0.0	Opisthokonta (fungi)	Mucoromycotina	NA	7
denovo699057	60.2	3.8	0.0	Opisthokonta (fungi)	Mucoromycotina	Mucor	7
denovo286979	79.3	3.8	0.0	Opisthokonta (fungi)	Mucoromycotina	NA	7
denovo729251	100.0	3.8	0.0	Opisthokonta (fungi)	Mucoromycotina	NA	7
denovo442445	304.1	3.7	0.0	Opisthokonta (fungi)	Ascomycota	NA	7
denovo458298	75.9	3.7	0.0	Opisthokonta (fungi)	Mucoromycotina	NA	7
denovo39608	72.2	3.7	0.0	Opisthokonta (fungi)	Mucoromycotina	NA	7
denovo817581	220.5	3.6	0.0	Opisthokonta (fungi)	Ascomycota	Aspergillus	7
denovo458059	127.0	3.6	0.0	Opisthokonta (fungi)	Ascomycota	Aspergillus	7
denovo227057	27.3	3.6	0.0	Opisthokonta (fungi)	Ascomycota	NA	7
denovo545213	60.9	3.6	0.0	Opisthokonta (fungi)	Ascomycota	NA	7
denovo147892	55.7	3.6	0.0	Opisthokonta (fungi)	Ascomycota	NA	7
denovo784077	69.3	3.6	0.0	Opisthokonta (fungi)	Mucoromycotina	NA	7
denovo597846	63.0	3.5	0.0	Opisthokonta (fungi)	Ascomycota	Aspergillus	7
denovo589530	68.4	3.5	0.0	Opisthokonta (fungi)	Ascomycota	Aspergillus	7
denovo753120	35.9	3.5	0.0	Opisthokonta (fungi)	Ascomycota	NA	7
denovo475609	44.9	3.5	0.0	Opisthokonta (fungi)	Mucoromycotina	NA	7
denovo590606	32.8	3.5	0.0	Opisthokonta (fungi)	NA	NA	7
denovo634093	83.7	3.5	0.0	Opisthokonta (fungi)	Ascomycota	Aspergillus	7
denovo53854	115.3	3.4	0.0	Opisthokonta (fungi)	Ascomycota	NA	7
denovo488029	23.5	3.4	0.0	Opisthokonta (fungi)	Ascomycota	NA	7
denovo656359	46.8	3.4	0.0	Opisthokonta (fungi)	Ascomycota	NA	7
denovo150578	154.3	3.4	0.0	Opisthokonta (fungi)	Ascomycota	NA	7
denovo723187	36.6	3.4	0.0	Opisthokonta (fungi)	Mucoromycotina	NA	7
denovo33256	45.8	3.4	0.0	Opisthokonta (fungi)	Mucoromycotina	NA	7

denovo524652	45.8	3.4	0.0	Opisthokonta (fungi)	Ascomycota	NA	7
denovo552576	43.1	3.4	0.0	Opisthokonta (fungi)	Mucoromycotina	NA	7
denovo11260	43.7	3.4	0.0	Opisthokonta (fungi)	Ascomycota	NA	7
denovo250958	33.0	3.3	0.0	Opisthokonta (fungi)	Mucoromycotina	Mucor	7
denovo12319	61.8	3.3	0.0	Opisthokonta (fungi)	Ascomycota	NA	7
denovo343405	36.0	3.3	0.0	Opisthokonta (fungi)	Mucoromycotina	NA	7
denovo267134	24.7	3.3	0.0	Opisthokonta (fungi)	Ascomycota	NA	7
denovo581058	58.6	3.3	0.0	Opisthokonta (fungi)	Ascomycota	NA	7
denovo309815	27.2	3.2	0.0	Opisthokonta (fungi)	Mucoromycotina	NA	7
denovo654768	71.2	3.2	0.0	Opisthokonta (fungi)	Ascomycota	NA	7
denovo527382	19.4	3.2	0.0	Opisthokonta (fungi)	Ascomycota	NA	7
denovo478002	20.6	3.2	0.0	Opisthokonta (fungi)	Ascomycota	NA	7
Total number of OTUs within the super-group				**52**			7
denovo526485	119.9	3.9	0.0	Bacteria	Proteobacteria	NA	7
denovo246454	403.0	3.9	0.0	Bacteria	Proteobacteria	Magnetospirillum	7
denovo568599	46.9	3.8	0.0	Bacteria	Proteobacteria	Burkholderia	7
denovo250777	207.8	3.8	0.0	Bacteria	Proteobacteria	Magnetospirillum	7
denovo181916	79.0	3.7	0.0	Bacteria	Proteobacteria	NA	7
denovo16632	89.5	3.6	0.0	Bacteria	Proteobacteria	Magnetospirillum	7
denovo460336	68.9	3.6	0.0	Bacteria	Proteobacteria	NA	7
denovo179717	135.4	3.6	0.0	Bacteria	Proteobacteria	NA	7
denovo744095	62.6	3.6	0.0	Bacteria	Proteobacteria	NA	7
denovo394000	978.9	3.5	0.0	Bacteria	Proteobacteria	Magnetospirillum	7
denovo689109	49.6	3.4	0.0	Bacteria	Proteobacteria	Variovorax	7
denovo174169	44.8	3.3	0.0	Bacteria	Proteobacteria	Pseudomonas	7
denovo444246	43.5	3.3	0.0	Bacteria	Proteobacteria	Burkholderia	7
denovo468972	107.9	3.3	0.0	Bacteria	Proteobacteria	uncultured bacterium	7
denovo800415	84.6	3.2	0.0	Bacteria	Proteobacteria	NA	7
denovo709927	68.2	3.1	0.0	Bacteria	Proteobacteria	Burkholderia	7
denovo726157	14.2	3.1	0.0	Bacteria	Proteobacteria	Azospirillum	7
denovo24385	26.6	3.0	0.0	Bacteria	Proteobacteria	Pseudomonas	7
denovo463897	25.3	3.0	0.0	Bacteria	Proteobacteria	Variovorax	7
denovo260085	26.6	3.0	0.0	Bacteria	Proteobacteria	Pseudomonas	7
denovo123236	47.0	3.0	0.0	Bacteria	Proteobacteria	Pseudomonas	7
denovo196673	30.3	2.9	0.0	Bacteria	Proteobacteria	Pseudomonas	7
denovo743937	143.5	2.7	0.0	Bacteria	Proteobacteria	NA	7
Total number of OTUs within the phylum					**23**		7
denovo353085	74.3	4.8	0.0	NA	NA	NA	7

denovo571736	51.2	4.6	0.0	NA	NA	NA	7
denovo220741	40.4	4.3	0.0	NA	NA	NA	7
denovo371508	34.1	4.2	0.0	NA	NA	NA	7
denovo440010	32.1	4.1	0.0	NA	NA	NA	7
denovo403659	32.8	4.1	0.0	NA	NA	NA	7
denovo488102	33.5	4.1	0.0	NA	NA	NA	7
denovo177876	26.6	3.9	0.0	NA	NA	NA	7
denovo401435	29.4	3.9	0.0	NA	NA	NA	7
denovo776631	57.4	3.8	0.0	NA	NA	NA	7
denovo436540	25.3	3.8	0.0	NA	NA	NA	7
denovo486427	151.2	3.8	0.0	NA	NA	NA	7
denovo604166	19.9	3.6	0.0	NA	NA	NA	7
denovo132034	20.1	3.6	0.0	NA	NA	NA	7
denovo296169	34.0	3.6	0.0	NA	NA	NA	7
denovo165899	21.6	3.6	0.0	NA	NA	NA	7
denovo48340	44.7	3.5	0.0	NA	NA	NA	7
denovo538875	81.9	3.5	0.0	NA	NA	NA	7
denovo763997	17.7	3.4	0.0	NA	NA	NA	7
denovo485132	24.7	3.4	0.0	NA	NA	NA	7
denovo398790	24.9	3.4	0.0	NA	NA	NA	7
denovo235624	15.6	3.3	0.0	NA	NA	NA	7
denovo290878	17.9	3.3	0.0	NA	NA	NA	7
denovo687253	14.2	3.3	0.0	NA	NA	NA	7
denovo495925	16.6	3.3	0.0	NA	NA	NA	7
denovo625983	26.7	3.2	0.0	NA	NA	NA	7
denovo722466	18.0	3.2	0.0	NA	NA	NA	7
denovo358854	29.8	3.2	0.0	NA	NA	NA	7
denovo448491	13.1	3.2	0.0	NA	NA	NA	7
denovo76658	15.4	3.2	0.0	NA	NA	NA	7
denovo117830	20.8	3.2	0.0	NA	NA	NA	7
denovo725433	13.6	3.2	0.0	NA	NA	NA	7
denovo830303	14.2	3.1	0.0	NA	NA	NA	7
denovo197185	26.0	3.1	0.0	NA	NA	NA	7
denovo523572	17.1	3.1	0.0	NA	NA	NA	7
denovo408788	11.5	3.1	0.0	NA	NA	NA	7
denovo229265	20.6	3.0	0.0	NA	NA	NA	7
denovo65405	13.6	3.0	0.0	NA	NA	NA	7
denovo410966	47.1	2.9	0.0	NA	NA	NA	7
denovo363207	42.0	2.9	0.0	NA	NA	NA	7
denovo530704	68.7	2.8	0.0	NA	NA	NA	7
denovo705508	60.8	-2.8	0.0	Bacteria	Bacteroidetes	NA	7
denovo410470	27.9	-2.9	0.0	Bacteria	Bacteroidetes	Bacteroidetes vadinHA17	28
denovo708433	95.9	-2.9	0.0	Bacteria	Bacteroidetes	NA	28
denovo512507	34.5	-2.9	0.0	Bacteria	Bacteroidetes	Bacteroidetes vadinHA17	28
denovo594451	28.7	-2.9	0.0	Bacteria	Bacteroidetes	NA	28

denovo674811	30.3	-3.0	0,0	Bacteria	Bacteroidetes	Bacteroidetes vadinHA17	28
denovo107205	68.9	-3.0	0.0	Bacteria	Bacteroidetes	Bacteroidetes vadinHA17	28
denovo356279	42.5	-3.0	0.0	Bacteria	Bacteroidetes	Bacteroidetes vadinHA17	28
denovo353205	21.6	-3.0	0.0	Bacteria	Bacteroidetes	Bacteroidetes vadinHA17	28
denovo801901	102.8	-3.0	0.0	Bacteria	Bacteroidetes	Bacteroidetes vadinHA17	28
denovo423850	237.5	-3.0	0.0	Bacteria	Bacteroidetes	Bacteroidetes vadinHA17	28
denovo570808	21.6	-3.0	0.0	Bacteria	Bacteroidetes	Bacteroidia	28
denovo498108	51.3	-3.0	0.0	Bacteria	Bacteroidetes	Bacteroidetes vadinHA17	28
denovo78165	33.3	-3.1	0.0	Bacteria	Bacteroidetes	NA	28
denovo467348	23.8	-3.1	0.0	Bacteria	Bacteroidetes	Bacteroidetes vadinHA17	28
denovo469062	28.2	-3.1	0.0	Bacteria	Bacteroidetes	Bacteroidetes vadinHA17	28
denovo333656	40.9	-3.1	0.0	Bacteria	Bacteroidetes	Bacteroidetes vadinHA17	28
denovo28934	31.9	-3.1	0.0	Bacteria	Bacteroidetes	Bacteroidetes vadinHA17	28
denovo241468	24.4	-3.2	0.0	Bacteria	Bacteroidetes	Bacteroidetes vadinHA17	28
denovo404293	42.5	-3.2	0.0	Bacteria	Bacteroidetes	Bacteroidetes vadinHA17	28
denovo529936	106.1	-3.2	0.0	Bacteria	Bacteroidetes	Bacteroidetes vadinHA17	28
denovo625413	70.3	-3.2	0.0	Bacteria	Bacteroidetes	Sphingobacteriia	28
denovo256021	25.8	-3.2	0.0	Bacteria	Bacteroidetes	Bacteroidetes vadinHA17	28
denovo505504	32.1	-3.2	0.0	Bacteria	Bacteroidetes	Bacteroidia	28
denovo346482	35.3	-3.2	0.0	Bacteria	Bacteroidetes	NA	28
denovo325036	52.9	-3.2	0.0	Bacteria	Bacteroidetes	Bacteroidetes vadinHA17	28
denovo560045	34.6	-3.3	0.0	Bacteria	Bacteroidetes	Sphingobacteriia	28
denovo278584	48.1	-3.3	0.0	Bacteria	Bacteroidetes	Bacteroidetes vadinHA17	28
denovo315164	48.1	-3.3	0.0	Bacteria	Bacteroidetes	NA	28
denovo723165	183.2	-3.3	0.0	Bacteria	Bacteroidetes	Bacteroidetes vadinHA17	28
denovo53317	30.2	-3.3	0.0	Bacteria	Bacteroidetes	Bacteroidetes vadinHA17	28
denovo71278	66.8	-3.4	0.0	Bacteria	Bacteroidetes	Bacteroidetes vadinHA17	28
denovo106581	69.5	-3.4	0.0	Bacteria	Bacteroidetes	Bacteroidetes vadinHA17	28
denovo85256	110.1	-3.4	0.0	Bacteria	Bacteroidetes	Bacteroidetes vadinHA17	28
denovo272445	36.0	-3.5	0.0	Bacteria	Bacteroidetes	Bacteroidetes vadinHA17	28
denovo69716	51.5	-3.5	0.0	Bacteria	Bacteroidetes	Bacteroidetes vadinHA17	28

denovo146108	105.3	-3.5	0.0	Bacteria	Bacteroidetes	Bacteroidetes vadinHA17	28
denovo386846	220.0	-3.5	0.0	Bacteria	Bacteroidetes	Bacteroidetes vadinHA17	28
denovo622327	57.3	-3.5	0.0	Bacteria	Bacteroidetes	Bacteroidetes vadinHA17	28
denovo108032	61.1	-3.5	0.0	Bacteria	Bacteroidetes	Bacteroidetes vadinHA17	28
denovo552997	62.5	-3.6	0.0	Bacteria	Bacteroidetes	Bacteroidetes vadinHA17	28
denovo528749	80.3	-3.6	0.0	Bacteria	Bacteroidetes	Bacteroidetes vadinHA17	28
denovo186586	101.2	-3.6	0.0	Bacteria	Bacteroidetes	Bacteroidetes vadinHA17	28
denovo623284	63.3	-3.6	0.0	Bacteria	Bacteroidetes	Bacteroidetes vadinHA17	28
denovo309655	76.7	-3.7	0.0	Bacteria	Bacteroidetes	Bacteroidetes vadinHA17	28
denovo757376	219.5	-3.8	0.0	Bacteria	Bacteroidetes	Bacteroidetes vadinHA17	28
denovo597240	158.8	-3.8	0.0	Bacteria	Bacteroidetes	NA	28
denovo79095	90.9	-3.8	0.0	Bacteria	Bacteroidetes	Bacteroidetes vadinHA17	28
denovo751797	98.1	-3.9	0.0	Bacteria	Bacteroidetes	Bacteroidetes vadinHA17	28
denovo415690	76.8	-4.0	0.0	Bacteria	Bacteroidetes	Bacteroidetes vadinHA17	28
denovo616727	394.0	-4.0	0.0	Bacteria	Bacteroidetes	Bacteroidetes vadinHA17	28
denovo382917	96.8	-4.1	0.0	Bacteria	Bacteroidetes	Bacteroidetes vadinHA17	28
denovo196788	126.9	-4.1	0.0	Bacteria	Bacteroidetes	NA	28
denovo192711	479.8	-4.2	0.0	Bacteria	Bacteroidetes	Bacteroidetes vadinHA17	28
denovo613907	600.3	-4.2	0.0	Bacteria	Bacteroidetes	Bacteroidetes vadinHA17	28
denovo215971	459.3	-4.3	0.0	Bacteria	Bacteroidetes	Bacteroidetes vadinHA17	28
denovo66425	172.7	-4.4	0.0	Bacteria	Bacteroidetes	Bacteroidetes vadinHA17	28
denovo333790	204.3	-4.6	0.0	Bacteria	Bacteroidetes	Bacteroidetes vadinHA17	28
Total number of OTUs within the phylum					**58**		28
denovo380515	47.6	-2.8	0.0	Bacteria	Chlorobi	NA	28
Total number of OTUs within the phylum					**1**		28
denovo444836	37.9	-2.9	0.0	Bacteria	Fibrobacteres	NA	28
denovo621214	40.0	-3.3	0.0	Bacteria	Fibrobacteres	NA	28
Total number of OTUs within the phylum					**2**		28
denovo49595	110.2	-2.8	0.0	Bacteria	Firmicutes	Oxobacter	28
denovo557703	49.1	-3.0	0.0	Bacteria	Firmicutes	Christensenellaceae R-7 group	28
denovo331980	32.7	-3.0	0.0	Bacteria	Firmicutes		28
denovo92210	34.5	-3.3	0.0	Bacteria	Firmicutes	NA	28

Total number of OTUs within the phylum					**4**		28
denovo627321	31.1	-3.0	0.0	Bacteria	Latescibacteria	Candidatus Latescibacter	28
denovo172228	71.7	-3.5	0.0	Bacteria	Latescibacteria	Candidatus Latescibacter	28
Total number of OTUs within the phylum					**2**		28
denovo146464	20.0	-3.0	0.0	Bacteria	Planctomycetes	NA	28
denovo325139	23.6	-3.1	0.0	Bacteria	Planctomycetes	NA	28
Total number of OTUs within the phylum					**2**		28
denovo445971	36.9	-2.9	0.0	Bacteria	Proteobacteria	Syntrophorhabdus	28
denovo610313	75.5	-3.1	0.0	Bacteria	Proteobacteria	NA	28
denovo216693	47.7	-3.1	0.0	Bacteria	Proteobacteria	Haliangium	28
denovo591220	116.1	-3.2	0.0	Bacteria	Proteobacteria	Methylomonas	28
denovo493791	338.1	-3.2	0.0	Bacteria	Proteobacteria	NA	28
denovo825732	82.5	-3.2	0.0	Bacteria	Proteobacteria	Methylomonas	28
denovo247377	149.1	-3.2	0.0	Bacteria	Proteobacteria	Methylomonas	28
denovo44108	50.2	-3.3	0.0	Bacteria	Proteobacteria	NA	28
denovo784224	207.1	-3.3	0.0	Bacteria	Proteobacteria	Azoarcus	28
denovo610295	105.8	-3.3	0.0	Bacteria	Proteobacteria	NA	28
denovo488888	135.6	-3.3	0.0	Bacteria	Proteobacteria	Sideroxydans	28
denovo216481	77.2	-3.3	0.0	Bacteria	Proteobacteria	Haliangium	28
denovo470603	159.4	-3.4	0.0	Bacteria	Proteobacteria	NA	28
denovo165417	127.6	-3.4	0.0	Bacteria	Proteobacteria	NA	28
denovo185038	103.9	-3.4	0.0	Bacteria	Proteobacteria	Methylomonas	28
denovo611304	57.3	-3.4	0.0	Bacteria	Proteobacteria	Haliangium	28
denovo592059	233.3	-3.4	0.0	Bacteria	Proteobacteria	Methylomonas	28
denovo634787	519.8	-3.7	0.0	Bacteria	Proteobacteria	Methylomonas	28
denovo15228	151.5	-3.8	0.0	Bacteria	Proteobacteria	Azoarcus	28
denovo237537	167.3	-4.0	0.0	Bacteria	Proteobacteria	Methylomonas	28
denovo736967	131.8	-4.0	0.0	Bacteria	Proteobacteria	Methylomonas	28
Total number of OTUs within the phylum					21		28
denovo6463	57.0	-3.0	0.0	Unassigned	NA	NA	28
denovo238337	26.6	-3.0	0.0	Unassigned	NA	NA	28
denovo248398	28.0	-3.1	0.0	Unassigned	NA	NA	28
denovo76260	26.8	-3.2	0.0	Unassigned	NA	NA	28
Total number of OTUs within the phylum					4		28

Table S10 *Transcripts overrepresented in flooded or drained soils within the combined flooded and drained data-sets (7 + 28 days flooded, and 7 + 28 days drainage)*

***KEGG Genes* (level 4)**	***log2FC*** [1]	***P value*** [2]	***Upregulate under***
K03235 elongation factor 3	-3.7	0.0	Drainage
K03891 ubiquinol-cytochrome c reductase cytochrome b subunit	-3.6	0.0	Drainage
K03379 cyclohexanone monooxygenase [EC:1.14.13.22]	-3.4	0.0	Drainage
K14161 protein ImuB	-3.1	0.0	Drainage
K00982 adenylyltransferase / [glutamine synthetase]-adenylyl-L-tyrosine phosphorylase	-3.1	0.0	Drainage
K04090 indolepyruvate ferredoxin oxidoreductase	-3.1	0.0	Drainage
K07788 multidrug efflux pump	-3.0	0.0	Drainage
K09800 translocation and assembly module TamB	-2.9	0.0	Drainage
K00990 [protein-PII] uridylyltransferase [EC:2.7.7.59]	-2.9	0.0	Drainage
K07789 multidrug efflux pump	-2.9	0.0	Drainage
K01854 UDP-galactopyranose mutase	-2.9	0.0	Drainage
K01690 phosphogluconate dehydratase [EC:4.2.1.12]	-2.8	0.0	Drainage
K01555 fumarylacetoacetase [EC:3.7.1.2]	-2.8	0.0	Drainage
K11927 ATP-dependent RNA helicase RhlE [EC:3.6.4.13]	-2.8	0.0	Drainage
K00547 homocysteine S-methyltransferase [EC:2.1.1.10]	-2.8	0.0	Drainage
K13571 proteasome accessory factor A [EC:6.3.1.19]	-2.8	0.0	Drainage
K00285 D-amino-acid dehydrogenase [EC:1.4.99.1]	-2.7	0.0	Drainage
K15174 RNA polymerase II-associated factor 1	-2.7	0.0	Drainage
K00549 5-methyltetrahydropteroyltriglutamate--homocysteine methyltransferase [EC:2.1.1.14]	-2.7	0.0	Drainage
K01414 oligopeptidase A [EC:3.4.24.70]	-2.7	0.0	Drainage
K00507 stearoyl-CoA desaturase (delta-9 desaturase) [EC:1.14.19.1]	-2.6	0.0	Drainage
K07147 methionine sulfoxide reductase catalytic subunit [EC:1.8.-.-]	-2.5	0.0	Drainage
K00381 sulfite reductase (NADPH) hemoprotein beta-component [EC:1.8.1.2]	-2.4	0.0	Drainage
K07552 MFS transporter, DHA1 family, multidrug resistance protein	-2.4	0.0	Drainage
K09162 chlorite dismutase [EC:1.13.11.49]	-2.4	0.0	Drainage
K00517 [EC: 1.14.-.-]	-2.3	0.0	Drainage
K01473 N-methylhydantoinase A [EC:3.5.2.14]	-2.3	0.0	Drainage
K09691 lipopolysaccharide transport system ATP-binding protein	-2.3	0.0	Drainage
K01474 N-methylhydantoinase B [EC:3.5.2.14]	-2.3	0.0	Drainage
K01488 adenosine deaminase [EC:3.5.4.4]	-2.3	0.0	Drainage
K13527 proteasome-associated ATPase	-2.2	0.0	Drainage
K01114 phospholipase C [EC:3.1.4.3]	-2.2	0.0	Drainage
K15371 glutamate dehydrogenase [EC:1.4.1.2]	-2.2	0.0	Drainage
K02301 protoheme IX farnesyltransferase [EC: 2.5.1.-]	-2.1	0.0	Drainage
K05365 penicillin-binding protein 1B [EC: 2.4.1.129 3.4.-.-]	-2.1	0.0	Drainage
K19302 undecaprenyl-diphosphatase [EC:3.6.1.27]	-2.1	0.0	Drainage
K03405 magnesium chelatase subunit I [EC:6.6.1.1]	-2.1	0.0	Drainage
K00117 quinoprotein glucose dehydrogenase [EC:1.1.5.2]	-2.1	0.0	Drainage
K02438 glycogen debranching enzyme [EC:3.2.1.196]	-2.0	0.0	Drainage
K00574 cyclopropane-fatty-acyl-phospholipid synthase [EC:2.1.1.79]	-2.0	0.0	Drainage
K01768 adenylate cyclase [EC:4.6.1.1]	-2.0	0.0	Drainage

K00193 acetyl-CoA decarbonylase/synthase complex subunit beta [EC: 2.3.1.-]	2.0	0.0	Flooded
K00200 formylmethanofuran dehydrogenase subunit A [EC:1.2.99.5]	2.0	0.0	Flooded
K03390 heterodisulfide reductase subunit C [EC:1.8.98.1]	2.0	0.0	Flooded
K06237 collagen. type IV. alpha	2.0	0.0	Flooded
K01572 oxaloacetate decarboxylase. beta subunit [EC:4.1.1.3]	2.1	0.0	Flooded
K00402 methyl-coenzyme M reductase gamma subunit [EC:2.8.4.1]	2.1	0.0	Flooded
K01938 formate--tetrahydrofolate ligase [EC:6.3.4.3]	2.1	0.0	Flooded
K06284 transcriptional pleiotropic regulator of transition state genes	2.1	0.0	Flooded
K02119 V/A-type H+-transporting ATPase subunit C	2.1	0.0	Flooded
K04480 methanol---5-hydroxybenzimidazolylcobamide Co-methyltransferase [EC:2.1.1.90]	2.1	0.0	Flooded
K00579 tetrahydromethanopterin S-methyltransferase subunit C [EC:2.1.1.86]	2.1	0.0	Flooded
K01805 xylose isomerase [EC:5.3.1.5]	2.2	0.0	Flooded
K07406 alpha-galactosidase [EC:3.2.1.22]	2.2	0.0	Flooded
K00441 coenzyme F420 hydrogenase subunit beta [EC:1.12.98.1]	2.2	0.0	Flooded
K00853 L-ribulokinase [EC:2.7.1.16]	2.2	0.0	Flooded
K02392 flagellar basal-body rod protein FlgG	2.2	0.0	Flooded
K00192 acetyl-CoA decarbonylase/synthase complex subunit alpha [EC:1.2.7.4]	2.2	0.0	Flooded
K03421 methyl-coenzyme M reductase subunit C	2.2	0.0	Flooded
K00177 2-oxoglutarate ferredoxin oxidoreductase subunit gamma [EC:1.2.7.3]	2.2	0.0	Flooded
K07466 replication factor A1	2.2	0.0	Flooded
K00171 pyruvate ferredoxin oxidoreductase. delta subunit [EC:1.2.7.1]	2.3	0.0	Flooded
K01960 pyruvate carboxylase subunit B [EC:6.4.1.1]	2.3	0.0	Flooded
K07469 aldehyde oxidoreductase [EC:1.2.99.7]	2.3	0.0	Flooded
K00584 tetrahydromethanopterin S-methyltransferase subunit H [EC:2.1.1.86]	2.4	0.0	Flooded
K08264 heterodisulfide reductase subunit D [EC:1.8.98.1]	2.4	0.0	Flooded
K10670 glycine/sarcosine/betaine reductase complex component A [EC:1.21.4.2 1.21.4.3 1.21.4.4]	2.4	0.0	Flooded
K00176 2-oxoglutarate ferredoxin oxidoreductase subunit delta [EC:1.2.7.3]	2.4	0.0	Flooded
K01818 L-fucose isomerase [EC:5.3.1.25]	2.4	0.0	Flooded
K00198 carbon-monoxide dehydrogenase catalytic subunit [EC:1.2.99.2 1.2.7.4]	2.4	0.0	Flooded
K01449 N-acetylmuramoyl-L-alanine amidase [EC:3.5.1.28]	2.4	0.0	Flooded
K01179 endoglucanase [EC:3.2.1.4]	2.4	0.0	Flooded
K01176 alpha-amylase [EC:3.2.1.1]	2.5	0.0	Flooded
K10119 raffinose/stachyose/melibiose transport system permease protein	2.5	0.0	Flooded
K06113 arabinan endo-1.5-alpha-L-arabinosidase [EC:3.2.1.99]	2.5	0.0	Flooded
K14081 methanol corrinoid protein	2.5	0.0	Flooded
K12264 anaerobic nitric oxide reductase flavorubredoxin	2.5	0.0	Flooded
K03737 pyruvate-ferredoxin/flavodoxin oxidoreductase [EC: 1.2.7.1 1.2.7.-]	2.5	0.0	Flooded
K02117 V/A-type H+-transporting ATPase subunit A [EC:3.6.3.14]	2.5	0.0	Flooded
K07171 mRNA interferase MazF [EC: 3.1.-.-]	2.5	0.0	Flooded
K02440 glycerol uptake facilitator protein	2.5	0.0	Flooded
K03420 proteasome regulatory subunit	2.5	0.0	Flooded

K01218 mannan endo-1.4-beta-mannosidase [EC:3.2.1.78]	2.5	0.0	Flooded
K15580 oligopeptide transport system substrate-binding protein	2.6	0.0	Flooded
K02795 PTS system. mannose-specific IIC component	2.6	0.0	Flooded
K03388 heterodisulfide reductase subunit A [EC:1.8.98.1]	2.6	0.0	Flooded
K14475 inhibitor of cysteine peptidase	2.6	0.0	Flooded
K00580 tetrahydromethanopterin S-methyltransferase subunit D [EC:2.1.1.86]	2.6	0.0	Flooded
K03422 methyl-coenzyme M reductase subunit D	2.6	0.0	Flooded
K15531 oligosaccharide reducing-end xylanase [EC:3.2.1.156]	2.6	0.0	Flooded
K14127 F420-non-reducing hydrogenase iron-sulfur subunit [EC: 1.12.99.-]	2.6	0.0	Flooded
K01224 arabinogalactan endo-1,4-beta-galactosidase [EC:3.2.1.89]	2.7	0.0	Flooded
K05878 dihydroxyacetone kinase. N-terminal domain [EC: 2.7.1.-]	2.7	0.0	Flooded
K04769 AbrB family transcriptional regulator. stage V sporulation protein T	2.7	0.0	Flooded
K10548 putative multiple sugar transport system ATP-binding protein	2.7	0.0	Flooded
K00442 coenzyme F420 hydrogenase subunit delta	2.7	0.0	Flooded
K01571 oxaloacetate decarboxylase. alpha subunit [EC:4.1.1.3]	2.7	0.0	Flooded
K03091 RNA polymerase sporulation-specific sigma factor	2.7	0.0	Flooded
K13276 bacillopeptidase F [EC: 3.4.21.-]	2.7	0.0	Flooded
K02588 nitrogenase iron protein NifH [EC:1.18.6.1]	2.7	0.0	Flooded
K17202 erythritol transport system substrate-binding protein	2.8	0.0	Flooded
K14126 F420-non-reducing hydrogenase large subunit [EC: 1.12.99.-]	2.8	0.0	Flooded
K04076 ATP-dependent Lon protease [EC:3.4.21.53]	2.8	0.0	Flooded
K10439 ribose transport system substrate-binding protein	2.8	0.0	Flooded
K00205 4Fe-4S ferredoxin	2.8	0.0	Flooded
K17319 putative aldouronate transport system permease protein	2.8	0.0	Flooded
K03738 aldehyde:ferredoxin oxidoreductase [EC:1.2.7.5]	2.9	0.0	Flooded
K00582 tetrahydromethanopterin S-methyltransferase subunit F [EC:2.1.1.86]	2.9	0.0	Flooded
K11751 5'-nucleotidase / UDP-sugar diphosphatase [EC:3.1.3.5 3.6.1.45]	2.9	0.0	Flooded
K13280 signal peptidase. endoplasmic reticulum-type [EC:3.4.-.-]	2.9	0.0	Flooded
K06382 stage II sporulation protein E [EC:3.1.3.16]	2.9	0.0	Flooded
K00443 coenzyme F420 hydrogenase subunit gamma [EC:1.12.98.1]	2.9	0.0	Flooded
K00319 methylenetetrahydromethanopterin dehydrogenase [EC:1.5.98.1]	2.9	0.0	Flooded
K00440 coenzyme F420 hydrogenase subunit alpha [EC:1.12.98.1]	2.9	0.0	Flooded
K00005 glycerol dehydrogenase [EC:1.1.1.6]	2.9	0.0	Flooded
K15023 5-methyltetrahydrofolate corrinoid/iron sulfur protein methyltransferase [EC:2.1.1.258]	2.9	0.0	Flooded
K02122 V/A-type H+-transporting ATPase subunit F	2.9	0.0	Flooded
K04523 ubiquilin	3.0	0.0	Flooded
K00577 tetrahydromethanopterin S-methyltransferase subunit A [EC:2.1.1.86]	3.0	0.0	Flooded
K14138 acetyl-CoA synthase [EC:2.3.1.169]	3.0	0.0	Flooded
K07325 archaeal flagellin FlaB	3.0	0.0	Flooded
K00394 adenylylsulfate reductase, subunit A [EC:1.8.99.2]	3.0	0.0	Flooded
K00125 formate dehydrogenase. beta subunit [EC:1.2.1.2]	3.0	0.0	Flooded
K01119 2'.3'-cyclic-nucleotide 2'-phosphodiesterase / 3'-nucleotidase [EC:3.1.4.16 3.1.3.6]	3.0	0.0	Flooded

K18332 NADP-reducing hydrogenase subunit HndD [EC:1.12.1.3]	3.0	0.0	Flooded
K10542 methyl-galactoside transport system ATP-binding protein [EC:3.6.3.17]	3.0	0.0	Flooded
K02058 simple sugar transport system substrate-binding protein	3.0	0.0	Flooded
K02824 uracil permease	3.1	0.0	Flooded
K10924 MSHA pilin protein MshA	3.1	0.0	Flooded
K07723 CopG family transcriptional regulator / antitoxin EndoAI	3.1	0.0	Flooded
K02406 flagellin	3.1	0.0	Flooded
K00527 ribonucleoside-triphosphate reductase [EC:1.17.4.2]	3.1	0.0	Flooded
K00929 butyrate kinase [EC:2.7.2.7]	3.1	0.0	Flooded
K03042 DNA-directed RNA polymerase subunit A [EC:2.7.7.6]	3.1	0.0	Flooded
K07812 trimethylamine-N-oxide reductase (cytochrome c) [EC:1.7.2.3]	3.2	0.0	Flooded
K17320 putative aldouronate transport system permease protein	3.2	0.0	Flooded
K10188 lactose/L-arabinose transport system substrate-binding protein	3.2	0.0	Flooded
K00581 tetrahydromethanopterin S-methyltransferase subunit E [EC:2.1.1.86]	3.2	0.0	Flooded
K01308 g-D-glutamyl-meso-diaminopimelate peptidase [EC:3.4.19.11]	3.3	0.0	Flooded
K17234 arabinosaccharide transport system substrate-binding protein	3.3	0.0	Flooded
K10547 putative multiple sugar transport system permease protein	3.3	0.0	Flooded
K07699 two-component system. response regulator. stage 0 sporulation protein A	3.3	0.0	Flooded
K06283 putative DeoR family transcriptional regulator. stage III sporulation protein D	3.3	0.0	Flooded
K01387 microbial collagenase [EC:3.4.24.3]	3.3	0.0	Flooded
K00702 cellobiose phosphorylase [EC:2.4.1.20]	3.3	0.0	Flooded
K01181 endo-1.4-beta-xylanase [EC:3.2.1.8]	3.4	0.0	Flooded
K06212 formate transporter	3.4	0.0	Flooded
K17213 inositol transport system substrate-binding protein	3.4	0.0	Flooded
K00260 glutamate dehydrogenase [EC:1.4.1.2]	3.5	0.0	Flooded
K14128 F420-non-reducing hydrogenase small subunit [EC:1.12.99.-]	3.5	0.0	Flooded
K00583 tetrahydromethanopterin S-methyltransferase subunit G [EC:2.1.1.86]	3.6	0.0	Flooded
K18331 NADP-reducing hydrogenase subunit HndC [EC:1.12.1.3]	3.6	0.0	Flooded
K01615 glutaconyl-CoA decarboxylase [EC:4.1.1.70]	3.6	0.0	Flooded
K10117 raffinose/stachyose/melibiose transport system substrate-binding protein	3.6	0.0	Flooded
K17992 NADP-reducing hydrogenase subunit HndB [EC:1.12.1.3]	3.7	0.0	Flooded
K00262 glutamate dehydrogenase (NADP+) [EC:1.4.1.4]	3.7	0.0	Flooded
K13653 AraC family transcriptional regulator	3.7	0.0	Flooded
K15924 glucuronoarabinoxylan endo-1.4-beta-xylanase [EC:3.2.1.136]	4.0	0.0	Flooded
K10540 methyl-galactoside transport system substrate-binding protein	4.0	0.0	Flooded
K10546 putative multiple sugar transport system substrate-binding protein	4.2	0.0	Flooded
K01225 cellulose 1.4-beta-cellobiosidase [EC:3.2.1.91]	5.0	0.0	Flooded
K15921 arabinoxylan arabinofuranohydrolase [EC:3.2.1.55	5.1	0.0	Flooded
K17318 putative aldouronate transport system substrate-binding protein	5.4	0.0	Flooded

[1] log2 foldchange between flooded and drained soil, blue colour (positive value) indicates a transcript that is enriched in flooded soils, while dark pink colour (negative value) indicates a transcript that is enriched in drained soils.
[2] FDR corrected *P* values

Table S11 *Soil physical and chemical parameters of the 7-day pre-incubated soil followed by drainage*

Parameters	***Drainage-7 days***
Oxygen (µmol/l)	236±4
Temperature (◦C)	28±0.4
Redox (mv)	386±16
Water potential (Kpa)	NA
Moisture content % (w/w)	18.3±1.7
Methane production potential (µmol h^{-1} gdw^{-1})	0.4±0.04

Appendix

List of abbreviation

2-bromoethanesulfonate	BES
Ammonium-oxidising bacteria/ Bacterial ammonia oxidisers	AOB
Auxiliary Activities	AA
Bacterial nitrite oxidisers./Bacterial nitrite oxidisers	NOB
Base pair	bp
Carbohydrate Esterases	CE
Carbohydrates-active Enzymes	CAZymes
Complementary DNA	cDNA
DataBase for automated Carbohydrate-active enzyme ANnotation	dbCAN
Denaturing gradient gel electrophoresis	DGGE
Denitrifying bacteria	DNB
Dissimilatory nitrate reduction to ammonia	DNRA
Encyclopedia of Genes and Genomes	KEGG
False discovery rate	FDR
GlycosyleHydrolase	GH
Greenhouse gases	GGC
GycosyleTransferase	GT
Iron-oxidising bacteria	FeOB
Iron-reducing bacteria	FeRB
Large Subunit rRNA	LSU
Lowest Common Ancestor	LCA
Methyl-coenzyme M reductase subunit alpha	*mcrA*

Methyl-coenzyme M reductase	MCR
Messenger RNA	mRNA
National center for Biotechnology Information	NCBI
Next Generation sequencing	NGS
Non-redundant	(nr)
Parts per billion	ppb
Particulate methane monooxygenase	pMMO
Particulate methane monooxygenase alpha	*pmoA*
Polysaccharide Lyases	PL
Principle coordinate analysis	PCoA
Quantitative Insights Into Microbial Ecology	QIIME
Quantitative PCR	qPCR
Reverse Transcription Quantitative PCR	RT-qPCR
RNA polymerase subunit β	*rpoB*
Small subunit rRNA (SSU rRNA)	SSU rRNA
Soil organic matter	SOM
Tera gram	Tg
Terminal restriction fragment length polymorphism	T-RFLP

Curriculum Vitae

PERSONAL INFORMATION

Rehab Abdallah

Place of Birth Giza, Egypt

Date of Birth 04.02.1986

WORK EXPERIENCE

01/10/2014–Present

Ph.D. researcher

Max Planck Institute for Terrestrial Microbiology, Marburg (Germany)

Project title: Response of soil microbial community to drainage and other environmental factors

01/04/2011–30/09/2014

Research biologist / Teaching assistant

The American University in Cairo, Cairo (Egypt)

01/09/2008–01/03/2011

Master researcher

The American University in Cairo, Cairo (Egypt)

Project title: The Red Sea Marine Metagenomics Project

01/06/2008–30/08/2008

Teaching assistant

Faculty of Biotechnology, October University for Modern Sciences and Arts, Cairo (Egypt)

EDUCATION AND TRAINING

01/10/2014–27/9/2018

Doctor rerum naturalium

EQF level 8

Max Planck Institute for Terrestrial Microbiology, Marburg (Germany)

- **Thesis title:** Community transcriptomics reveals drainage effects on paddy soil microbial community across the three domains of life
- **Thesis advisor:** Dr. Werner Liesack

01/09/2008–20/02/2012

Master of Science in Biotechnology

EQF level 7

The American University in Cairo, Cairo (Egypt)

- **GPA:** 3.738 (high honors)
- **Thesis title:** Exploring the Aerobic Methanotrophs community in the Red Sea Atlantis II Deep Brine area
- **Thesis advisor:** Dr. Rania Siam

01/09/2003–01/05/2008

Bachelor of Science in Biotechnology

EQF level 6

Montana State University, Bozeman, Montana (United States)

- **Major:** Biotechnology microbial system **Minor:** Biochemistry
- **GPA:** 3.92 (highest honors)

ADDITIONAL INFORMATION

Publications

- Kopf A., Bicak M., Kottmann R., Schnetzer J., Kostadinov I., Lehmann K., Fernandez-Guerra A., Jeanthon C., Rahav E., Ullrich M., Wichels A.,Gerdts G, Polymenakou P., Kotoulas G., Siam R., **Abdallah R. Z.**, The ocean sampling day consortium, 2015, Gigascienc 4 (1), 27
- **Abdallah R. Z.**, Adel M., Ouf A., Sayed A., Ghazy M. A., Alam I., Essack M., Lafi F.F., Bajic V.B., El-Dorry H., Siam R., Aerobic methanotrophic communities at the Red Sea brine-seawater interface, 2014, Frontiers in microbiology 5, 487
- **Abdallah R. Z.**, Wegner C.E., Liesack W., Community transcriptomics reveals drainage effects on paddy soil microbiome across the three domains of life, submitted to Soil Biology and Biogeochemistry
- **Abdallah R. Z.**, Wegner C.E., Liesack W., Effect of incubation periods on paddy soil microbial community after drainage, manuscript in preparation as short report

Honors and awards

- International Max Planck Research Schools fellowship from the Max Planck Institute for terrestrial microbiology, 2014-present
- Ph.D.Mentor in the DAAD “Research Internships in Science and Engineering (RISE)" scholarship, May-August 2017
- FEMS Travel Grant 14th Symposium on Bacterial Genetics and Ecology (BAGECO), June 2017
- King Abdullah University of Science and Technology (KAUST) fellowship from The American University in Cairo, 2008-2011
- Outstanding Senior Scholarship Award, the Microbiology Department, Montana State University, 2008
- Certificate of Achievement, Department of State, Washington, D.C., 2008
- Montana INBRE Award for enhancing biomedical research opportunities, 2007-2008
- Partnerships for Learning Undergraduate Studies Program (PLUS) from the Department of State, 2006-2008

Contribution to conferences

- The collaborative research center SFB 987 retreat, April 2018, Marburg, Germany (Oral presentation)
- 14th Symposium on Bacterial Genetics and Ecology (BAGECO), Aberdeen UK, June 2017, (Poster presentation)
- 3rd Thünen Symposium on Soil Metagenomics, December 2016, Braunschweig, Germany, (Poster presentation)
- Annual Meeting of the Association for General and Applied Microbiology (VAAM), March 2016, Jena, Germany, (Poster presentation)

Other activities

- Active member of the KMT foundation for Science and Philosophy (BioKMT), a non-profit organization that aims at advancing science and philosophy education in Egypt, 2014-present (http://www.biokmt.org/)

Acknowledgements

I would like to thank PD Dr. Werner Liesack not only for the opportunity to conduct my PhD studies in his laboratory but also for his support and the valuable scientific supervision.

Many thanks to Prof. Dr. Ralf Conrad and his group for providing the soil samples used in this study and for the interesting scientific discussions.

I am grateful to my thesis advisory committee – Prof. Dr. Ralf Conrad, Prof. Dr. Erhard Bremer, and Dr. Tobi Erb.

I am also very thankful to Dr. Carl Eric Wegner for all his help during my PhD. It would have been quite tough without your support in the laboratory since day one. Thank you so much for all your help with the computational analyses and for the constructive scientific discussions during the course of my PhD. I wish you a very bright future and am happy to have you as a friend.

I would also like to thank my friend Anna Hakobyan for the pleasant work atmosphere and her emotional and scientific support. I am thankful that you have been there for me.

Sincere thanks to Dr. Jingjing Peng, Dr. Dongfei Han, Dr. Qicheng Bei, Jing Zhu, Mehrdad Rabiei Nematabad, all the members of the Department of Biogeochemistry, and all the members of the Department of Organismic Interactions, for the pleasant work atmosphere.

I am deeply grateful to my husband for his love, support, encouragement, and understanding during the final phase of my PhD. I am also grateful to my friends especially Alejandra, Samada , Hala and Gihan for their support and the nice time we had together. Last but not least, I am deeply grateful to my family for their continuous and loving support

This research was supported by the Deutsche Forschungsgemeinschaft (collaborative research center SFB 987).

Pledge

Ich versichere, dass ich meine Dissertation

“**Community transcriptomics reveals drainage effects on paddy soil microbiome across the three domains of life**”

selbstständig und ohne unerlaubte Hilfe angefertigt habe und mich keiner als der von mir ausdrücklich bezeichneten Quellen und Hilfen bedient habe. Diese Dissertation wurde in der jetzigen oder ähnlichen Form noch bei keiner anderen Hochschule eingereicht und hat noch keinen sonstigen Prüfungszwecken gedient.

Marburg, Juli 2018 Rehab Abdallah

Pledge (English)

I certify that the present thesis entitled:

"**Community transcriptomics reveals drainage effects on paddy soil microbiome across the three domains of life**"

Was carried out without any unlawful means. This work has never been submitted before in this or in a similar format to any other university and has not been used before in any examination.

Marburg, July 2018

Rehab Abdallah